University of California
Los Angeles

An Energy-Based Approach to Power System Analysis

A dissertation submitted in partial satisfaction
of the requirements for the degree
Doctor of Philosophy in Electrical Engineering

by

Sina Yamaç Çalışkan

2015

Abstract of the Dissertation

An Energy-Based Approach to Power System Analysis

by

Sina Yamaç Çalışkan

Doctor of Philosophy in Electrical Engineering

University of California, Los Angeles, 2015

Professor Paulo Tabuada, Chair

Power systems are part of the nation's critical infrastructure and they support several indispensable services of our civilization such as hospitals, transportation systems, and telecommunications. Among the many requirements that power systems need to satisfy, power systems need to ensure that voltages and currents in the power grid are sinusoidal with a synchronous frequency of 50 or 60 Hz. Failure to do so would cause damage in appliances as well as in electrical industrial machinery that were developed under the assumption of sinusoidal voltages and currents with constant frequency. Furthermore, according to the North American Electric Reliability Corporation, frequency divergence of one or more of the generators that supply power to the grid, i.e., loss of synchronization, can lead to vibrations causing serious damage to the generators. As documented in the United States Department of Energy report on the August 14, 2003 blackout in Canada and the Northeast of the United States, frequency swings are the main reason for blackouts to spread across power systems. This makes the preservation of synchronization of generator frequencies one of the most important problems in power systems. This problem is also known as the transient stability problem in the power systems literature.

The classical models used to study the transient stability problem implicitly assume that all the generators are rotating at angular velocities close to the synchronous frequency. This assumption is known not to hold in real power systems.

A well documented example by the Department of Energy is the final stage of the August 14, 2003 blackout. This makes us question the validity of the existing tools and methods, based on classical assumptions and models, to predict and prevent the spread of blackouts.

In this work, we abandon the classical models and replace them with energy-based models derived from first principles that are not subject to hard-to-justify classical assumptions. In addition to eliminate assumptions that are known not to be satisfied, we derive intuitive conditions ensuring the transient stability of power systems. Providing such conditions in the classical framework with lossy transmission lines is a problem that has remained unsolved for more than sixty years and partial solutions under very restrictive assumptions have only recently been found. This is to be contrasted with the conditions described in this thesis that naturally handle lossy transmission lines. With the help of the insights we gained in the analysis performed in Section 4.3, we design easy-to-implement controllers that solve the transient stability problem in power systems. We also provide a novel way of performing circuit reduction, aiming to reduce the complexity of transmission grid models. Kron reduction, which is performed under steady state assumptions, is the standard circuit reduction technique used in the power systems literature. The novel circuit reduction method described in Section 3.1 shows how to perform Kron reduction for a class of electrical networks without these steady state assumptions.

The dissertation of Sina Yamaç Çalışkan is approved.

Mani Srivastava

Jason L. Speyer

Rajit Gadh

Panagiotis D. Christofides

Paulo Tabuada, Committee Chair

University of California, Los Angeles

2015

To my parents, Oğuz and Handan.

Table of Contents

List of Figures

Vita

2008	B.S. (Electrical and Electronics Engineering), ODTÜ (METU), Ankara, Turkey
2010	M.S. (Electrical and Electronics Engineering), Bilkent University, Ankara, Turkey
2010-2015	Graduate Student Researcher, Department of Electrical Engineering, University of California, Los Angeles, CA, USA.
2013–present	Ph.D. Candidate (Electrical Engineering), University of California, Los Angeles, CA, USA.
2015–present	Software Developer, MathWorks, MA, USA.

CHAPTER 1

Introduction

1.1 Power Systems

One of the major achievements in the history of our civilization is the invention of fire. The discovery of fire was also the inception of our ongoing search for the generation of energy to meet our basic needs. Power systems arise from this ongoing search. A power system is responsible for generating, transmitting, and distributing electrical energy to the customers connected to it. We can think of a power system as an interconnection of several building blocks, each of which is designed to achieve a different objective.

The first building block consists of generators which produce electrical energy. This production is achieved by means of converting some form of energy into electrical energy. The only form of energy that was required by our primal ancestors was heat energy, which was used for warming shelters or cooking food. In the contemporary society, we know how to build devices that use electrical energy to achieve a wide spectrum of tasks. This is one of the reasons behind converting different forms of energy into electrical energy in the generator units of a power system.

The electrical energy is "the common currency" of power systems because it is easier to transmit electrical energy to a wide area in an efficient manner. This efficiency in the transfer of electrical energy allows us to separate generation from consumption. In contrast to our ancestors, who kindled a fire to generate energy and use this generated energy on the spot, the customers of contemporary power systems are free from the laborious task of generating electrical energy by themselves. The second building block, the transmission grid, is responsible for transmitting the

energy produced by the generators to the distribution substations. The final building block consists of distribution grids. Each distribution grid is connected to one of the distributing substations. The energy received from the substation is routed to the customers connected to the distribution grid. When we connect our computer to an electrical plug, we form a connection between our device and the distribution grid.

Due to historical reasons, alternating currents in a power system are perfect sinusoidal waveforms with a fixed *utility frequency* of 60 Hz (in the United States, Canada, Mexico, etc.) or 50 Hz (in the European Union, Africa, Russia, China, etc). The whole system is designed based on the assumption that the electrical waveforms will be "close" to these ideal sinusoidal waveforms. Due to disturbances such as equipment failure and short-circuits caused by a tree contact, or the mismatch between the generated electrical energy and the consumed electrical energy, the electrical waveforms deviate from these ideal waveforms. One of the most important engineering objectives is to make sure that these deviations do not have significant effects on the power system operation. Another important objective is to make sure that the currents flowing on the transmission lines do not violate the predefined operational limits. Failure to achieve this objective results in high currents, and consequently, overheating of the transmission lines due to resistive losses. We want to avoid such excess heating since it has the potential to cause significant damage to the transmission line.

We can ensure that these two engineering objectives are satisfied by making sure that the frequencies of the generated electrical waveforms at the generator units are equal to the utility frequency, and the differences between the phase angles of the waveforms at the generator terminals are at the desired values. Transient stability, one of the most important problems in the power systems literature, can be informally defined as the problem of maintaining the frequencies and the phase angle differences of the generated electrical waveforms at the desired values.

1.2 The Future of the Power Systems

Our successful journey from the invention of fire to contemporary power systems is an impressive achievement. However, we are not at the end of this journey; and the evolution of power systems is an ongoing process. Researchers and engineers around the world give us glimpses of the next destinations that we will reach on this journey. It is important to see the path forward, because if we are blind to the vision of future power systems, in the words of Robert Shapard and Scott Prochazka in the US Department of Energy's "The Future of the Grid" report [68], "the changes will happen to us, rather than our industry leading the way to our future and that of the electric grid (system)". In the same report, the future directions of the power systems are investigated.

It is expected that the power grid, i.e., the combination of the transmission grid and the distribution grids of a power system, will be the most important part of the future power system. The interaction of customers with the future grid will also evolve into a more active relationship. In contemporary power systems, energy flows from the generation sources to the customers. The only role of the customer is to pay for the price of generation, transmission and distribution of this energy; and use this purchased energy passively. This paradigm of unidirectional flow of energy will evolve into a bidirectional flow, where a household or a factory can both be a customer and a producer. Current highly regulated structures will be replaced by a mixture of regulated and competitive markets. There will be a retail market where the prices of generation, transmission and distribution are determined. We will observe a power shift from traditional actors of the energy sector to the customers. This active involvement of the customers to the energy market will cause the power system to become more complex.

The contribution of the distributed energy sources to the power system will increase significantly. Although the conventional energy sources such as nuclear reactors will still be the key component of generation, there will be a shift from such sources to renewable energy sources such as solar panels, and power generators using

wind energy or natural gas. Maintaining the balance between the produced energy and the demand will still be the key objective in the future. Due to the increasing contribution of renewable sources, bidirectional energy flows and the increasing complexity of the grid, it will be harder to achieve this task. Together with the increasing societal need for robust and reliable power, the future power systems, although more flexible and adaptable, will be more complex and harder to control.

We expect that these changes will result in a paradigm shift in power systems that will render one of the fundamental assumptions that is widely used in the power systems literature false. This assumption can be summarized as follows: the models derived for steady-state are good approximations to study problems of dynamical nature, such as transient stability. In the past, this was a reasonable assumption due to the centralized and highly regularized structure of power systems. However, as illustrated by the future projections in this section, this picture is bound to change. This change motivates us to question the traditional models used to derive the theory behind the operation of power systems in the past century. Moreover, the current theory is also not sufficient to explain important phenomena such as the spread of a blackout, because the underlying assumptions are known to be violated during these events, as exemplified by the United States Department of Energy report [66] on the August 14, 2003 blackout in Canada and the Northeast of the United States. In this work, we show that it is possible to develop a theory of power systems without relying on these assumptions that have a debatable future.

The remainder of the dissertation is organized as follows. In Chapter 2, we introduce notation and concepts that are used in the rest of the dissertation. In Chapter 3, we explain how to perform circuit reduction *dynamically*, that is, without relying on the usage of phasors that are only well defined at the steady-state; and we illustrate how these results can be applied to obtain reduced transmission grid models. Finally, in Chapter 4, we review the traditional way of analyzing transient stability of power systems. In the same chapter, we show that it is possible to perform this analysis without posing the restrictive assumptions required by the traditional analysis.

CHAPTER 2

Preliminaries

In this chapter, we present several standard definitions and results that will be used in the subsequent chapters. We refer to [36, 45] for linear algebra, [35, 73] for graph theory, [19, 22, 41, 73] for electrical circuits, and [70, 71] for control theory and port-Hamiltonian systems. We use $\mathbb{S}$, $\mathbb{N}$, $\mathbb{R}$, $\mathbb{R}_+$ and $\mathbb{C}$ to denote the unit circle, the natural numbers, the real numbers, the positive real numbers, and the complex numbers, respectively. The cardinality of a set S is denoted by $|S|$. Given a complex number $c = x + jy \in \mathbb{C}$, the complex conjugate of c is $c^* = x - jy$, where $j^2 = -1$. We denote the set of smooth maps with domain A and codomain B by $\mathcal{C}(A, B)$.

We denote the $(i, j)^{\text{th}}$ component of a matrix M and i^{th} component of a vector v by $M_{i,j}$ and $v(i)$. The Hermitian M^H and the transpose M^T of a matrix $M \in \mathbb{C}^{n\times m}$ are defined as $M^H_{i,j} = M^*_{j,i}$ and $M^T_{i,j} = M_{j,i}$ for all $i \in \{1, \ldots, n\}$ and $j \in \{1, \ldots, m\}$, respectively. The diagonal matrix with diagonal elements $\{d_1, \ldots, d_n\}$ is denoted by $\mathbf{diag}\{d_1, \ldots, d_n\}$. If $M \in \mathbb{R}^{n\times n}$, then we have $M^H = M^T$. If $M = M^H$ $(M = M^T)$, the matrix M is called Hermitian (symmetric). The identity matrix $\mathbf{1}_{n\times n} \in \mathbb{R}^{n\times n}$ is a matrix where all diagonal elements are one and all off-diagonal elements are zero. A matrix M is invertible if there exists a matrix called the inverse of M, denoted by M^{-1}, that satisfies $MM^{-1} = M^{-1}M = \mathbf{1}_{n\times n}$. If $\lambda \in \mathbb{C}$ satisfies $Mv = \lambda v$ for some matrix $M \in \mathbb{C}^{n\times n}$ and a nonzero vector $v \in \mathbb{C}^n$, then λ is called an eigenvalue of M and v is called the eigenvector of M associated with the eigenvalue λ. Let M be a Hermitian matrix and λ be an eigenvalue of M. We have $Mv = \lambda v$, which in turn implies $M^H v = \lambda^* v$. Therefore, $\lambda = \lambda^*$, and this implies that every eigenvalue λ of an Hermitian matrix M is real.

For a subset $S \subseteq V$, where $(V, +, \cdot)$ is a vector space over a field F, if $(S, +, \cdot)$ is

a vector space over the same field, we say $(S, +, \cdot)$ is a subspace of $(V, +, \cdot)$. Abusing the notation, we use V to denote the vector space $(V, +, \cdot)$. The zero vector, denoted by $\mathbf{0}_n \in \mathbb{R}^n$, is a vector with all entries equal to zero. The span of a set vectors $S = \{v_1, \ldots, v_n\}$ is denoted by **span** S. Let B be a basis for a vector space V. The dimension of the vector space V, denoted by **dim** V, is defined as **dim** $V = |B|$. If **dim** $V \in \mathbb{N}$ (**dim** $V = \pm\infty$), then V is finite (infinite) dimensional.

The kernel and the image of the linear map defined by a matrix $M \in \mathbb{R}^{n\times m}$ are the vector spaces defined by the sets:

$$\textbf{ker } M = \{x \in \mathbb{R}^m \mid Mx = \mathbf{0}_n\},$$

$$\textbf{im } M = \{z \in \mathbb{R}^n \mid z = Mx \text{ for some } x \in \mathbb{R}^m\}$$

Let $\langle x, y\rangle$ be the Euclidean product of vectors

$$x = \begin{bmatrix} x_1 \\ \vdots \\ x_n \end{bmatrix}, \; y = \begin{bmatrix} y_1 \\ \vdots \\ y_n \end{bmatrix} \in \mathbb{R}^n$$

defined as $\langle x, y\rangle = \sum_{i=1}^{n} x_i y_i$. The orthogonal complement $S^\perp$ of a subspace $S \subseteq V$ is defined as

$$S^\perp = \{v \in V \mid \langle x, v\rangle = 0 \text{ for all } x \in S\}.$$

A matrix $M \in \mathbb{R}^{n\times n}$ is called positive-definite (positive-semidefinite), denoted by $M > 0$ ($M \geq 0$), if $x^T Mx > 0$ ($x^T Mx \geq 0$) for all $x \in \mathbb{R}^n$. If $-M$ is positive-definite (positive-semidefinite), then M is negative-definite (negative-semidefinite).

Theorem 2.0.1 *The spaces* $\boldsymbol{ker}\ M^T$ *and* $\boldsymbol{im}\ M$ *are subspaces of* $\mathbb{R}^m$ *that are orthogonal complements, i.e.,* $\left(\boldsymbol{ker}\ M^T\right)^\perp = \boldsymbol{im}\ M$.

Theorem 2.0.2 *Let* $M \in \mathbb{R}^{n\times n}$ *be a symmetric matrix. The following statements are equivalent:*

- *M is positive-semidefinite (positive-definite).*
- *If λ is an eigenvalue of M, then $\lambda \geq 0$ ($\lambda > 0$).*

If the matrices M_i for $i \in \{1, \ldots, n\}$ are positive-semidefinite, we have

$$x^T \left(\sum_{i=1}^{n} M_i \right) x = \sum_{i=1}^{n} x^T M_i x \geq 0,$$

and the sum of matrices $\sum_{i=1}^{n} M_i$ is also positive-semidefinite.

2.1 Graphs

In this section, we introduce graphs. A graph is a mathematical abstraction that represents how the elements of a given set of objects are connected to each other. We begin with a presentation of the formal definition of a graph. In Section 2.1.2, we present some of the results from graph theory, which will be used in the subsequent chapters of this work.

2.1.1 Graph Theory Related Definitions

We suppose that we are given a set of objects $\mathcal{V}$ and we ask the following question: "Given two objects from the set $\mathcal{V}$, are these objects connected?". The answer to this question can be encoded as a set $\mathcal{E} \subseteq \mathcal{V} \times \mathcal{V}$, where any element $e = (v_1, v_2) \in \mathcal{E}$ represents a connection from the object $v_1 \in \mathcal{V}$ to the object $v_2 \in \mathcal{V}$. The resulting data structure is called a graph where the objects, and the connections between these objects are represented by the vertices $\mathcal{V}$, and the edges $\mathcal{E}$ of this graph, respectively. The edges have a sense of direction: for every edge $(v_1, v_2) \in \mathcal{E}$, the direction is from the vertex v_1 to the vertex v_2. If for every edge $(v_1, v_2) \in \mathcal{E}$, we also have $(v_2, v_1) \in \mathcal{E}$, then the direction information becomes redundant. A graph that satisfies this property is called an undirected graph.

Definition 2.1.1 *A graph $\mathcal{G} = (\mathcal{V}, \mathcal{E})$ is a tuple, where $\mathcal{V}$ is the set of vertices and $\mathcal{E} \subseteq \mathcal{V} \times \mathcal{V}$ is the set of edges. A graph is undirected if*

$$(v_1, v_2) \in \mathcal{E} \implies (v_2, v_1) \in \mathcal{E},$$

for every $(v_1, v_2) \in \mathcal{V}$.

The following examples illustrate objects that can be represented as a graph:

Example 2.1.2 *(Connectivity of the buildings at the UCLA South Campus) It is possible to go from some of the buildings located at the UCLA South Campus to another building in the same area without leaving any of these two buildings. If we consider the Engineering* 4 *(E*4*), Engineering* 5 *(E*5*), Boelter Hall (BH), Math Sciences (MS) and California Nanoscience Institute buildings, the following graph in Figure 2.1 describes which of these buildings are connected.*

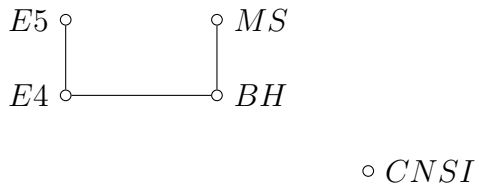

Figure 2.1: Connectivity of the buildings at the UCLA South Campus

The graph is undirected because if we can go from building A to building B without leaving any of these building, we can also go from building B to building A, i.e., $(A, B) \in \mathcal{E}$ *implies* $(B, A) \in \mathcal{E}$*. In the graph, an edge connecting two vertices A and B represents these two edges. In this example we have*

$$\mathcal{V} = \{E4, E5, BH, MS, CNSI\},$$

and

$$\mathcal{E} = \{(E4, E5), (E5, E4), (E4, BH), (BH, E4), (BH, MS), (MS, BH)\} \subseteq \mathcal{V} \times \mathcal{V}.$$

Since $(E4, E5) \in \mathcal{E}$*, we can go from Engineering* 4 *to Engineering* 5 *without leaving any of these buildings. However, since* $(E4, CNSI) \notin \mathcal{E}$*, we have to leave Engineering* 4 *to reach CNSI.*

Example 2.1.3 *(Followers in a social network) Let Alice (A), Bob (B), Carol (C) and Dave (D) be the users of a social network where people can follow other people's posts. We can use a directed graph to represent who is following who for this subset*

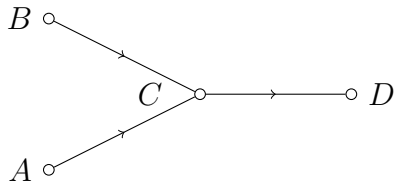

Figure 2.2: Followers in a social network

of users represented by

$$\mathcal{V} = \{A, B, C, D\}.$$

The scenario in which Alice and Bob follow Carol and Carol follows Dave is captured by the graph in Figure 2.2. The set of edges for this graph is

$$\mathcal{E} = \{(A, C), (B, C), (C, D)\}.$$

One can define a map $\Gamma : \mathcal{E} \to \mathcal{W}$. Given any edge e, this map assigns a *weight* $w = \Gamma(e) \in \mathcal{W}$ to this edge. A graph with weighted edges is called a *weighted graph.*

Definition 2.1.4 *A weighted graph $\mathcal{G} = (\mathcal{V}, \mathcal{E}, \Gamma, \mathcal{W})$ is a quadruple, where $\mathcal{V}$ is the set of vertices, $\mathcal{E} \subseteq \mathcal{V} \times \mathcal{V}$ is the set of edges, $\mathcal{W}$ is the set of edge weights and*

$$\Gamma : \mathcal{E} \to \mathcal{W},$$

is the weight function.

Example 2.1.5 *(Connectivity of the buildings at the UCLA South Campus - continued) The graph in Figure 2.1 shows the connectivity of the UCLA South Campus buildings. Some of these buildings are connected via suspension bridges. We can incorporate this information into the graph in Figure 2.1 by converting this graph into a weighted graph. We define $\mathcal{W} = \mathbb{N} \cup \{0\}$, and a map $\Gamma : \mathcal{E} \to \mathcal{W}$ which assigns each edge that connects two building the number of suspension bridges that form this connection. The resulting weighted graph $\mathcal{G} = (\mathcal{V}, \mathcal{E}, \Gamma, \mathcal{W})$ is given in Figure 2.3. We have*

$$\Gamma((E4, E5)) = 1, \quad \Gamma((E4, BH)) = 4, \quad \Gamma((BH, MS)) = 0.$$

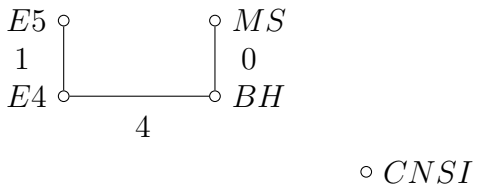

Figure 2.3: Number of suspension bridges connecting UCLA South Campus buildings

Any directed or undirected graph can be uniquely represented by a matrix

$$B \in \{-1, 0, 1\}^{|\mathcal{V}| \times |\mathcal{E}|},$$

which is called the *incidence matrix* of the graph.

Definition 2.1.6 *The incidence matrix* $B \in \{-1, 0, 1\}^{|\mathcal{V}| \times |\mathcal{E}|}$ *of a directed graph* $\mathcal{G} = (\mathcal{V}, \mathcal{E})$ *is a matrix defined by*

$$B_{i,j} = \begin{cases} -1 & \text{if} \quad \exists x \in \mathcal{V} \quad \text{such that} \quad e_i = (j, x) \in \mathcal{E} \\ 1 & \text{if} \quad \exists x \in \mathcal{V} \quad \text{such that} \quad e_i = (x, j) \in \mathcal{E} \\ 0 & \text{otherwise} \end{cases}.$$

For any undirected graph, for every edge $(i, j) \in \mathcal{E}$, we know that the symmetric edge $(j, i) \in \mathcal{E}$ is also an edge of the graph. We can always obtain a directed graph by randomly eliminating one of the edges from the pair of edges $(i, j), (j, i) \in \mathcal{E}$. Let B be the incidence matrix of the obtained graph. The incidence matrix of the undirected graph can be obtained by replacing every occurrence of -1 in B by 1.

Example 2.1.7 *The incidence matrix of the directed graph given in Figure 2.2 is*

$$B_{directed} = \begin{bmatrix} -1 & -1 & 0 & 0 \\ 0 & 0 & 0 & 0 \\ 1 & 0 & -1 & 0 \\ 0 & 0 & 1 & 0 \end{bmatrix}$$

In order to obtain the incidence matrix of the undirected graph given in Figure 2.1, we first eliminate the edges $(E5, E4)$, $(BH, E4)$, (MS, BH) *from the set of edges of the undirected graph to obtain a directed graph* $\mathcal{G}'$ *with*

$$\mathcal{V}' = \{E4, E5, BH, MS, CNSI\},$$

and

$$\mathcal{E}' = \{(E4, E5), (E4, BH), (BH, MS)\}$$

The incidence matrix of the undirected graph is obtained by replacing every occurrence of -1 *in the incidence matrix of the resulting directed graph* $\mathcal{G}'$ *by* 1*:*

$$B_{undirected} = \begin{bmatrix} 1 & 1 & 0 \\ 1 & 0 & 0 \\ 0 & 1 & 1 \\ 0 & 0 & 1 \\ 0 & 0 & 0 \end{bmatrix}.$$

The obtained incidence matrix $B_{undirected}$ *is independent of the choices of the eliminated edges from the pairs of symmetric edges.*

We conclude this section by defining connected graphs, paths and cycles.

Definition 2.1.8 *A path on graph* $\mathcal{G} = (\mathcal{V}, \mathcal{E})$ *from vertex* $v_0 \in \mathcal{V}$ *to vertex* $v_\ell \in \mathcal{V}$ *is the subset of vertices* $\{v_0, \ldots, v_i, \ldots, v_\ell\} \subseteq \mathcal{V}$ *that satisfies*

$$(v_{i-1}, v_i) \in \{(x, y) \in \mathcal{V} \times \mathcal{V} \mid (x, y) \in \mathcal{E} \text{ or } (y, x) \in \mathcal{E}\},$$

for all $i \in \{1, \ldots, \ell\}$*. If* $v_0 = v_\ell$*, then the path is called a cycle.*

Definition 2.1.9 *A graph* $\mathcal{G} = (\mathcal{V}, \mathcal{E})$ *is connected if for every* $v_i, v_j \in \mathcal{V}$ *with* $v_i \neq v_j$*, there exists a path from* v_i *to* v_j*.*

Example 2.1.10 *The graph in Figure 2.1 is not connected because for every*

$$v \in \{E4, E5, BH, MS\},$$

there exists no path from $CNSI$ *to* v*. The graph in Figure 2.2 is connected.*

2.1.2 Some Useful Results from Graph Theory

In this section, we present several graph-theoretical results that will later be used in Chapter 3. We begin by defining the graph Laplacian of a weighted directed graph.

Definition 2.1.11 *Let $\mathcal{G} = (\mathcal{V}, \mathcal{E}, \Gamma, \mathbb{R})$ be a weighted directed graph with the set of edges $\mathcal{E} = \{e_1, \ldots, e_{|\mathcal{E}|}\}$ and the incidence matrix B. The weight matrix W defined by the weight map Γ is given by*

$$W = \boldsymbol{diag}\left\{\Gamma(e_1), \ldots, \Gamma(e_{|\mathcal{E}|})\right\},$$

and the graph Laplacian of the weighted directed graph $\mathcal{G}$ is defined as BWB^T.

Let $\{\mathcal{V}_b, \mathcal{V}_i\}$ be a partition of the set of vertices $\mathcal{V}$ of a graph $\mathcal{G}$. We have $\mathcal{V} = \mathcal{V}_b \cup \mathcal{V}_i$ with $\mathcal{V}_b \cap \mathcal{V}_i = \emptyset$. This decomposition induces a decomposition of the incidence matrix

$$B = \begin{bmatrix} B_b \\ B_i \end{bmatrix},$$

where B_b and B_i are the matrices that are composed of the rows of the incidence matrix that correspond to the elements of $\mathcal{V}_b$, and $\mathcal{V}_i$, respectively. For the rest of the discussion, we will call the elements of $\mathcal{V}_b$, and $\mathcal{V}_i$ *boundary vertices*, and *internal vertices*, respectively. The following theorems illustrate important properties of the graph Laplacian of a weighted connected directed graph.

Theorem 2.1.12 *([73, Theorem 3.1]) Let $\mathcal{G} = (\mathcal{V}, \mathcal{E}, \Gamma, \mathbb{R}_+)$ be a weighted connected directed graph with the set of vertices $\mathcal{V} = \mathcal{V}_b \cup \mathcal{V}_i$, the weight matrix W, and the incidence matrix B. Then, the matrix $M = BWB^T$ is a symmetric, positive-semidefinite matrix with positive diagonal elements and non-positive off-diagonal elements. Moreover, the column sums and row sums of M are zero.*

Theorem 2.1.13 *([73, Theorem 3.1]) Let $M \in \mathbb{R}^{n \times n}$ be a symmetric, positive-semidefinite matrix with zero row and column sums, positive diagonal elements and non-positive off diagonal elements. There exists a weighted connected directed graph*

$\mathcal{G} = (\mathcal{V}, \mathcal{E}, \Gamma, \mathbb{R}_+)$ *with incidence matrix* B *and weight matrix* W *that satisfy* $M = BWB^T$.

Theorem 2.1.14 *([73, Theorem 3.1] and [11, Lemma 1]) Let* $\mathcal{G} = (\mathcal{V}, \mathcal{E}, \Gamma, \mathbb{R}_+)$ *be a weighted connected directed graph with the set of vertices* $\mathcal{V} = \mathcal{V}_b \cup \mathcal{V}_i$*, the weight matrix* W*, and the incidence matrix* B*. We assume that* $\mathcal{V}_b \neq \emptyset$ *and* $\mathcal{V}_i \neq \emptyset$*. There exists a weighted connected directed graph* $\hat{\mathcal{G}} = (\mathcal{V}_b, \hat{\mathcal{E}}, \hat{\Gamma}, \mathbb{R}_+)$ *with the weight matrix* $\hat{W}$ *and the incidence matrix* $\hat{B}$ *that satisfy*

$$\hat{B}\hat{W}\hat{B}^T = B_b W B_b^T - B_b W B_i^T \left(B_i W B_i^T\right)^{-1} B_i W B_b^T. \tag{2.1}$$

The following example shows that, in general, we cannot apply Theorem 2.1.14 to a graph with complex weights.

Example 2.1.15 *We consider the weighted directed graph* $\mathcal{G} = (\mathcal{V}, \mathcal{E}, \Gamma, \mathbb{C})$ *given in Figure 2.4 with* $\mathcal{V} = \{1, 2, 3\}$ *and* $\mathcal{E} = \{(1, 3), (3, 2)\}$*. The weight map is defined as*

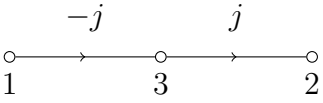

Figure 2.4: A weighted directed graph with complex weights

$$\Gamma(e) = \begin{cases} -j & \text{if} \quad e = (1,3) \\ \\ j & \text{if} \quad e = (3,2) \end{cases}.$$

The corresponding weight matrix and the incidence matrix are

$$W = \begin{bmatrix} -j & 0 \\ \\ 0 & j \end{bmatrix}, \quad B = \begin{bmatrix} -1 & 0 \\ \\ 0 & 1 \\ \\ 1 & -1 \end{bmatrix}.$$

We choose $\mathcal{V}_b = \{1, 2\}$ *and* $\mathcal{V}_i = \{3\}$*, which results in the partition*

$$\mathcal{B} = \begin{bmatrix} B_b \\ \\ B_i \end{bmatrix} \text{ with } B_b = \begin{bmatrix} -1 & 0 \\ \\ 0 & 1 \end{bmatrix}, \; B_i = \begin{bmatrix} 1 & -1 \end{bmatrix}.$$

Since $B_i W B_i^T = 0$*, the term* $(B^T W B_i^T)^{-1}$ *in* (2.2) *does not exist, therefore Theorem 2.1.14 is not applicable.*

This problem can be solved by enforcing the following assumption on edge weights:

Assumption 2.1.16 *The complex weights of the weighted directed graph* $\mathcal{G} = (\mathcal{V}, \mathcal{E}, \Gamma, \mathbb{C})$ *satisfy*

$$\sum_{(i,j)\in\mathcal{E}} \Gamma((i,j)) + \sum_{(j,i)\in\mathcal{E}} \Gamma((j,i)) \neq 0,$$

for every $i \in \mathcal{V}$.

By posing Assumption 2.1.16, we can generalize Theorem 2.1.14 to graphs with complex weights.

Theorem 2.1.17 *Let* $\mathcal{G} = (\mathcal{V}, \mathcal{E}, \Gamma, \mathbb{C})$ *be a weighted connected directed graph with the set of vertices* $\mathcal{V} = \mathcal{V}_b \cup \mathcal{V}_i$*, the set of edges* $\mathcal{E}$ *with weights satisfying Assumption 2.1.16, the weight matrix* W*, and the incidence matrix* B*. We assume that* $\mathcal{V}_b \neq \emptyset$ *and* $\mathcal{V}_i \neq \emptyset$*. There exists a weighted connected directed graph* $\hat{\mathcal{G}} = (\mathcal{V}_b, \hat{\mathcal{E}}, \hat{\Gamma}, \mathbb{C})$ *with the weight matrix* $\hat{W}$ *and the incidence matrix* $\hat{B}$ *that satisfy*

$$\hat{B}\hat{W}\hat{B}^T = B_b W B_b^T - B_b W B_i^T \left(B_i W B_i^T\right)^{-1} B_i W B_b^T. \tag{2.2}$$

2.2 Electrical Circuits

In this section, we focus on electrical circuits which are composed of two-terminal elements. In the remainder of this section, we assume that all the elements in the circuit are lumped. In Section 2.2.1, we present Kirchhoff's Voltage and Current Laws, which relate quantities defined on the terminals of the circuit elements to the quantities defined on the branches of the elements. In Section 2.2.1, we explain common two-terminal circuit elements in detail. Finally, in Section 2.2.2, we discuss how to analyze electrical circuits *at steady state* using phasors.

2.2.1 Kirchhoff's Laws and Circuit Elements

This section begins with the explanation on how to represent lumped electrical circuits as directed graphs. After we acquaint the reader with the graph theoretical

representation of electrical circuits, we present Kirchhoff's Laws using the language of graph theory.

2.2.1.1 Electrical Circuits as Graphs

A lumped electrical circuit is constructed by combining two-terminal lumped elements. This combination can be achieved by performing series and parallel connections of two-terminal elements. Given a new element to be connected to the rest of the circuit, in a series connection, we connect one of the terminals of the new element to one of the terminals to the rest of the circuit, whereas in a parallel connection we connect *both* of the terminals of the new element to the rest of the circuit.

Example 2.2.1 *We are given three two-terminal elements. The end points of the* i^{th} *elements are represented by* p_i *and* p_i'*. We connect elements* 1 *and* 2 *in series by connecting* p_1' *to* p_2*, and we connect element* 3 *in parallel to the circuit which is composed of elements* 1 *and* 2 *by connecting* p_3 *to* p_1 *and* p_3' *to* p_2'*. The final circuit is given in Figure 2.5*

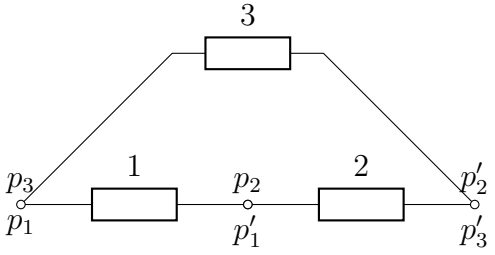

Figure 2.5: A lumped electrical circuit with three elements

We can think of the lumped circuit as a directed graph $\mathcal{G} = (\mathcal{V}, \mathcal{E})$, where we assign arbitrary reference directions to the edges. In Example 2.5, the set of vertices is $\mathcal{V} = \{v_1, v_2, v_3\}$ and the set of edges $\mathcal{E} = \{(v_1, v_2), (v_2, v_3), (v_1, v_3)\}$, where we identify the terminals p_1 and p_3 with the vertex v_1, the terminals p_1' and p_2 with the vertex v_2 and the terminals p_2' and p_3' with the vertex v_3. The edges of the graph represent the branches of the elements. This discussion generalizes to arbitrary lumped electrical circuits: we can represent any circuit as a directed graph $\mathcal{G} = (\mathcal{V}, \mathcal{E})$, where the set

of vertices $\mathcal{V}$ and edges $\mathcal{E}$ coincide with the terminals (nodes) and the branches of the lumped circuit elements.

2.2.1.2 Kirchhoff's Laws on Graphs

Let $\mathcal{G} = (\mathcal{V}, \mathcal{E})$ be a directed graph with the incidence matrix B that represents an electrical circuit. We define the smooth maps $I, V \in \mathcal{C}\left(\mathcal{I}, \mathbb{R}^{|\mathcal{E}|}\right)$ and $\eta, \psi \in \mathcal{C}\left(\mathcal{I}, \mathbb{R}^{|\mathcal{V}|}\right)$ for some $\mathcal{I} \subset \mathbb{R}$, where $I(e)(t)$ and $V(e)(t)$ are the current flowing through and voltage across the branch that is represented by edge e in the directed graph at time t. Similarly, $\eta(v)(t)$ and $\psi(v)(t)$ are the net current entering into and the potential at the terminal that is represented by vertex v at time t. For the rest of the discussion, we can use branch and edge, similarly terminal (node) and vertex, interchangeably.

From the definition of the incidence matrix B, we can verify that the i^{th} row B^i of the incidence matrix can be defined as

$$B^i(j) = \begin{cases} -1 & \text{if} \quad \text{the branch } j \text{ is leaving from the terminal } i \\ 1 & \text{if} \quad \text{the branch } j \text{ is entering into the terminal } i \\ 0 & \text{otherwise} \end{cases} \cdot$$

If the branch b is leaving from the terminal n, this means that the edge is from the vertex v that represents the terminal n to another vertex v'. Similarly, if the the branch b is entering into the terminal n, then the edge that represents b is from a vertex v' to the vertex v that represents the terminal n. With this observation on the rows of the incidence matrix, one can verify that $(B^i)^T I(t)$ represents the net current entering into the terminal at time t, i.e. the difference between the sums of currents at time t entering into and leaving from the terminal i. Repeating this process for every terminal node, we conclude that $BI(t)$ is the vector of currents injected on the terminals at time t. Kirchhoff's Current Law states that the net injection into the terminal nodes is zero, which is summarized as

$$0 = BI(t), \tag{2.3}$$

for all t. We note that this circuit is closed to outside current injections. We can

partition the set of nodes $\mathcal{V}$ into $\mathcal{V}_b$, the set of boundary nodes that one can interact with by injecting currents to the node or setting the potential of the node, and $\mathcal{V}_i$, the set of internal nodes that cannot be accessed from the outside. As explained in Section 2.1.2, this induces a decomposition of the incidence matrix B into B_b and B_i. Using the vector of net current injection η, Kirchhoff's Current Law can be expressed as

$$\eta(t) = \begin{bmatrix} \eta_b(t) \\ \mathbf{0}_{|\mathcal{V}_i|} \end{bmatrix} = BI(t) = \begin{bmatrix} B_b I(t) \\ B_i I(t) \end{bmatrix}, \tag{2.4}$$

for all t, where we assumed without loss of generality that the nodes are enumerated in a way that the first $|\mathcal{V}_b|$ nodes represent boundary nodes and the remaining nodes represent internal nodes. The last $|\mathcal{V}_i|$ elements of η are zero for all t, because these entries represent internal nodes, therefore we cannot inject currents into these nodes.

Kirchhoff's Voltage Law states that the sum of branch voltages around any loop in the electrical circuit is zero. Formally, V is orthogonal to any element of the cycle space of the graph, which is defined by $\mathbf{ker}\ B$, i.e., $V \in (\mathbf{ker}\ B)^{\perp}$. By Theorem 2.0.1, this implies that $V \in \mathbf{im}\ B^T$. Therefore, Kirchhoff Voltage Law can be stated as

$$V(t) = B^T\psi(t) = \begin{bmatrix} B_b^T & B_i^T \end{bmatrix} \psi(t) = B_b^T\psi_b(t) + B_i^T\psi_i(t), \tag{2.5}$$

for all $t \in \mathcal{I}$ for some $\psi \in \mathcal{C}\left(\mathcal{I}, \mathbb{R}^{|\mathcal{V}|}\right)$. The vector

$$\psi = \begin{bmatrix} \psi_b \\ \psi_i \end{bmatrix}$$

in (2.5) is precisely the vector of potentials at the terminals that we have defined earlied in this section where $\psi_b \in \mathcal{C}\left(\mathcal{I}, \mathbb{R}^{|\mathcal{V}_b|}\right)$ and $\psi_i \in \mathcal{C}\left(\mathcal{I}, \mathbb{R}^{|\mathcal{V}_i|}\right)$ are restrictions of ψ into $\mathcal{V}_b$ and $\mathcal{V}_i$, respectively.

Kirchhoff's Laws relate quantities defined on terminals to the quantities defined on branches. The next step is to understand how boundary variables, the voltage across the branches V and the currents flowing through the branches I are related. We cover three types of circuit elements: resistors, inductors and capacitors. If the circuit element represented by branch $b \in \mathcal{E}$ is a linear time invariant resistance,

an inductor or a capacitor, the voltage across the branch b and the current flowing through branch b satisfy

$$p_0(b)I(b)(t) + p_1(b)\dot{I}(b)(t) = q_0(b)V(b)(t) + q_1(b)\dot{V}(b)(t), \tag{2.6}$$

for all t. If the element is a resistor, we have $p_1 = 0$, $q_1 = 0$ and $r = \frac{p_0}{q_0} > 0$ is called the resistance of the element. In the case of an inductor, the zero coefficients are p_0 and q_1, and the constant $\ell = \frac{p_1}{q_0}$ is called the inductance of the element. Finally, $p_1 = 0$ and $q_0 = 0$ if the element is a capacitor; and $c = \frac{q_1}{p_0}$ is called the capacitance of the element.

2.2.2 Phasors and Steady-State Behavior

One can simplify (2.6), if the circuit is asymptotically stable, that is, if the effect of initial capacitor voltages and inductor currents at time $t = 0$ disappear as time goes to infinity. It is common in circuit analysis to implicitly assume that the circuit is asymptotically stable, and study the behavior of the circuit as time goes to infinity, also known as the steady state behavior of the circuit, by setting all initial conditions to zero and assuming that all terminal and branch waveforms are sinusoidals with a *constant* frequency ω. This implies that for branch b, we have

$$V(b) = \sqrt{2}V_{\text{rms, b}}\sin(\omega_s + \phi(b)), \tag{2.7}$$

and

$$I(b) = \sqrt{2}I_{\text{rms, b}}\sin(\omega_s + \rho(b)). \tag{2.8}$$

Since we know that the frequency is fixed and it is equal to ω_s, the only information we need to construct (2.7) is the amplitude V_{rms} and phase $\phi(b)$. Therefore the smooth waveform (2.7) can be represented by a complex number defined by $\bar{V}(b) = V_{\text{rms, b}}e^{j\phi(b)}$. This complex representation is called a *phasor*. Similarly, (2.8) can be replaced with the phasor representation $\bar{I}(b) = I_{\text{rms, b}}e^{j\rho(b)}$. Similarly, the time derivatives

$$\dot{V}(b) = \omega_s\sqrt{2}V_{\text{rms, b}}\cos(\omega_s + \phi(b)) = \omega_s\sqrt{2}V_{\text{rms, b}}\sin\left(\omega_s + \phi(b) + \frac{\pi}{2}\right), \tag{2.9}$$

and

$$\dot{I}(b) = \omega_s \sqrt{2} I_{\text{rms, b}} \cos(\omega_s + \rho(b)) = \omega_s \sqrt{2} I_{\text{rms, b}} \sin\left(\omega_s + \rho(b) + \frac{\pi}{2}\right) \tag{2.10}$$

can be replaced with phasor representations

$$\omega_s V_{\text{rms, b}} e^{j\phi(b)+\frac{\pi}{2}} = \omega_s \bar{V}(b) e^{\frac{\pi}{2}} = j\omega_s \bar{V}(b),$$

and

$$\omega_s I_{\text{rms, b}} e^{j\rho(b)+\frac{\pi}{2}} = \omega_s \bar{I}(b) e^{\frac{\pi}{2}} = j\omega_s \bar{I}(b),$$

respectively. We note that $\bar{V}(b), \bar{I}(b) \in \mathbb{C}$ *do not* depend on time. Replacing the smooth waveforms in (2.6) with phasor representations, we obtain

$$p_0(b)\bar{I}(b) + jp_1(b)\omega_s \bar{I}(b) = q_0(b)\bar{V}(b) + jq_1(b)\omega_s \bar{V}(b). \tag{2.11}$$

By juxtaposing (2.11) for every $b \in \mathcal{E}$, we obtain

$$\bar{I} = \mathbf{diag}\left(\frac{q_0(e_1) + j\omega_s q_1(e_1)}{p_0(e_1) + j\omega_s p_1(e_1)}, \ldots, \frac{q_0(e_{|\mathcal{E}|}) + j\omega_s q_1(e_{|\mathcal{E}|})}{p_0(e_{|\mathcal{E}|}) + j\omega_s p_1(e_{|\mathcal{E}|})}\right) \bar{V} = \Gamma \bar{V}, \tag{2.12}$$

where

$$\bar{I} = \begin{bmatrix} \bar{I}(e_1) \\ \vdots \\ \bar{I}(e_{|\mathcal{E}|}) \end{bmatrix}, \ \bar{V} = \begin{bmatrix} \bar{V}(e_1) \\ \vdots \\ \bar{V}(e_{|\mathcal{E}|}) \end{bmatrix} \in \mathbb{C}^{|\mathcal{E}|},$$

and $\Gamma \in \mathbb{C}^{|\mathcal{E}| \times |\mathcal{E}|}$. Since η and ψ are vectors of sinusoidal waveforms in $\mathcal{C}(\mathcal{I}, \mathbb{R}^{|\mathcal{V}|})$, we can also construct phasor representations of these vectors: $\bar{\eta}, \bar{\psi} \in \mathbb{C}^{|\mathcal{V}|}$. Using the phasor representations, Kirchhoff's Laws (2.4) and (2.5) can be expressed as

$$\bar{\eta} = \begin{bmatrix} \bar{\eta}_b \\ \mathbf{0}_{|\mathcal{V}_i|} \end{bmatrix} = B\bar{I} = \begin{bmatrix} B_b \bar{I} \\ B_i \bar{I} \end{bmatrix}, \tag{2.13}$$

and

$$\bar{V} = B^T \bar{\psi} = B_b^T \bar{\psi}_b + B_i^T \bar{\psi}_i. \tag{2.14}$$

Combining (2.13), (2.12) and (2.14), we obtain

$$\bar{\eta} = B\bar{I} = B\Gamma\bar{V} = B\Gamma B^T \bar{\psi}, \tag{2.15}$$

or equivalently,

$$\begin{bmatrix} \bar{\eta}_b \\ \mathbf{0}_{|\mathcal{V}_i|} \end{bmatrix} = \begin{bmatrix} B_b \Gamma B_b^T & B_b \Gamma B_i^T \\ B_i \Gamma B_b^T & B_i \Gamma B_i^T \end{bmatrix} \begin{bmatrix} \bar{\psi}_b \\ \bar{\psi}_i \end{bmatrix}. \tag{2.16}$$

By applying Theorem 2.2, we can eliminate the potentials of the internal nodes $\bar{\psi}_i$(2.16), and we express (2.16) as

$$\bar{\eta} = B_b W B_b^T - B_b W B_i^T \left(B_i W B_i^T\right)^{-1} B_i W B_b^T \bar{\psi}_b = \hat{B} \hat{W} \hat{B}^T \bar{\psi}_b. \tag{2.17}$$

This elimination process is also known as Kron reduction [27]. In order to perform this reduction on (2.16), we need to pose Assumption 2.1.16. Moreover, (2.16) is well defined only at the steady state. In Chapter 3, we will explain how to perform this reduction process without posing the Assumption 2.1.16 and assuming that the waveforms in the electrical circuit are sinusoidals.

2.3 Port-Hamiltonian Systems

We consider the affine control system

$$\dot{x} = f(x) + g(x)u \tag{2.18}$$

where $x \in \mathcal{M}$, $u \in \mathcal{U}$, $\mathcal{M}$ is a manifold and $\mathcal{U} \subseteq \mathbb{R}^m$ is a compact set. The affine control system (2.18) admits a port-Hamiltonian representation if there exists a smooth function $H : \mathbb{R}^n \to \mathbb{R}$, which is called Hamiltonian, together with smooth functions $g : \mathbb{R}^n \to \mathbb{R}^{n \times m}$, $\mathcal{J} : \mathbb{R}^n \to \mathbb{R}^{n \times n}$ and $\mathcal{R} : \mathbb{R}^n \to \mathbb{R}^{n \times n}$ satisfying $\mathcal{J}^T(x) = -\mathcal{J}(x)$ and $\mathcal{R}(x) = \mathcal{R}^T(x) \geq 0$ for all $x \in \mathbb{R}^n$ such that (2.18) can be written in the form

$$\dot{x} = (\mathcal{J}(x) - \mathcal{R}(x)) \frac{\partial H}{\partial x} + g(x)u, \tag{2.19}$$

where $\frac{\partial H}{\partial x}$ is the gradient of the Hamiltonian with respect to the vector

$$x = \begin{bmatrix} x_1 \\ \vdots \\ x_n \end{bmatrix},$$

which is given by

$$\frac{\partial H}{\partial x} = \begin{bmatrix} \frac{\partial H}{\partial x_1} & \cdots & \frac{\partial H}{\partial x_n} \end{bmatrix}^T.$$

We note that the gradient is assumed to be a column vector. The output of the port-Hamiltonian representation is defined as

$$y = g^T(x)\frac{\partial H}{\partial x}.$$

In the port-Hamiltonian representation, we can think of the Hamiltonian H as the total energy of the system. Taking the time derivative of the Hamiltonian H yields

$$\frac{dH}{dt} = \frac{\partial H}{\partial x}^T \dot{x} = -\frac{\partial H}{\partial x}^T \mathcal{R}\frac{\partial H}{\partial x} + u^T y \leq u^T y. \tag{2.20}$$

Here, the term $u^T y$ in the property (2.20) represents the power supplied to the system through the ports. Hence, this property states that the rate of increase of the Hamiltonian is less than the power supplied to the system.

CHAPTER 3

Circuit Reduction of Transmission Grids

In Section 2.2.2, we presented a circuit reduction technique, called Kron reduction, that relies on the usage of phasors. In this chapter, we show how to perform this reduction technique without using phasors for a class of circuits called generalized electrical networks. After introducing the theory, we use this reduction method on transmission grids to reduce the number of states that are needed to describe the grid. The results presented in this chapter are published in [11].

3.1 Circuit Reduction of Generalized Electrical Networks

As in Section 2.2.1, we assume that we have a network of electrical components which is represented by a directed graph $\mathcal{G} = (\mathcal{V}, \mathcal{E})$ and each electrical component has two terminals. The constitutive relation of the electrical component is a relation between the current flowing through the electrical component and the voltage across its terminals. We consider electrical components with constitutive relations given by

$$\sum_{i=0}^{\nu} p_{ki} \frac{d^i}{dt^i} I_{1,k} = \sum_{i=0}^{\nu} q_{ki} \frac{d^i}{dt^i} V_k^1. \tag{3.1}$$

where $p_{ki}, q_{ki} \in \mathbb{R}_+$, $\nu \in \mathbb{N}$ is the highest degree of differentiation, $I_{1,k}$ is the current flowing through the electrical component $k \in \bar{e}$ with $\bar{e} = \{1, \ldots, |\mathcal{E}|\}$ and V_k^1 is the voltage across the terminals of the electrical component k. The *coefficient vectors* of (3.1) are defined as $p_k = (p_{k0}, \ldots, p_{k\nu}) \in \mathbb{R}_+^{\nu+1}$, $q_k = (q_{k0}, \ldots, q_{k\nu}) \in \mathbb{R}_+^{\nu+1}$. The *coefficient matrices* are defined as

$$P = \begin{bmatrix} p_1 & \ldots & p_e \end{bmatrix},$$

and

$$Q = \begin{bmatrix} q_1 & \dots & q_e \end{bmatrix}.$$

We note that (2.6) is a special case of (3.1). The constitutive relation for a linear ideal resistor is given by $rI_{1,k} = V_k^1$ and can be described by (3.1) if we take $\nu = 0$ and $\frac{p_{k0}}{q_{k0}} = r$. Similarly, the constitutive relations for inductors and capacitors, $\ell \dot{I}_{1,k} = V_k^1$ and $I_{1,k} = c\dot{V}_k^1$, are described by (3.1) when we set $\nu = 1$, $p_{k0} = 0$, $p_{k1} = \ell$, $q_{k0} = 0$, $q_{k1} = 1$, and $\nu = 1$, $p_{k0} = 0$, $p_{k1} = 1$, $q_{k0} = 0$, $q_{k1} = c$, respectively.

The constant upper bound ν in (3.1) is the same for every electrical component. In other words, the highest degree of differentiation in (3.1), which is a measure of the complexity of the electrical component, is independent of the electrical component. We can think of an electrical network as a directed graph in which each edge in the graph represents an electrical component. In this framework, electrical components relate the space of trajectories of currents flowing through the edges Λ_1 and its dual space, the space of trajectories of voltages across the edges Λ^1. In other words, for the directed graph $\mathcal{G}$, $(I_1, V^1) \in \Lambda_1 \times \Lambda^1$ satisfies the constitutive relations (3.1) if for every edge $e_k \in \mathcal{E}$, the relationship between $I_{1,k}$ and V_k^1 is given by (3.1), where $I_{1,k}$ is the k^{th} element of I_1 and V_k^1 is the k^{th} element of V^1. For every edge $e_k \in \mathcal{E}$, the coefficient vectors of (3.1) are p_k and q_k. For the rest of the paper, we will assume that $p_k \neq \mathbf{0}_{\nu+1}$ (i.e. no short-circuit edges) and $q_k \neq \mathbf{0}_{\nu+1}$ (i.e. no open-circuit edges).

Definition 3.1.1 *A generalized electrical network is a five-tuple $\mathcal{N} = (\mathcal{G}, \mathcal{V}_b, \nu, P, Q)$. It consists of an open directed graph $\mathcal{G} = (\mathcal{V}, \mathcal{E})$ with boundary vertices $\mathcal{V}_b \subset \mathcal{V}$ on which KCL (2.4), KVL (2.5), and constitutive relations (3.1) are satisfied on $\mathcal{G}$; ν is the constant in (3.1), and $P, Q \in \mathbb{R}^{(\nu+1)\times e}$ are the coefficient matrices.*

We adapt the notion of terminal behavior, which was introduced in [76, 81], to our framework.

Definition 3.1.2 *The terminal behavior $\mathcal{B}_\mathcal{N} \subset \Lambda_b^0 \times \Lambda_{0b}$ of a generalized electrical network $\mathcal{N} = (\mathcal{G}, \mathcal{V}_b, \nu, P, Q)$ is the relation defined by: $(\psi^{0b}, I_{0b}) \in \mathcal{B}_\mathcal{N}$ iff there exists*

a $\psi^{0i} \in \Lambda^{0i}$ *such that* $\psi^0 = (\psi^{0b}, \psi^{0i}) \in \Lambda^0$ *and* $I_0 = (I_{0b}, \mathbf{0}_{|\mathcal{V}_e|}) \in \Lambda_{0b} \times \Lambda_{0i}$ *satisfy KCL (2.4), KVL (2.5) and constitutive relations (3.1) on* $\mathcal{G}$*.*

The problem addressed in this note is:

Problem 3.1.3 (Kron Reduction [26]) *Given a generalized electrical network*

$$\mathcal{N} = (\mathcal{G}, \mathcal{V}_b, \nu, P, Q),$$

when can we construct another generalized electrical network

$$\hat{\mathcal{N}} = (\hat{\mathcal{G}}, \mathcal{V}_b, \nu, \hat{P}, \hat{Q}),$$

with $\hat{\mathcal{G}} = (\mathcal{V}_b, \hat{\mathcal{E}})$ *and* $\mathcal{B}_{\mathcal{N}} = \mathcal{B}_{\hat{\mathcal{N}}}$*?*

Note that every node in the graph $\hat{\mathcal{G}}$ is a boundary vertex. Moreover, the highest degree of differentiation in the constitutive relations, ν, is the same for $\mathcal{N}$ and $\hat{\mathcal{N}}$. Therefore, Problem 3.1.3 is equivalent to eliminating all the internal vertices of the generalized electrical network $\mathcal{N}$ without changing the terminal behavior and the complexity of the constitutive relations, as measured by ν. Problem 3.1.3 admits the following solution.

Theorem 3.1.4 *Problem 3.1.3 is solvable for the generalized electrical network*

$$\mathcal{N} = (\mathcal{G}, \mathcal{V}_b, \nu, P, Q)$$

if we have

$$\textbf{\textit{dim span}} \{p_1, \ldots, p_e\} = \textbf{\textit{dim span}} \{q_1, \ldots, q_e\} = 1, \tag{3.2}$$

where p_i*,* q_i *are the coefficient vectors of (3.1) for edge* $e_i \in \mathcal{E}$*, where* $i \in \{1, \ldots, e\}$*.*

Proof. Assume that $\mathcal{N} = (\mathcal{G}, \mathcal{V}_b, \nu, P, Q)$ is a generalized electrical network satisfying (3.2). Condition (3.2) states that the vector space **span** $\{p_1, \ldots, p_e\}$ has dimension one. This implies that the basis for this vector space consists of a single vector $\tilde{p} = (\tilde{p}_1, \ldots, \tilde{p}_e) \neq \mathbf{0}_{(\nu+1)e}$. Thus for every $k \in \bar{e}$, there exists a constant λ_k such that $p_k = \lambda_k \tilde{p}$. Since every element of p_k is nonnegative for all $k \in \bar{e}$,

we can assume without loss of generality that every element of $\tilde{p}$ is nonnegative. Hence, we can assume $\lambda_k \geq 0$ for all $k \in \bar{e}$. Similarly, the basis for the vector space $\textbf{span}\,\{q_1, \ldots, q_e\}$ consists of a single vector $\tilde{q} = (\tilde{q}_1, \ldots, \tilde{q}_e) \neq \mathbf{0}_{(\nu+1)e}$. From the same reasoning, we can assume $\gamma_k \geq 0$. Replacing p_k and q_k in (3.1) with $p_k = \lambda_k \tilde{p}$ and $q_k = \gamma_k \tilde{q}$, we obtain

$$\lambda_k \sum_{i=0}^{\nu} \tilde{p}_i \frac{d^i}{dt^i} I_{1,k} = \gamma_k \sum_{i=0}^{\nu} \tilde{q}_i \frac{d^i}{dt^i} V_k^1, \tag{3.3}$$

for every edge $e_k \in \mathcal{E}$. By assumption, we have $p_k \neq \mathbf{0}_{\nu+1}$ and $q_k \neq \mathbf{0}_{\nu+1}$. This implies that $\lambda_k \neq 0$ and $\gamma_k \neq 0$. Dividing (3.3) by λ_k for each $k \in \mathcal{E}$ and writing equation (3.3) for every edge $e_k \in \mathcal{E}$ in vector form, we obtain

$$\sum_{i=0}^{\nu} \tilde{p}_i \frac{d^i}{dt^i} I_1 = \Gamma \sum_{i=0}^{\nu} \tilde{q}_i \frac{d^i}{dt^i} V^1, \tag{3.4}$$

where $I_1 = (I_{1,1}, \ldots, I_{1,e})$, $V^1 = (V_1^1, \ldots, V_e^1)$ and Γ is a diagonal matrix with strictly positive diagonal elements. The matrix Γ is defined as $\Gamma_{kk} = \frac{\gamma_k}{\lambda_k}$ for all $k \in \bar{e}$. From KVL (2.5), we have $V^1 = B^T \psi^0$ for $\psi^0 \in \Lambda_0$. Replacing V^1 in (3.4), we obtain

$$\sum_{i=0}^{\nu} \tilde{p}_i \frac{d^i}{dt^i} I_1 = \Gamma \sum_{i=0}^{\nu} \tilde{q}_i \frac{d^i}{dt^i} B^T \psi^0 = \Gamma B^T \sum_{i=0}^{\nu} \tilde{q}_i \frac{d^i}{dt^i} \psi^0. \tag{3.5}$$

Multiplying both sides of (3.5) by B results in

$$B \sum_{i=0}^{\nu} \tilde{p}_i \frac{d^i}{dt^i} I_1 = B\Gamma B^T \sum_{i=0}^{\nu} \tilde{q}_i \frac{d^i}{dt^i} \psi^0 \iff \sum_{i=0}^{\nu} \tilde{p}_i \frac{d^i}{dt^i} B I_1 = B\Gamma B^T \sum_{i=0}^{\nu} \tilde{q}_i \frac{d^i}{dt^i} \psi^0. \tag{3.6}$$

Using the previously defined partitioning of B into B_i and B_b, we obtain the following set of equations from (3.6)

$$\sum_{i=0}^{\nu} \tilde{p}_i \frac{d^i}{dt^i} B_b I_1 = B_b \Gamma B_i^T \sum_{i=0}^{\nu} \tilde{q}_i \frac{d^i}{dt^i} \psi^{0i} + B_b \Gamma B_b^T \sum_{i=0}^{\nu} \tilde{q}_i \frac{d^i}{dt^i} \psi^{0b}, \tag{3.7}$$

$$\sum_{i=0}^{\nu} \tilde{p}_i \frac{d^i}{dt^i} B_i I_1 = B_i \Gamma B_i^T \sum_{i=0}^{\nu} \tilde{q}_i \frac{d^i}{dt^i} \psi^{0i} + B_i \Gamma B_b^T \sum_{i=0}^{\nu} \tilde{q}_i \frac{d^i}{dt^i} \psi^{0b}. \tag{3.8}$$

From KCL (2.4), we have $B_b I_1 = I_{0b}$ and $B_i I_1 = \mathbf{0}_{|\mathcal{V}_i|}$. Replacing $B_b I_1 = I_{0b}$ in (3.7) and $B_i I_1 = \mathbf{0}_{|\mathcal{V}_i|}$ in (3.8), we have

$$\sum_{i=0}^{\nu} \tilde{p}_i \frac{d^i}{dt^i} I_{0b} = B_b \Gamma B_i^T \sum_{i=0}^{\nu} \tilde{q}_i \frac{d^i}{dt^i} \psi^{0i} + B_b \Gamma B_b^T \sum_{i=0}^{\nu} \tilde{q}_i \frac{d^i}{dt^i} \psi^{0b}, \tag{3.9}$$

$$\mathbf{0}_{|\mathcal{V}_i|} = B_i \Gamma B_i^T \sum_{i=0}^{\nu} \tilde{q}_i \frac{d^i}{dt^i} \psi^{0i} + B_i \Gamma B_b^T \sum_{i=0}^{\nu} \tilde{q}_i \frac{d^i}{dt^i} \psi^{0b}.$$

The matrix $B_i\Gamma B_i^T$ is invertible by Theorem 2.1.12. Therefore, we obtain from the previous equality:

$$\sum_{i=0}^{\nu} \tilde{q}_i \frac{d^i}{dt^i}\psi^{0i} = -(B_i\Gamma B_i^T)^{-1}B_i\Gamma B_b^T \sum_{i=0}^{\nu} \tilde{q}_i \frac{d^i}{dt^i}\psi^{0b}. \tag{3.10}$$

Substituting $\sum_{i=0}^{\nu} \tilde{q}_i \frac{d^i}{dt^i}\psi^{0i}$ into (3.9), we obtain

$$\sum_{i=0}^{\nu} \tilde{p}_i \frac{d^i}{dt^i} I_{0b} = \left(B_b\Gamma B_b^T - B_b\Gamma B_i^T(B_i\Gamma B_i^T)^{-1}B_i\Gamma B_b^T\right) \sum_{i=0}^{\nu} \tilde{q}_i \frac{d^i}{dt^i}\psi^{0b}. \tag{3.11}$$

Smoothness of ψ^{0b} implies that the left hand side of (3.11) and the left hand side of (3.10) are continuous functions. Since $\tilde{p} \neq \mathbf{0}_{\nu+1}$ for any $\psi^{0b} \in \Lambda_b^0$, there exists a unique $I_{0b} \in \Lambda_{0b}$ that satisfies (3.11) and a unique ψ^{0i} that satisfies (3.10). Therefore, if I_{0b} and ψ_{0b} satisfy (3.11), then there exists a unique $\psi^{0i} \in \Lambda^{0i}$ such that $\psi^0 = (\psi^{0b}, \psi^{0i}) \in \Lambda^0$ and $I_0 = (I_{0b}, \mathbf{0}_{|\mathcal{V}_e|}) \in \Lambda_0$ satisfy KCL (2.4), KVL (2.5) and constitutive relations (3.1). Thus $(\psi_b, I_b) \in \mathcal{B}_{\mathcal{N}}$ iff I_{0b} and ψ_{0b} satisfy (3.11). We now want to construct a generalized electrical network $\hat{\mathcal{N}} = (\hat{\mathcal{G}}, \mathcal{V}_b, \nu, \hat{P}, \hat{Q})$ with $\hat{\mathcal{G}} = (\mathcal{V}_b, \hat{\mathcal{E}})$ and $\mathcal{B}_{\mathcal{N}} = \mathcal{B}_{\hat{\mathcal{N}}}$. From Theorem 2.1.14, there exists a graph $\hat{\mathcal{G}} = (\mathcal{V}_b, \hat{\mathcal{E}})$ with incidence matrix $\hat{B}$ and a diagonal matrix $\hat{\Gamma}$ with strictly positive diagonal elements such that

$$\hat{B}\hat{\Gamma}\hat{B}^T = B_b\Gamma B_b^T - B_b\Gamma B_i^T(B_i\Gamma B_i^T)^{-1}B_i\Gamma B_b^T. \tag{3.12}$$

We construct a generalized electrical network $\hat{\mathcal{N}}$ from the directed graph $\hat{\mathcal{G}}$ by defining the constitutive relations on $\hat{\mathcal{G}}$ as

$$\sum_{i=0}^{\nu} \tilde{p}_i \frac{d^i}{dt^i} \hat{I}_1 = \hat{\Gamma} \sum_{i=0}^{\nu} \tilde{q}_i \frac{d^i}{dt^i} \hat{V}^1. \tag{3.13}$$

Multiplying both sides of (3.13) by $\hat{B}$ and using (2.4), (2.5), (3.12); we obtain (3.11) from (3.13). Therefore we can construct a generalized electrical circuit $\hat{\mathcal{N}}$ that has the same terminal behavior as $\mathcal{N}$. □

We emphasize that the reduction process detailed in the proof of Theorem 3.1.4 is performed in the time domain and requires no steady state assumptions. We start with the generalized electrical network $\mathcal{N}$ that describes the relation between voltages and currents in the time domain and we constructed the Kron reduced

generalized electrical network $\hat{\mathcal{N}}$ that has the same terminal behavior also described in the time domain by the constitutive relations (3.13). In the proof, we are assuming that the sum of the currents entering to the internal nodes are zero. However, the proof is extendable to the case in which we have current injections at internal nodes.

The following example illustrates that Condition (3.2) in Theorem 3.1.4 is not necessary.

Example 3.1.5 *Consider the generalized electrical network* $\mathcal{N} = (\mathcal{G}, \mathcal{V}_b, \nu, P, Q)$ *with* $\mathcal{G}$ *given below:*

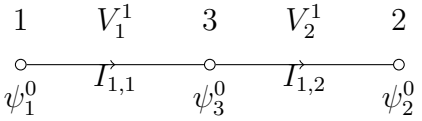

The constitutive relations for the edges $e_1 = (1, 3)$ *and* $e_2 = (3, 2)$ *are* $I_{1,1} = V_1^1$ *and* $\frac{d}{dt} I_{1,2} = V_2^1$*, respectively. Note that* $\nu = 1$*. From KCL (2.4), we have* $I_{0b,1} = I_{1,1}$*,* $I_{1,1} = I_{1,2}$ *and* $I_{1,2} = -I_{0b,2}$*. From KVL (2.5), we have* $V_1^1 = \psi_3^0 - \psi_1^0$ *and* $V_2^1 = \psi_2^0 - \psi_3^0$*. Replacing* $I_{1,1}$*,* $I_{1,2}$*,* V_1^1 *and* V_2^1 *in the constitutive relations, we obtain*

$$I_{0b,1} = -I_{0b,2} = \psi_3^0 - \psi_1^0,$$
$$\frac{d}{dt} I_{0b,1} = -\frac{d}{dt} I_{0b,2} = \psi_2^0 - \psi_3^0.$$

Combining these equations, we obtain

$$I_{0b,1} + \frac{d}{dt} I_{0b,1} = -I_{0b,2} - \frac{d}{dt} I_{0b,2} = \psi_2^0 - \psi_1^0. \tag{3.14}$$

There exists a ψ_3^0 *such that* $(\psi_1^0, \psi_2^0, \psi_3^0)$ *and* $(I_{0b,1}, I_{0b,2})$ *satisfy KCL (2.4), KVL (2.5) and the constitutive relations if and only if* (ψ_1^0, ψ_2^0) *and* $(I_{0b,1}, I_{0b,2})$ *satisfy (3.14). Therefore* $(\psi_1^0, \psi_2^0, I_{0b,1}, I_{0b,2}) \in \mathcal{B}_{\mathcal{N}}$ *if and only if* $(\psi_1^0, \psi_2^0, I_{0b,1}, I_{0b,2})$ *satisfy (3.14). We now construct a generalized electrical network* $\hat{\mathcal{N}} = (\hat{\mathcal{G}}, \mathcal{V}_b, 1, P, Q)$ *such that* $\mathcal{B}_{\hat{\mathcal{N}}} = \mathcal{B}_{\mathcal{N}}$*. The directed graph* $\hat{\mathcal{G}}$ *is given below:*

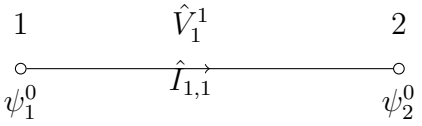

We pick the constitutive relation of the single edge in $\hat{\mathcal{N}}$ as

$$\hat{I}_{1,1} + \frac{d}{dt}\hat{I}_{1,1} = \hat{V}_1^1.$$

*From KCL (2.4), we have $I_{0b,1} = -I_{0b,2} = \hat{I}_{1,1}$. From KVL (2.5), we have $\hat{V}_1^1 = \psi_2^0 - \psi_1^0$. Replacing $\hat{I}_{1,1}$ and $\hat{V}_1^1$ in the constitutive relations, we recover (3.14). Therefore $(\psi_1^0, \psi_2^0, I_{0b,1}, I_{0b,2}) \in \mathcal{B}_{\hat{\mathcal{N}}}$ if and only if $(\psi_1^0, \psi_2^0, I_{0b,1}, I_{0b,2})$ satisfy (3.14). This implies that $\mathcal{B}_{\mathcal{N}} = \mathcal{B}_{\hat{\mathcal{N}}}$. Hence Problem 3.1.3 is solvable. However $p_1 = (1, 0)$ and $p_2 = (0, 1)$. Therefore **dim span**$\{p_1, p_2\} = 2$ and Condition (3.2) does not hold.*

*If we pick the constitutive relations for the edges of $\mathcal{N}$ as $I_{1,1} = V_1^1$ and $I_{1,2} = \frac{d}{dt}V_2^1$, we can also verify that Problem 3.1.3 is solvable. In this case, **dim span**$\{q_1, q_2\} = 2$ and Condition (3.2) does not hold.* □

Example 3.1.6 *Consider the generalized electrical network in the previous example. If we pick the constitutive relations for the edges of $\mathcal{N}$ as $\frac{d}{dt}I_{1,1} = V_1^1$ and $I_{1,2} = \frac{d}{dt}V_2^1$, Condition (3.2) does not hold. Nevertheless, we can compute the constitutive relation for the Kron reduced network as*

$$\frac{d}{dt}(V_1^1 + V_2^1) = \frac{d}{dt}(\psi_2^0 - \psi_1^0) = \frac{d^2}{dt^2}I_{1,1} + I_{1,2}. \tag{3.15}$$

Observe that $\nu = 1$. However, the constitutive relation for the single edge in the reduced graph has a second order derivative. Problem 3.1.3 is not solvable.

3.2 Applications

3.2.1 Application to RLC Circuits and Power Networks

Every RLC circuit can be modeled as a generalized electrical network by taking the electric components to be combinations of resistors, inductors, or capacitors. When all the circuit elements are resistors we speak of a purely resistive circuit. Purely inductive and purely capacitive circuits can be defined similarly. It is shown in [73] that Problem 3.1.3 is solvable for purely resistive, inductive, or capacitive circuits. The same result can be obtained by the following corollary of Theorem 3.1.4.

Corollary 3.2.1 *Problem 3.1.3 is solvable for the generalized electrical network $\mathcal{G}$ if $\mathcal{G}$ is a purely resistive, purely inductive or purely capacitive circuit.*

Proof. We will prove the corollary for purely resistive circuits. The proofs for purely inductive and purely capacitive circuits are very similar. In a purely resistive circuit, $\mathbf{p}_i = (r_i, 0)$, and $\mathbf{q}_i = (1, 0)$, where $r_i \in \mathbb{R}^e_+$ is the resistance of the branch i. Hence, Condition (3.2) holds. The result follows from Theorem 3.1.4. □

One particular example of generalized electrical networks is *homogeneous* RL circuits [10]. Every branch of an homogeneous RL circuit is a series connection of a resistor and an inductor. The term homogeneous comes from the fact that for every two edges $e_i, e_j \in \mathcal{E}$ with resistance values r_i, r_j and inductor values ℓ_i, ℓ_j, we have $\frac{r_i}{r_j} = \frac{\ell_i}{\ell_j}$. In order to represent RL circuits, it is enough to set $\nu = 1$ and $(p_{i1}, p_{i2}, q_{i1}, q_{i2}) = (r_i, \ell_i, 1, 0)$ in (3.1) for all $i \in \bar{e}$, where r_i is the resistance value of the resistive component of branch i and ℓ_i is the inductance value of the inductive component of branch i. Note that homogeneity implies that there exists a constant $c \in \mathbb{R}$, $c > 0$ such that $\mathbf{p}_i = c\mathbf{p}_j$ for every $i, j \in \bar{e}$. Therefore Condition (3.2) holds and we can recover Theorem 4.4 in [10] as a corollary of Theorem 3.1.4. The concept of homogeneity can be generalized to RLC circuits. A *homogeneous* RLC circuit is an electrical circuit such that every branch is a series combination of a resistor, an inductor and a capacitor with the following condition: for every two edges $e_i, e_j \in \mathcal{E}$ with resistance values r_i, r_j, inductor values ℓ_i, ℓ_j, and capacitor values c_i, c_j; we have $\frac{r_i}{r_j} = \frac{\ell_i}{\ell_j} = \frac{c_i}{c_j}$. *Homogeneous RC* circuits and *homogeneous LC* circuits can be defined in a similar fashion. The previous discussion is summarized in the next result.

Corollary 3.2.2 *Problem 3.1.3 is solvable for homogeneous RLC, RL, RC or LC circuits.*

There are various transmission line models available in the literature [21], [59], [5]. If the transmission line is relatively short (less than 60 kilometers [21], or 50 miles [5]), the short line approximation can be used. In the short line approximation

the line is modeled as a series connection of a resistor and an inductor [5]. Hence every network of short transmission lines can be modeled as a generalized electrical network with $\nu = 1$, $\mathbf{p}_i = (r_i, \ell_i)$ and $\mathbf{q}_i = (1, 0)$ in (3.1), where r_i is the resistance value of the resistive component of branch i and ℓ_i is the inductance value of the inductive component of branch i. Moreover, if the network is a homogeneous RL circuit, it follows from Corollary 3.2.2 that we can perform Kron reduction. In such models, we would describe loads as possibly nonlinear current sources connected to the internal nodes. This ensures that homogeneity assumption only depends on the characteristics of the line. Our main theorem can be easily generalized to the case in which we have current injections at initial nodes. Therefore we can perform Kron reduction on the power network and the aggregated effect of loads is modeled as current sources connected to the boundary nodes. One can argue that the assumption that allows us to use the short line approximation (sinusoidal voltages and currents) to study electromechanical transients also allows us to use phasors. However, in our framework we do not need to assume sinusoidal waveforms *per se*. As long as the short line approximation can accurately describe the transients in consideration, we can use the reduced model for transient analysis.

CHAPTER 4

Transient Stability Analysis of Power Systems

In this chapter, we introduce generator models, a first principles model and the traditional swing equation model used in the power systems literature. After comparing these two models and showing that the traditional model is a special case of the first principles model, we first review how to perform transient stability analysis using the traditional model. We conclude this section by showing that the transient stability analysis can be performed using the first principles model where the assumptions required in the derivation of the traditional model is lifted.

4.1 Generator Models

In this section, we present a comparison of a first principles model of a synchronous generator and the traditional swing equation model. The results in this section are published in [12, 13, 14]

4.1.1 A First Principles Model

In this section, we derive the equations of motion for a two-pole synchronous generator from first principles. The first step in this derivation is to identify the Hamiltonian, the sum of the kinetic and the potential energy, of a single generator. We then derive a stability condition, using the Hamiltonian as a Lyapunov function, for the synchronous generator when the terminal voltages are known. Although we only consider two-pole synchronous machines, the results in this section can easily be generalized to machines with more than two poles.

4.1.1.1 Mechanical Model

Every synchronous generator consists of two parts: rotor and stator. Several torques act on the rotor shaft and cause the rotor to rotate around its axis. Explicitly, we can write the torque balance equation for the torques acting on the rotor shaft as follows:

$$M\ddot{\theta} + D\dot{\theta} = \tau_m - \tau_e, \tag{4.1}$$

where θ is the rotor angle, M is the moment of inertia of the rotor shaft, D is the damping coefficient, τ_m is the applied mechanical torque and τ_e is the electrical torque. The angular velocity of the rotor shaft is $\omega = \dot{\theta}$. The total kinetic energy of the rotor can be expressed as

$$H_{\text{kinetic}} = \frac{1}{2}M\omega^2.$$

Using the definition of the angular velocity ω, we can write (4.1) in the form

$$\dot{\theta} = \omega, \tag{4.2}$$

$$M\dot{\omega} = -D\omega + \tau_m - \tau_e. \tag{4.3}$$

Remark 4.1.1 *In the classical power systems literature, the torque balance equation* (4.1) *is scaled by* ω. *Defining* $P_m = \omega\tau_m$, $P_e = \omega\tau_e$, $M' = M\omega$, $D' = D\omega$ *and dividing both sides of* (4.1) *by a constant value called rated power, the following set of mechanical equations is obtained:*

$$\dot{\theta} = \omega, \tag{4.4}$$

$$M'\dot{\omega} = -D'\omega + P_m - P_e. \tag{4.5}$$

In these equations, the parameters M' *and* D' *are assumed to be constant, which implies that* ω *is either constant or slowly changing. Equations (4.2) and (4.3) do not require such assumptions on* ω.

4.1.1.2 Electrical Model

There are three identical circuits connected to the stator. These circuits are called *stator windings* and they are labeled with letters a, b and c. There are also windings

connected to the rotor. These winding are called *field windings*. In this work, we consider a synchronous generator with a single field winding. In a cylindrical rotor synchronous generator, which are predominantly used in nuclear and thermal generation units, the aggregated effect of the field windings can be modeled by a single circuit [32]. Hence, the single field winding assumption is reasonable for such generators. We label the single field winding with the letter f. The electrical diagram for the phase-a stator winding is given in Figure 4.2. In this diagram, λ_a

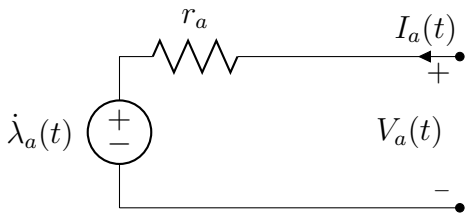

Figure 4.1: Phase-a stator winding

is the flux generated at the phase-a winding, r_a is the winding resistance, V_a is the voltage at the terminals of the winding and I_a is the current *entering* through the positive pole of the winding terminal. The notation we choose for the current is called the *motor notation*. One can obtain the *generator notation* by replacing I_a with $-I_a$. The diagram for the other phases (b and c) and the field winding can be obtained by replacing the subscript a in the diagram with the corresponding letters. From Kirchoff's Voltage Law, we have

$$\dot{\lambda}_a = -r_a I_a + V_a$$

for the phase a winding. The equations for the phases b and c can be obtained by replacing subscript a with b and c, respectively. Since the stator winding circuits are identical, we have $r = r_a = r_b = r_c$. We can write these equations in the vector form

$$\dot{\lambda}_{abc} = -RI_{abc} + V_{abc}, \tag{4.6}$$

where $\lambda_{abc} = (\lambda_a, \lambda_b, \lambda_c, \lambda_f)$, $I_{abc} = (I_a, I_b, I_c, I_f)$, $V_{abc} = (V_a, V_b, V_c, V_f)$ and $R = \mathbf{diag}(r, r, r, r_f)$. In a synchronous generator with a single field winding, we can

relate fluxes and currents using the equation

$$\lambda_{abc} = \mathbb{L}_{abc} I_{abc}, \tag{4.7}$$

where

$$\mathbb{L}_{abc} = \begin{bmatrix} L_s + L_{s0} & -L_{s0} & -L_{s0} & L_{sf}\cos(\theta) \\ -L_{s0} & L_s + L_{s0} & -L_{s0} & L_{sf}\cos\left(\theta - \frac{2\pi}{3}\right) \\ -L_{s0} & -L_{s0} & L_s + L_{s0} & L_{sf}\cos\left(\theta + \frac{2\pi}{3}\right) \\ L_{sf}\cos(\theta) & L_{sf}\cos\left(\theta - \frac{2\pi}{3}\right) & L_{sf}\cos\left(\theta + \frac{2\pi}{3}\right) & L_f \end{bmatrix}.$$

The inductance matrix $\mathbb{L}_{abc}$ is obtained from the inductance matrix in [32, page 273] by neglecting the saliency terms. We can define the total magnetic energy stored in the windings as

$$H_{\text{magnetic}} = \frac{1}{2}\lambda_{abc}^T \mathbb{L}_{abc}^{-1} \lambda_{abc}$$

and express the electrical equation (4.6) using H_{magnetic} as

$$\dot{\lambda}_{abc} = -R\frac{\partial H_{\text{magnetic}}}{\partial \lambda_{abc}} + V_{abc}. \tag{4.8}$$

4.1.2 Port-Hamiltonian Model of a Single Generator

Using the total magnetic energy H_{magnetic} defined in Section 4.1.1.2, we can explicitly compute the electrical torque τ_e in (4.3) as

$$\tau_e = \frac{\partial H_{\text{magnetic}}}{\partial \theta}.$$

The Hamiltonian for the single generator is the sum of the kinetic and magnetic energies, i.e.,

$$H = H_{\text{kinetic}} + H_{\text{magnetic}}.$$

Note that H_{kinetic} does not depend on θ and λ_{abc} and H_{magnetic} does not depend on $M\omega$. Replacing the electrical torque expression in (4.3), the equations (4.2),(4.3) and (4.6) can be written in the form

$$\dot{\theta} = \omega, \tag{4.9}$$

$$M\dot{\omega} = -D\frac{\partial H}{\partial (M\omega)} + \tau_m - \frac{\partial H}{\partial \theta}, \tag{4.10}$$

$$\dot{\lambda}_{abc} = -R\frac{\partial H}{\partial \lambda_{abc}} + V_{abc}. \tag{4.11}$$

If we define the energy variables $\chi = (\theta, M\omega, \lambda_{abc})$ we obtain the port-Hamiltonian representation of equations (4.9)-(4.11) with state χ, input (τ_m, V_{abc}) and:

$$\mathcal{J} - \mathcal{R} = \begin{bmatrix} 0 & 1 & 0_{1\times 4} \\ -1 & -D & 0_{1\times 4} \\ 0_{4\times 1} & 0_{4\times 1} & -R \end{bmatrix}, \quad g_{abc} = \begin{bmatrix} 0 & 0_{1\times 4} \\ 1 & 0_{1\times 4} \\ 0_{4\times 1} & 1_4 \end{bmatrix}.$$

4.1.2.1 Transformation from *abc* Domain to *xyz* Domain and a Simplifying Assumption

Steady state currents and voltages for the *abc* phases of the single generator are sinusoidal waveforms. In order to focus on the simpler problem of stability of equilibrium points, we perform a change of coordinates $T_\theta : \mathbb{R}^4 \to \mathbb{R}^4$ defined by the point-wise linear map

$$T_\theta = \sqrt{\frac{2}{3}} \begin{bmatrix} \cos(\theta) & \cos(\theta - \frac{2\pi}{3}) & \cos(\theta + \frac{2\pi}{3}) & 0 \\ \sin(\theta) & \sin(\theta - \frac{2\pi}{3}) & \sin(\theta + \frac{2\pi}{3}) & 0 \\ \frac{\sqrt{2}}{2} & \frac{\sqrt{2}}{2} & \frac{\sqrt{2}}{2} & 0 \\ 0 & 0 & 0 & \sqrt{\frac{3}{2}} \end{bmatrix}. \tag{4.12}$$

with the inverse $T_\theta^{-1} = T_\theta^T$.

Remark 4.1.2 *In the power systems literature, it is assumed that the generator rotor angles rotate with a speed that is very close to synchronous speed ω_s, i.e., $\dot{\theta} \approx \omega_s$. If we integrate this approximation and assume zero initial conditions, we obtain $\theta = \omega_s t$. When we replace $\theta = \omega_s t$ in* (4.12)*, the upper* 3*-by-*3 *matrix of* (4.12) *becomes a transformation that maps balanced waveforms with frequency ω_s to constant values, also known as Park's transformation [59].*

Using (4.12), we can map *abc*-domain currents $I_{abc} = (I_a, I_b, I_c, I_f)$ to *xyz*-domain currents $I_{xyz} = (I_x, I_y, I_z, I_f) = T_\theta I_{abc}$. Note that the field winding current I_f is not affected by the change of coordinates. We define *xyz*-winding voltages as $V_{xyz} = (V_x, V_y, V_z, V_f) = T_\theta V_{abc}$ and *xyz*-winding fluxes as $\lambda_{xyz} = (\lambda_x, \lambda_y, \lambda_z, \lambda_f) = T_\theta \lambda_{abc}$

in a similar fashion. We obtain the Hamiltonian H in the new coordinates as

$$H = \frac{1}{2}\lambda_{abc}^T \mathbb{L}_{abc}^{-1} \lambda_{abc} + \frac{1}{2} M\omega^2 = \frac{1}{2}\lambda_{xyz}^T \mathbb{L}_{xyz}^{-1} \lambda_{xyz} + \frac{1}{2} M\omega^2,$$

where $\mathbb{L}_{xyz} = \left(T_\theta \mathbb{L}_{abc}^{-1} T_\theta^{-1}\right)^{-1}$ is given by

$$\mathbb{L}_{xyz} = \begin{bmatrix} L_s + 2L_{s0} & 0 & 0 & \sqrt{\frac{3}{2}} L_{sf} \\ 0 & L_s + 2L_{s0} & 0 & 0 \\ 0 & 0 & L_s - L_{s0} & 0 \\ \sqrt{\frac{3}{2}} L_{sf} & 0 & 0 & L_f \end{bmatrix}. \tag{4.13}$$

Equations (4.9)-(4.11) can be written in the xyz-domain as

$$\dot{\theta} = \omega, \tag{4.14}$$

$$\dot{\xi} = \left(\mathcal{J}(\xi) - \mathcal{R}\right) \frac{\partial H}{\partial \xi} + g \begin{bmatrix} \tau_m \\ V_{xyz} \end{bmatrix}, \tag{4.15}$$

where $\xi = (M\omega, \lambda_{xyz})$ and

$$\mathcal{J}(\xi) = \begin{bmatrix} 0 & \lambda_y & -\lambda_x & 0 & 0 \\ -\lambda_y & 0 & 0 & 0 & 0 \\ \lambda_x & 0 & 0 & 0 & 0 \\ 0 & 0 & 0 & 0 & 0 \\ 0 & 0 & 0 & 0 & 0 \end{bmatrix}, \quad g = 1_5.$$

At the desired steady state operation, the fluxes λ_{xyz} are constant and ω is the synchronous velocity ω_s. Therefore, we can safely disregard (4.14) and focus on the stability of the equilibria of (4.15). From the last row of (4.15), we have

$$\dot{\lambda}_f = -r_f I_f + V_f \tag{4.16}$$

which can be expressed in terms of currents as:

$$L_f \dot{I}_f = -\sqrt{\frac{3}{2}} L_{sf} \dot{I}_x - r_f I_f + V_f$$

by using the equality $\lambda_f = \sqrt{\frac{3}{2}} L_{sf} I_x + L_f I_f$ that follows from $\lambda_{xyz} = \mathbb{L}_{xyz} I_{xyz}$. Note that we can always design a control law acting on the field winding terminals by

choosing the voltage V_f according to

$$V_f = \sqrt{\frac{3}{2}} L_{sf} \dot{I}_x + r_f I_f + \alpha \left(I_f - I_f^* \right)$$

for some $\alpha < 0$ and a constant reference value I_f^*. This controller keeps the field current constant and justifies the following assumption:

Assumption 4.1.3 *The field winding current I_f is constant.*

If we use (4.7), and consider the field winding current I_f to be constant, we can express (4.15) in terms of currents:

$$M\dot{\omega} = -D\omega - L_m I_f I_y + \tau_m, \tag{4.17}$$

$$L_{ss}\dot{I}_x = -rI_x - \omega L_{ss} I_y + V_x, \tag{4.18}$$

$$L_{ss}\dot{I}_y = -rI_y + \omega L_{ss} I_x + \omega L_m I_f + V_y, \tag{4.19}$$

$$(L_{ss} - 3L_{s0})\dot{I}_z = -rI_z + V_z, \tag{4.20}$$

where $L_{ss} = L_s + 2L_{s0}$ and $L_m = \sqrt{\frac{3}{2}} L_{sf}$.

4.1.2.2 Equilibria of a Single Generator

In this section, we study the equilibria of a single generator. Recall that sinusoidal waveforms in the *abc* coordinates are mapped to constant values on the *xyz* coordinates. Therefore, equilibria of (4.17)-(4.69) are points rather than sinusoidal trajectories. We can find the equilibrium currents I_x^*, I_y^*, and I_z^* that satisfy (4.18)-(4.69) when the voltages across the generator terminals, V_x, V_y, and V_z, are constant and equal to V_x^*, V_y^*, and V_z^*, respectively, by solving the algebraic equations

$$0 = -rI_x^* - \omega L_{ss} I_y^* + V_x^*, \tag{4.21}$$

$$0 = -rI_y^* + \omega L_{ss} I_x^* + \omega L_m I_f + V_y^*, \tag{4.22}$$

$$0 = -rI_z^* + V_z^*, \tag{4.23}$$

to obtain $I_z^* = \frac{V_z^*}{r}$ and

$$I_x^* = \frac{-\omega^2 L_m L_{ss} I_f - \omega L_{ss} V_y^* + r V_x^*}{r^2 + \omega^2 L_{ss}^2} \tag{4.24}$$

$$I_y^* = \frac{\omega L_{ss} V_x^* + \omega r L_m I_f + r V_y^*}{r^2 + \omega^2 L_{ss}^2}. \tag{4.25}$$

The values of ω are obtained by replacing (4.71) into the algebraic equation obtained by setting $\dot{\omega} = 0$ in (4.17). This results in a third order polynomial equation in ω. For any given $\omega_s \in \mathbb{R}$, if we choose

$$\tau_m^* = L_m I_f \left(\frac{\omega_s L_{ss} V_x^* + \omega_s r L_m I_f + r V_y^*}{r^2 + (\omega_s)^2 L_{ss}^2} \right) + D\omega_s, \tag{4.26}$$

it is easy to show that one of the solutions of $\dot{\omega} = 0$ is $\omega = \omega_s$. Therefore, we can always choose a torque value τ_m such that for any given steady state inputs (V_x^*, V_y^*, V_z^*) and desired synchronous velocity ω_s, one of the solutions of the equations (4.17)–(4.69) is

$$(M\omega, L_{ss} I_x, L_{ss} I_y, L_{ss} I_z) = (M\omega_s, L_{ss} I_x^*, L_{ss} I_y^*, L_{ss} I_z^*), \tag{4.27}$$

with I_x^* and I_y^* given by (4.70) and (4.71), respectively and $I_z^* = \frac{V_z^*}{r}$. Note that, in addition to ω_s, the equation $\dot{\omega} = 0$ has two other solutions. For each solution we potentially have an equilibrium point. Hence, in general we have three equilibrium points. By analyzing the coefficients of the polynomial equation $\dot{\omega} = 0$ it is not difficult to show that the only real solution of $\dot{\omega} = 0$ is ω_s iff

$$-4D^2 r^2 - 4D I_f L_m r \left(I_f L_m + L_{ss} I_x^* \right) + \left(I_f L_m L_{ss} I_y^* \right)^2 < 0, \tag{4.28}$$

where I_x^* and I_y^* are obtained by replacing ω with ω_s in (4.70) and (4.71), respectively. Inequality (4.28) is a necessary condition for global asymptotic stability of the equilibrium ξ^*. In the next section, we obtain sufficient conditions by identifying constraints on the generator parameters that lead to a global Lyapunov function for the equilibrium ξ^*.

4.1.3 Models Derived from the First Principles Model

The simplest model for a synchronous generator, also known as the swing equation model, is described by

$$M'\ddot{\theta} + D'(\dot{\theta} - \omega_s) = \omega_s\tau_m - \omega_s\tau_e = P_m - P_e, \tag{4.29}$$

where $M' = \frac{\omega_s M}{S_{\text{rated}}}$, $D' = \frac{\omega_s D}{S_{\text{rated}}}$, and S_{rated} is the rated power. The constants M, D, θ, τ_m, τ_e, and ω_s are defined as in Section 4.1.1; P_m is the supplied mechanical power, and P_e is the electrical power [59]. In the literature, abusing notation, the constants M' and D' are also referred to as the moment of inertia and the damping coefficient, respectively. We assume, without loss of generality, that $S_{\text{rated}} = 1$ VA. When the supplied mechanical power is equal to the electrical power drawn by the circuit, i.e., the demand is matched by the supply, (4.29) becomes a first order differential equation on the unknown $\omega = \dot{\theta}$ with a single globally asymptotically stable equilibrium point at $\omega = \omega_s$. It is common in the literature to use the relative angle $\delta = \theta - \omega_s t$ instead of the rotor shaft angle θ. At steady state, the relative angular velocity $\dot{\delta} = \dot{\theta} - \omega_s$ is zero.

We can obtain an explicit expression for the electrical power by posing the so-called *constant voltage behind transient reactance* assumption [59]. This assumption essentially states that the phase-a winding of a generator can be thought of as an independent voltage source $E_a(t) = \sqrt{\frac{2}{3}}E\sin(\theta(t))$ in series connection with the winding circuit represented in Figure 4.2. The diagrams for phases-b and c can be obtained by substituting the subscript a with the letters b and c, respectively. Since the winding circuits for all phases are identical, we have $r := r_a = r_b = r_c$ and $\ell = \ell_a = \ell_b = \ell_c$. The phase-$b$ and the phase-c voltages are obtained by introducing the phase differences of $\frac{-2\pi}{3}$ and $\frac{2\pi}{3}$, respectively.

Finally, the electrical power P_e is assumed to be equal to real power. For later use, we denote this assumption by **A1**. In time domain, the real power is defined as

$$P_e = \frac{1}{T}\int_{t-T}^{t} \left(V_a(t)I_a(t) + V_b(t)I_b(t) + V_c(t)I_c(t)\right) dt, \tag{4.30}$$

where $T := \frac{2\pi}{\omega_s}$. Typically, the resistor r and the inductor ℓ are incorporated into

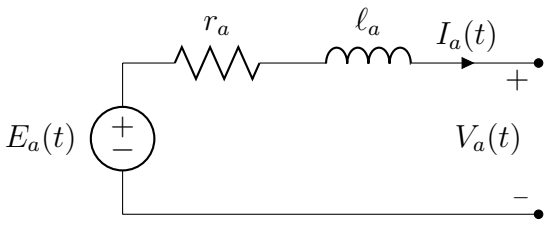

Figure 4.2: Phase-a stator winding

the power grid model and the electrical power is defined as the energy transfer at the port where the voltage behind the transient reactance $E_a(t)$ is connected to this aggregated circuit. In this case, V_i, $i \in \{a, b, c\}$ in (4.30) can be replaced with E_i.

4.1.3.1 Recovering the Swing Equation Model from the First Principles Model

In order to recover the swing equation model from the first principles model, we first assume that the generator has a cylindrical rotor structure (**A2**) and saliency effects are neglected (**A3**). Synchronous generators with cylindrical rotor structure are typically used in nuclear power plants [32] and the validity of Assumption **A3** is considered to be well established in the literature [20]. Under Assumptions **A2** and **A3**, there is a single field winding and the inductance matrix is given by

$$L(\theta) = \begin{bmatrix} L_s + L_{s0} & -L_{s0} & -L_{s0} & L_{sf}\cos(\theta) \\ -L_{s0} & L_s + L_{s0} & -L_{s0} & L_{sf}\cos\left(\theta - \frac{2\pi}{3}\right) \\ -L_{s0} & -L_{s0} & L_s + L_{s0} & L_{sf}\cos\left(\theta + \frac{2\pi}{3}\right) \\ L_{sf}\cos(\theta) & L_{sf}\cos\left(\theta - \frac{2\pi}{3}\right) & L_{sf}\cos\left(\theta + \frac{2\pi}{3}\right) & L_f \end{bmatrix}. \quad (4.31)$$

This matrix is the same inductance matrix in [32, page 273] where we neglect the saliency terms due to Assumption **A3**. We also assume that the field winding current is kept constant by means of a control signal applied to the field winding terminals (**A4**) and the angular velocity is equal to the synchronous velocity (**A5**). Assumptions **A4** and **A5** are used in the power systems in the derivation of traditional generator models [59]. Assumption **A5** implies that on the right hand side of (4.9)-(4.11), we set ω to ω_s.

We define $E = \omega_s\sqrt{\frac{3}{2}}L_{sf}I_f$; and the voltages E_i, $i \in \{a, b, c\}$ are defined as in Section 4.1.3. Under Assumptions **A4** and **A5**, the electrical power in the first principles model can be written as

$$\begin{aligned} P_e &= \frac{\omega_s}{2} I_{abc}^T \frac{\partial L(\theta)}{\partial \theta} I_{abc} \\ &= -\omega_s L_{sf} I_f I_a \sin(\theta) - \omega_s L_{sf} I_f I_b \sin\left(\theta - \frac{2\pi}{3}\right) \\ &\quad - \omega_s L_{sf} I_f I_c \sin\left(\theta + \frac{2\pi}{3}\right) \\ &= -\left(E_a I_a + E_b I_b + E_c I_c\right). \end{aligned} \tag{4.32}$$

Since the currents are in motor direction, we substitute I_i, $i \in \{a, b, c\}$ by $-I_i$ to obtain

$$P_e = (E_a I_a + E_b I_b + E_c I_c) = P_{real} + P_{reactive},$$

where P_{real} is the real power given in (4.30) and P_{reactive} is the reactive power. Here, we note that P_e is the total power exchanged between the generator and the circuit through the stator winding terminals. We obtain the swing equation model by neglecting P_{reactive} due to Assumption **A1** and replacing $P_e = P_{real}$, as given in (4.30), into (4.29).

4.1.3.2 Single-machine Infinite-Bus Power System

By setting the stator winding terminal voltages for phases-a, b and c of a synchronous generator, described by the swing equation model introduced in Section 4.1.3, to

$$V_a = V_\infty \sin(\omega_s t), \tag{4.33}$$

$$V_b = V_\infty \sin\left(\omega_s t - \frac{2\pi}{3}\right), \tag{4.34}$$

$$V_c = V_\infty \sin\left(\omega_s t + \frac{2\pi}{3}\right), \tag{4.35}$$

respectively, we obtain the renowned Single-Machine Infinite-Bus (SMIB) power system. The ideal three-phase voltage source described by (4.33)-(4.35) is called an *infinite bus*, and it represents a power system that is so large, when compared to

a single generator, that its voltage is unaffected by the single generator [59]. By applying Kirchoff's voltage law to the phase-a winding, we obtain

$$E_a = \sqrt{\frac{2}{3}} E \sin(\theta) = r_a I_a + \ell_a \dot{I}_a + V_\infty \sin(\omega_s t). \tag{4.36}$$

We assume $\ell \neq 0$ and $r = 0$, and choose $V_\infty = \sqrt{\frac{2}{3}} E$, $E = \sqrt{\frac{\omega_s \ell P_{\max}}{3}}$, where $P_{\max}$ is the maximum electrical power that can be injected by the generator. By solving (4.36) for I_a, we obtain

$$I_a = \sqrt{\frac{2P_{\max}}{\omega_s \ell}} \sin\left(\frac{\delta}{2}\right) \cos\left(\frac{\delta}{2} + \omega_s t\right),$$

and

$$V_a I_a = \frac{P_{\max}}{3} \left(\sin\delta + \sin(\delta + 2\omega_s t) + \sin(2\omega_s t)\right).$$

Repeating the same arguments, we obtain for phases b and c

$$V_b I_b = \frac{P_{\max}}{3} \left(\sin\delta + \sin\left(\delta + 2\omega_s t - \frac{4\pi}{3}\right) + \sin\left(2\omega_s t - \frac{4\pi}{3}\right)\right),$$

$$V_c I_c = \frac{P_{\max}}{3} \left(\sin\delta + \sin\left(\delta + 2\omega_s t + \frac{4\pi}{3}\right) + \sin\left(2\omega_s t + \frac{4\pi}{3}\right)\right).$$

One can also choose $r \neq 0$; and by properly modifying the constants V_∞ and E, the same expressions can be obtained. Replacing $V_i I_i$ for $i \in \{a, b, c\}$ into (4.30) yields $P_e = P_{\max} \sin\delta$. By substituting the obtained electrical power expression in (4.29), we obtain the SMIB equation

$$M'\ddot{\delta} + D'\dot{\delta} = P_m - P_{\max} \sin\delta. \tag{4.37}$$

4.1.4 Traditional Multi-machine Power System Model

We consider a multi-machine power system with N generators, where the i^{th} generator is modeled by

$$M_i\ddot{\theta} + D_i(\dot{\theta}_i - \omega_s) = P_{m,i} - P_{e,i}. \tag{4.38}$$

It is assumed that for every generator i, we have

$$E_{a,i}(t) = \sqrt{\frac{2}{3}} E_i \sin(\theta_i) = \sqrt{\frac{2}{3}} E_i \sin(\omega_s t + \delta_i), \tag{4.39}$$

for some constant E_i. In a single-input single-output linear circuit, if the input is a sinusoidal waveform, the output is also a sinusoidal with the same frequency. This output sinusoidal is an amplified and phase-shifted version of the input signal [22]. Using this information, if we short-circuit all the ports except port j by setting $E_{a,i} = 0$ for all $i \neq j$, we can compute the current entering to the circuit through port i as

$$\begin{aligned} I_{a,ij}(t) &= \sqrt{\frac{2}{3}} Y_{ij} E_j \sin(\omega_s t + \delta_j + \phi_{ij}) \\ &= \sqrt{\frac{2}{3}} \Bigg(E_j Y_{ij} \cos(\phi_{ij}) \sin(\omega_s t + \delta_j) + E_j Y_{ij} \sin(\phi_{ij}) \cos(\omega_s t + \delta_j) \Bigg). \end{aligned}$$

Defining $G_{ij} = Y_{ij} \cos(\phi_{ij})$ and $B_{ij} = Y_{ij} \sin(\phi_{ij})$, we get

$$I_{a,ij}(t) = \sqrt{\frac{2}{3}} E_j G_{ij} \sin(\omega_s t + \delta_j) + \sqrt{\frac{2}{3}} E_j B_{ij} \cos(\omega_s t + \delta_j). \tag{4.40}$$

We can repeat this procedure for every generator. Since the circuit is linear, we can superpose the solutions (4.40) to obtain the solution for $I_{a,i}$. This is the current entering to the circuit through port i when all the generators are active. From this superposition of solutions, we get

$$I_{a,i}(t) = \sum_{j=1}^{N} I_{a,ij}(t) = \sqrt{\frac{2}{3}} \sum_{j=1}^{N} E_j G_{ij} \sin(\omega_s t + \delta_j) + E_j B_{ij} \cos(\omega_s t + \delta_j). \tag{4.41}$$

We can obtain the current and voltage waveforms for phase b and phase c by adding $\frac{-2\pi}{3}$ and $\frac{2\pi}{3}$ for the phase, respectively. Hence,

$$E_{b,i}(t) = \sqrt{\frac{2}{3}} E_i \sin\left(\theta_i - \frac{2\pi}{3}\right) = \sqrt{\frac{2}{3}} E_i \sin\left(\omega_s t - \frac{2\pi}{3} + \delta_i\right), \tag{4.42}$$

$$E_{c,i}(t) = \sqrt{\frac{2}{3}} E_i \sin\left(\theta_i + \frac{2\pi}{3}\right) = \sqrt{\frac{2}{3}} E_i \sin\left(\omega_s t + \frac{2\pi}{3} + \delta_i\right), \tag{4.43}$$

and

$$I_{b,i}(t) = \sqrt{\frac{2}{3}} \sum_{j=1}^{N} E_j G_{ij} \sin\left(\omega_s t - \frac{2\pi}{3} + \delta_j\right) + E_j B_{ij} \cos\left(\omega_s t - \frac{2\pi}{3} + \delta_i\right), \tag{4.44}$$

$$I_{c,i}(t) = \sqrt{\frac{2}{3}} \sum_{j=1}^{N} E_j G_{ij} \sin\left(\omega_s t + \frac{2\pi}{3} + \delta_j\right) + E_j B_{ij} \cos\left(\omega_s t + \frac{2\pi}{3} + \delta_i\right). \tag{4.45}$$

There is a transformation, called Park transformation [5, 59], that is commonly used in the power systems literature. This transformation takes the waveforms $f_a(t)$ in phase a, $f_b(t)$ in phase b and $f_c(t)$ in phase c and maps them to the so called d-axis (direct axis or positive-sequence), q-axis (quadrature axis or negative-sequence) and 0-axis (zero sequence) variables using the equation

$$\begin{bmatrix} f_d(t) \\ f_q(t) \\ f_0(t) \end{bmatrix} = T \begin{bmatrix} f_a(t) \\ f_b(t) \\ f_c(t) \end{bmatrix} = \sqrt{\frac{2}{3}} \begin{bmatrix} \sin(\omega_s t) & \sin(\omega_s t - \frac{2\pi}{3}) & \sin(\omega_s t + \frac{2\pi}{3}) \\ \cos(\omega_s t) & \cos(\omega_s t - \frac{2\pi}{3}) & \cos(\omega_s t + \frac{2\pi}{3}) \\ \frac{\sqrt{2}}{2} & \frac{\sqrt{2}}{2} & \frac{\sqrt{2}}{2} \end{bmatrix} \begin{bmatrix} f_a(t) \\ f_b(t) \\ f_c(t) \end{bmatrix}. \tag{4.46}$$

The matrix T in (4.46) is invertible, hence we can uniquely construct the phase a, phase b and phase c waveforms from the d-axis, q-axis and 0-axis waveforms. Using the Park transformation (4.46), we compute the d-axis, q-axis and 0-axis voltages and currents as

$$\begin{bmatrix} E_{d,i}(t) \\ E_{q,i}(t) \\ E_{0,i}(t) \end{bmatrix} = T \begin{bmatrix} E_{a,i}(t) \\ E_{b,i}(t) \\ E_{c,i}(t) \end{bmatrix} \qquad \begin{bmatrix} I_{d,i}(t) \\ I_{q,i}(t) \\ I_{0,i}(t) \end{bmatrix} = T \begin{bmatrix} I_{a,i}(t) \\ I_{b,i}(t) \\ I_{c,i}(t) \end{bmatrix}. \tag{4.47}$$

Explicitly, we have

$$E_{d,i} = E_i \cos(\delta_i), \quad E_{q,i} = E_i \sin(\delta_i), \quad E_{0,i} = 0,$$

and

$$I_{d,i}(t) = \sum_{j=1}^{N} E_j G_{ij} \cos(\delta_j) - E_j B_{ij} \sin(\delta_j), \tag{4.48}$$

$$I_{q,i}(t) = \sum_{j=1}^{N} E_j G_{ij} \sin(\delta_j) + E_j B_{ij} \cos(\delta_j), \tag{4.49}$$

$$I_{0,i}(t) = 0. \tag{4.50}$$

We can see that the 0-axis parameters can be neglected, since they are equal to zero. Hence we can represent the voltage and the current variables using the complex numbers defined as

$$\mathbf{E}_i = E_d + jE_q = E_i(\cos(\delta_i) + j\sin(\delta_i)) = E_i \underline{/\delta_i} \tag{4.51}$$

$$\mathbf{I}_i = I_d + jI_q \tag{4.52}$$

The bold variables $\mathbf{E}_i$ and $\mathbf{I}_i$ in (4.51) and (4.52) are renowned *phasor* variables that are currently being used in almost every work in the power systems literature. Moreover, if we define $\mathbf{Y}_{ij} = G_{ij} + jB_{ij}$, it is a simple computation to check that

$$\mathbf{I}_i = \mathbf{Y}_{ij}\mathbf{E}_j$$

This is the i^{th} equation of the current-balance form network equations [59, Chapter 7], where $\mathbf{Y}_{ij}$ is the $(i,j)^{\text{th}}$ element of the bus admittance matrix. At this point, we have recovered the standard equations, and it is clear that we need the assumption (**A1**) for these equations to be well-defined. So far, we have not scaled the equations by rated currents and voltages. However, without loss of generality, we can assume that all the variables are scaled by rated values. Now, we can write the electrical power expression. It is *assumed* that the electrical power is equal to the real power (**A5**). This is expressed as

$$P_{e,i} = \text{Re}\{\mathbf{E}_i^*\mathbf{I}_i\} = E_{d,i}I_{d,i} + E_{q,i}I_{q,i},$$

where $\mathbf{E}_i^*$ is the complex conjugate of the complex number $\mathbf{E}_i$ and Re{.} is an operator returning the real part of a complex number. An equivalent statement for this assumption is the following: the electrical power is equal to the total average power in three phases. This average is computed by integrating the instantaneous power over a time interval of length $2\pi/\omega_s$ and dividing the result by the length of this time interval. Note that this definition also assumes that we have sinusoidal waveforms in all phases. By direct computation, we obtain

$$P_{e,i} = \sum_{j=1}^{N} E_iE_jG_{ij}\cos(\theta_i - \theta_j) + E_iE_jB_{ij}\sin(\theta_i - \theta_j). \tag{4.53}$$

Replacing (4.53) in (4.38) and setting $\theta_i = \omega_s t + \delta_i$, we obtain

$$\dot{\delta}_i = \omega_i - \omega_s, \tag{4.54}$$

$$M_i'\ddot{\delta}_i + D_i'\dot{\delta}_i = P_{m,i} - D_i'\omega_s - \sum_{j=1}^{N} E_iE_jG_{ij}\cos(\delta_i - \delta_j) + E_iE_jB_{ij}\sin(\delta_i - \delta_j). \tag{4.55}$$

Define $\hat{\omega}_i = \omega - \omega_s$. Incorporating the term $D'_i\omega_s$ into the mechanical torque by setting $P'_{m,i} = P_{m,i} + D'_i\omega_s$ and seperating the term in the sum that corresponds to $j = i$, we have

$$\dot{\delta}_i = \hat{\omega}_i, \tag{4.56}$$

$$M'_i\dot{\hat{\omega}}_i + D'_i\hat{\omega}_i = P'_{m,i} - E_{ii}^2 G_{ii} - \sum_{j=1, j\neq i}^{N} E_i E_j G_{ij}\cos(\delta_i - \delta_j) + E_i E_j B_{ij}\sin(\delta_i - \delta_j). \tag{4.57}$$

The equation (4.57) is called the swing equation for multi-machine power systems. The equations (4.56) and (4.57), which assumes (**A1**), are used in the transient stability analysis in the power systems literature.

4.1.5 Comparison between the Derived Models and the First Principles Model

4.1.5.1 Comparing Equilibria of Generator Models

In this section, we study the mismatch in the equilibria of generator models. The existence of such a mismatch provides clear evidence of behavior in the first principles model that cannot be reproduced by the swing equation model. We start with a change of coordinates that simplifies the analysis. We set the terminal voltages V_i, $i \in \{a, b, c\}$ to balanced sinusoidal waveforms, the field winding voltage V_f to a control signal that renders the field winding current constant (Assumption **A4**), and we omit the dynamical equation for the field winding in the rest of this section. The equations for the first principles model under these conditions are

$$\dot{\theta} = \omega \tag{4.58}$$

$$M\dot{\omega} + D(\omega - \omega_s) = \tau_m - \frac{1}{2} I_{abc}^T \frac{\partial L(\theta)}{\partial \theta} I_{abc}, \tag{4.59}$$

$$\dot{\lambda}_{abc} = -RI_{abc} + V_{abc}. \tag{4.60}$$

We can rewrite the equations (4.58)-(4.60) in a form that is simpler to analyze if we perform a change of coordinates by defining $V_{xyz} = T_\theta V_{abc}$, and similarly,

$I_{xyz} = T_\theta I_{abc}$, and $\lambda_{xyz} = T_\theta \lambda_{xyz}$, where

$$T_\theta = \sqrt{\frac{2}{3}} \begin{bmatrix} \cos(\theta) & \cos(\theta - \frac{2\pi}{3}) & \cos(\theta + \frac{2\pi}{3}) & 0 \\ \sin(\theta) & \sin(\theta - \frac{2\pi}{3}) & \sin(\theta + \frac{2\pi}{3}) & 0 \\ \frac{\sqrt{2}}{2} & \frac{\sqrt{2}}{2} & \frac{\sqrt{2}}{2} & 0 \\ 0 & 0 & 0 & \sqrt{\frac{3}{2}} \end{bmatrix},$$

$V_{xyz} = (V_x, V_y, V_z, V_f)$, $V_{xyz} = (V_x, V_y, V_z, V_f)$, and $V_{xyz} = (V_x, V_y, V_z, V_f)$. The transformation T_θ maps a vector of balanced sinusoidals to a point if the angular speed of the rotor angle is constant, i.e., $\dot{\theta} = \omega_s$. In the xyz coordinates, (4.58)-(4.60) become

$$M\dot{\omega} = -D(\omega - \omega_s) + \tau_m - \ell_m I_f I_y, \tag{4.61}$$

$$\ell \dot{I}_x = -rI_x - \omega \ell I_y + V_x, \tag{4.62}$$

$$\ell \dot{I}_y = -rI_y + \omega \ell I_x + \omega \ell_m I_f + V_y, \tag{4.63}$$

$$\ell_z \dot{I}_z = -rI_z + V_z, \tag{4.64}$$

where $0 < \ell_z < \ell$, $\ell_m = \sqrt{\frac{3}{2}} L_{sf}$. Equations (4.61)-(4.64) do not depend on θ. Therefore we can neglect the dynamics of the phase angle θ in xyz coordinates.

Our aim is to compare the equilibria of the SMIB described by

$$\dot{\delta} = \omega - \omega_s \tag{4.65}$$

$$M'\dot{\omega}_2 + D'(\omega - \omega_s) = P_m - P_{e,max} \sin \delta, \tag{4.66}$$

with the equilibria of the first principles model in the xyz coordinates (4.61)-(4.63). This comparison easily generalizes to multi-machine power systems. We can think of a multi-machine power system *in steady state* as a collection of isolated single-machine systems with fixed terminal voltages. These fixed terminal voltage values can be computed from the equilibrium point of the multi-machine power system, and they satisfy all the operational constraints. Finally, the equilibria of the multi-machine power system can be obtained by repeating the steps for the SMIB for each of these individual machines.

4.1.5.2 Equilibria of the First Principles Model

Since in the SMIB model, terminal voltages are set to (4.33)-(4.35), we have to assume that the terminal voltages in the first principles model are also described by (4.33)-(4.35) so that we can compare the equilibria of these two models *under the same terminal voltages*. This assumption implies that the terminal voltages are constant *in the xyz-domain*, i.e., $V_x = V_x^*$, $V_y = V_y^*$ and $V_z = V_z^*$ where V_x^*, V_y^*, and V_z^* are constants. By solving

$$0 = -rI_x^{\omega^*} - \omega^* \ell I_y^{\omega^*} + V_x, \tag{4.67}$$

$$0 = -rI_y^{\omega^*} + \omega^* \ell I_x^{\omega^*} + \omega^* \ell_m I_f + V_y, \tag{4.68}$$

$$0 = -rI_z^{\omega^*} + V_z, \tag{4.69}$$

we obtain the equilibrium currents as a function of the angular velocity ω^*

$$I_x^{\omega^*} = \frac{-(\omega^*)^2 \ell_m \ell I_f - \omega^* \ell V_y^* + rV_x^*}{r^2 + (\omega^* \ell)^2}, \tag{4.70}$$

$$I_y^{\omega^*} = \frac{\omega^* \ell V_x^* + \omega^* r \ell_m I_f + rV_y^*}{r^2 + (\omega^* \ell)^2}, \tag{4.71}$$

and $I_z^{\omega^*} = \frac{V_z^*}{r}$. In order to characterize all the values that the angular velocity can assume, we substitute $I_y = I_y^{\omega^*}$ in (4.61). At equilibrium, the angular velocity ω^* satisfies

$$0 = -D(\omega^* - \omega_s) + \tau_m - \ell_m I_f I_y^{*,\omega^*}. \tag{4.72}$$

The right-hand side of the equation (4.72) defines a third order polynomial on ω^*, and (4.72) has three solutions: $\omega^{*,i}$ for $i \in \{1, 2, 3\}$. We have two distinct cases:

- For a given constant field winding current I_f, we choose the mechanical torque τ_m to be
$$\tau_m = \ell_m I_f \left(\frac{\omega_s \ell V_x^* + \omega_s r \ell_m I_f + rV_y^*}{r^2 + (\omega_s \ell)^2} \right) + D\omega_s. \tag{4.73}$$
- For a given constant mechanical torque τ_m, we solve the algebraic constraint on the field winding current I_f defined by (4.73). Since in any practical scenario, the supplied mechanical torque τ_m will be greater than the mechanical

dissipation $D\omega_s$, it is reasonable to assume that $\tau_m > D\omega_s$. Under this assumption, we have two real solutions for I_f and at least one of these solutions is positive. We choose this solution as the constant field winding current.

In both of the preceding two cases, one of the solutions of (4.72) is $\omega^{*,1} = \omega_s$. Depending on the generator parameters, the other solutions $\omega^{*,2}$ and $\omega^{*,3}$ are either both real or they form a complex conjugate pair. A necessary and sufficient condition for having a unique real solution $\omega^{*,1} = \omega_s$ of (4.72) is given in [13]. In general, we have three equilibrium points: $\xi^{*,i} := (\omega^{*,i}, I^{\omega^{*,i}})$, where

$$I^{\omega^{*,i}} = (I_x^{\omega^{*,i}}, I_y^{\omega^{*,i}}, I_z^{\omega^{*,i}}),$$

for $i \in \{1, 2, 3\}$. However, if there is a unique real solution of (4.72), the points $\xi^{*,2}, \xi^{*,3}$ do not lie in $\mathbb{R}^4$ and therefore, they are not physically meaningful. In this case, we have a unique equilibrium $\xi^{*,1} = (\omega_s, I^{\omega_s})$. In [13], a sufficient condition for the global asymptotic stability of this unique equilibrium is also presented.

4.1.5.3 Equilibria of the SMIB

The SMIB model (4.65)-(4.66) has two equilibrium points if $P_m < P_{max}$: (ω_s, δ_2^*) and $(\omega_s, \pi - \delta_2^*)$, where $\delta_2^* = \arcsin\left(\frac{P_m}{P_{max}}\right)$ and $-\frac{\pi}{2} < \delta_2^* \leq \frac{\pi}{2}$. There exists no equilibrium if $P_m > P_{max}$. If we recall the derivation of the SMIB equations, we can give a physical interpretation to these equilibrium points. The first equilibrium corresponds to the scenario where for the phase-a winding, we have $E_a^{*,1} = \sqrt{\frac{2}{3}} E \sin(\omega_s t + \delta_2^*)$ and $V_a^* = V_\infty \sin(\omega_s t)$. For the second equilibrium, the terminal voltage V_a^* does not change, but the voltage behind the transient is different:

$$E_a^{*,2} = \sqrt{\frac{2}{3}} E \sin(\omega_s t + \pi - \delta_2^*) \neq E_a^{*,1}.$$

The currents leaving the winding can be found by solving the differential equation

$$\ell \dot{I}_a^{*,i} = -r I_a^{*,i} + E_a^{*,i} - V_a^*.$$

for $i \in \{1, 2\}$.

4.1.5.4 Comparison of Equilibria

In this concluding subsection, we compare the equilibria of the SMIB with the equilibria of the first principles model under constant terminal voltages. In the SMIB, the equilibria are computed based on the assumption that the phase-*abc* terminal voltages are balanced sinusoidals. These balanced sinusoidals can be mapped to phase-xyz via the transformation $V_{xyz} = T_\theta V_{abc}$. Here, we emphasize that the transformation T_θ depends on θ. Therefore, we have to apply it twice: once for the equilibrium (ω_s, δ_2^*) and once for the equilibrium $(\omega_s, \pi - \delta_2^*)$. At the first equilibrium point, the phase angle is $\theta^{*,1} = \omega_s t + \delta_2^* + \theta_0$, where θ_0 is an initial angle value that can assumed to be zero without loss of generality. We have

$$V_{xyz}^{*,1} = (V_x^{*,1}, V_y^{*,1}, V_y^{*,1}, V_f) = T_{\theta^{*,1}} V_{abc},$$

where $V_{abc} = (V_a, V_b, V_c, V_f)$ and V_i for $i \in \{a, b, c\}$ are defined as in (4.33)-(4.35). Explicitly,

$$V_x^{*,1} = \sqrt{\frac{3}{2}} V_\infty \sin(\delta_2^*), \quad V_y^{*,1} = -\sqrt{\frac{3}{2}} V_\infty \cos(\delta_2^*),$$

and $V_z^{*,1} = 0$. By setting the terminal voltage of the first principles model to

$$V_{xyz}^{*,1} = (V_x^{*,1}, V_y^{*,1}, V_z^{*,1}),$$

we obtain three equilibrium points following the discussion in Section 4.1.5.2. One of these equilibrium points, (ω_s, I^{ω_s}), represents the equilibrium point (ω_s, δ_2^*) in the SMIB model. The other two points correspond to operating points where the angular velocity is different from ω_s. These points are not visible in the SMIB equations due to the restrictive assumption that is required in the derivation of this model: $\omega = \omega_s$ (Assumption **A4**).

For the second equilibrium point, the phase angle is $\theta^{*,2} = \omega_s t + \pi - \delta_2^*$. Following a similar argument, we obtain

$$V_x^{*,2} = \sqrt{\frac{3}{2}} V_\infty \sin(\pi - \delta_2^*) = \sqrt{\frac{3}{2}} V_\infty \sin(\delta_2^*) = V_x^{*,1},$$

$$V_y^{*,2} = -\sqrt{\frac{3}{2}} V_\infty \cos(\pi - \delta_2^*) = \sqrt{\frac{3}{2}} V_\infty \cos(\delta_2^*) = -V_y^{*,1},$$

and $V_z^{*,2} = 0 = V_z^{*,1}$. Setting the terminal voltage to $V_{xyz}^{*,2} = (V_x^{*,1}, -V_y^{*,1}, V_z^{*,1})$ will yield three new equilibrium points. This time, one of these points represents the equilibrium point $(\omega_s, \pi - \delta_2^*)$ in the first principles model. In summary, if we set the phase-*abc* winding terminal voltages to a balanced set of sinusoidals, the SMIB has two equilibrium points and the first principles model has six equilibrium points, two of which corresponds to the equilibrium points of the SMIB model. Therefore, the SMIB model cannot reproduce all the behaviors of the first principles model due to these additional equilibrium points. One of the goals of the next section is to assess the significance of these missing behaviors.

4.1.5.5 Mismatch in the Behavior of Generator Models

Our aim in this section is to understand: 1) if we can use the swing equation for performing stability analysis of power systems under small oscillations, and 2) if the missing behaviors in the SMIB model due to the mismatch in the equilibria of the generator models are significant. In order to answer the first question, we compare the *theoretical* conclusions predicted by the SMIB model with the behavior observed in the first principles model. The second question is addressed by observing how the SMIB model behaves if the initial state is a point which is an equilibrium point of the first principles model, but not an equilibrium point of the SMIB model.

In [59, Example 9.2], the stability of the equilibrium point of the SMIB described by

$$0.2\ddot{\delta} = 1 - 2\sin\delta - 0.02\dot{\delta} \tag{4.74}$$

is analyzed. The SMIB has two equilibrium points: the stable equilibrium point at $(\delta^*, \omega^* - \omega_s) = (\pi/6, 0)$ and the unstable equilibrium point at $(\pi - \delta^*, \omega^* - \omega_s) = (5\pi/6, 0)$. It has been shown in [59, Example 9.2] that the region of attraction S_{ROA} of the stable equilibrium point is given by

$$S_{\text{ROA}} = \{(\delta, \omega) \in \,]-\pi, 5\pi/6[\times \mathbb{R} \mid V(\delta, \omega) < V(\pi - \delta^*, 0)\},$$

where

$$V(\delta, \omega) = 0.1(\omega - \omega_s)^2 - (\delta - \delta^*) - 2\left(\cos(\delta) - \cos(\delta^*)\right).$$

We showed that the swing equation model is a special case of the first principles model. The parameters for the generator are not provided in [59, Example 9.2]. We use the parameters given in [1, Example 4.1]. The synchronous angular velocity is $\omega_s = 2\pi 60$ rad/s. The parameter ℓ can be found by taking the average of the parameters L_d and L_q in [1, Example 4.1]. The stator winding resistances are neglected, a standard assumption due to the fact that $r \ll \omega_s \ell$. We use the value given in [1, Example 4.1] for the inertia constant M. The field winding current is given as $I_f = 926A$ and ℓ_m in our example is equal to the parameter kM_F in [1, Example 4.1]. The damping coefficient is not provided. In order to be consistent with the SMIB equation (4.74), we choose $D = 0.1M$ and we set $\tau_m = 5M$. With this choice of parameters, (4.61)-(4.63) become

$$0.2\dot{\omega} = -0.02(\omega - \omega_s) + 1 - 4.31 I_y, \tag{4.75}$$

$$\dot{I}_x = -\omega I_y + 160.52 V_x, \tag{4.76}$$

$$\dot{I}_y = \omega I_x + 1.08\omega + 160.52 V_y. \tag{4.77}$$

The terminal voltages of the SMIB in *abc* coordinates are in the form (4.33)-(4.35). If we redefine our reference angle as δ^* and compute the xyz voltages that correspond to the stable equilibrium point using $V^*_{xyz} = T_{\delta^* + \omega_s t} V_{abc}$, we obtain $V^*_x = V_\infty$ and $V^*_y = 0$. The xyz voltages that correspond to the unstable equilibrium point are obtained from $V_{abc} = T_{\pi - \delta^* + \omega_s t} V_{abc}$ as $V^*_x = V_\infty$ and $V^*_y = 0$. The exact value of V^*_x can be computed by solving

$$0 = -0.02(\omega_s - \omega_s) + 1 - 4.31 I^*_y,$$
$$0 = -\omega_s I^*_y + 160.52 V^*_x.$$

We have $I^*_y = 0.232$ and $V^*_x = 0.545$. From

$$0 = \omega I^*_x + 1.08\omega_s,$$

we find $I^*_x = -1.08$. From this discussion, we can see that one of the equilibrium points of (4.61)-(4.63) is $(\omega_s, 0.232, -1.08)$ given the fixed terminal voltages $V^*_x = 0.545$ and $V^*_y = 0$. For the same terminal voltages, the other equilibrium point

is $(0.133\omega_s, 1.74933, -1.08)$. Finally, we note that in the SMIB model, the terminal voltages are sinusoidal in *abc* coordinates, and this does not imply that they stay constant in *xyz* coordinates, since this would require the equality: $\dot{\theta} = \omega_s$. If the angle error is $\Delta\delta = \delta - \delta^*$, using the formula

$$V_{xyz} = T_\theta V_{abc} = T_{\delta+\omega_s t} V_{abc} = T_{\delta+\omega_s t} T^{-1}_{\delta^*+\omega_s t} V^*_{xyz},$$

we can show that the x axis and y axis voltages can be expressed as

$$V_x = V_x^* \cos(\Delta\delta) - V_y^* \sin(\Delta\delta) = V_x^* \cos(\Delta\delta), \tag{4.78}$$

and

$$V_y = V_x^* \sin(\Delta\delta) + V_y^* \cos(\Delta\delta) = V_x^* \sin(\Delta\delta). \tag{4.79}$$

At the stable and unstable equilibrium points of the SMIB, it is easy to verify that we have $V_x = V_x^*$ and $V_y = V_y^* = 0$. Replacing (4.78) and (4.79) into (4.76) and (4.77), respectively, the first principles equations together with the angle dynamics become

$$\dot{\delta} = \omega - \omega_s \tag{4.80}$$

$$0.2\dot{\omega} = -0.02(\omega - \omega_s) + 1 - 4.31 I_y, \tag{4.81}$$

$$\dot{I}_x = -\omega I_y + 87.4689 \ \cos(\delta - \delta^*), \tag{4.82}$$

$$\dot{I}_y = \omega I_x + 1.08\omega + 87.4689 \ \sin(\delta - \delta^*). \tag{4.83}$$

4.1.5.6 Example 1

We now provide a counter-example to the theoretical conclusion obtained from the swing equation model that suggests the stability of the equilibrium point $(\delta^*, \omega^* - \omega_s)$ of the SMIB model. We choose $(\delta_0, \omega_0) = (\frac{\pi}{4}, \omega_s)$ as the initial condition of the SMIB model and $(\delta_0, \omega_0, I_{x,0}, I_{y,0}) = (\frac{\pi}{4}, \omega_s, I_x^*, I_y^*)$ as the initial condition of the first principles model. It is easy to check that $(\delta_0, \omega_0) \in S_{\text{ROA}}$. Therefore, we expect the trajectory in the SMIB simulation to converge to the stable SMIB equilibrium $(\pi/6, \omega_s)$. We also note that the initial angular velocity is ω_s, which is the synchronous velocity. The evolution of the angular velocity according to

the SMIB dynamics and the first principles model dynamics is given in Figure 4.3 and Figure 4.4, respectively. The angular velocity in Figure 4.3 is in the range $[59.85, 60.15]$ Hz. Since the SMIB model is considered to be a valid model to study local oscillations in the range $[59, 61]$ Hz [59, page 215], the conclusions obtained from the simulation of the SMIB model and the first principles model should match.

These plots suggest that the SMIB model concludes stability in scenarios where the corresponding first-principles model exhibits a significantly different behavior. Although the initial angular velocity is the synchronous velocity (60 Hz), the angular velocity of the first principles model steers away from this angular velocity and the generator starts operating at a dangerous regime where the angular velocity is 68 Hz. It is known that the angular velocities above 65 Hz upper limit can cause serious equipment damage, and they may even result in loss of generation [66]. Therefore, this example strongly suggests the usage of first principles models for stability analysis of power systems even under small oscillations.

4.1.5.7 Example 2

It is also possible to construct scenarios in which the SMIB model is unstable whereas the first principles model is stable. We consider the scenario in which the initial conditions of the SMIB model and the first principles model are $(\delta_0, \omega_0) = (\frac{11\pi}{12}, \omega_s)$ and $(\delta_0, \omega_0, I_{x,0}, I_{y,0}) = (\frac{11\pi}{12}, \omega_s, I_x^*, I_y^*)$. We can obtain the damped equations

$$\begin{aligned}
\dot{\delta} &= \omega - \omega_s \\
0.2\dot{\omega} &= -0.02(\omega - \omega_s) + 1 - 4.31 I_y, \\
\dot{I}_x &= -100(I_x - I_x^*) - \omega I_y + 87.4689\ \cos(\delta - \delta^*), \\
\dot{I}_y &= -100(I_y - I_y^*) + \omega I_x + 1.08\omega + 87.4689\ \sin(\delta - \delta^*),
\end{aligned}$$

by introducing a stator resistance $r = 100\ell$ and readjusting the steady state terminal voltages. Although, it is very unlikely to encounter a practical situation in which the stator winding resistances are a hundred times greater than the stator winding inductances, for the sake of showing the possibility of false-negative scenarios in which the SMIB model concludes instability whereas the first principles model is

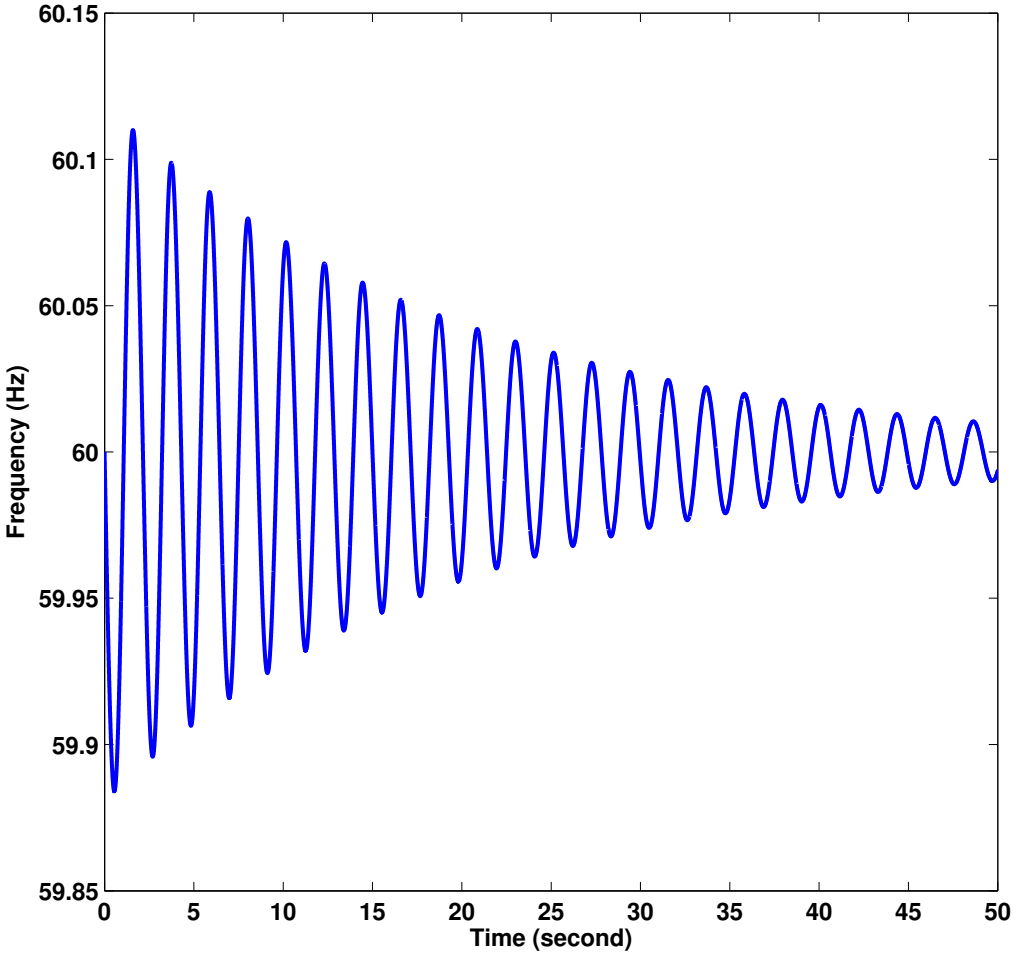

Figure 4.3: Evolution of the SMIB model angular velocity (Example 1).

stable, we neglect this practical issue. The evolution of the angular velocity with respect to SMIB dynamics and first principles dynamics is given in Figure 4.5 and Figure 4.6, respectively. In Figure 4.5, we can observe that the angular velocity does not converge to 68 Hz, but oscillates.

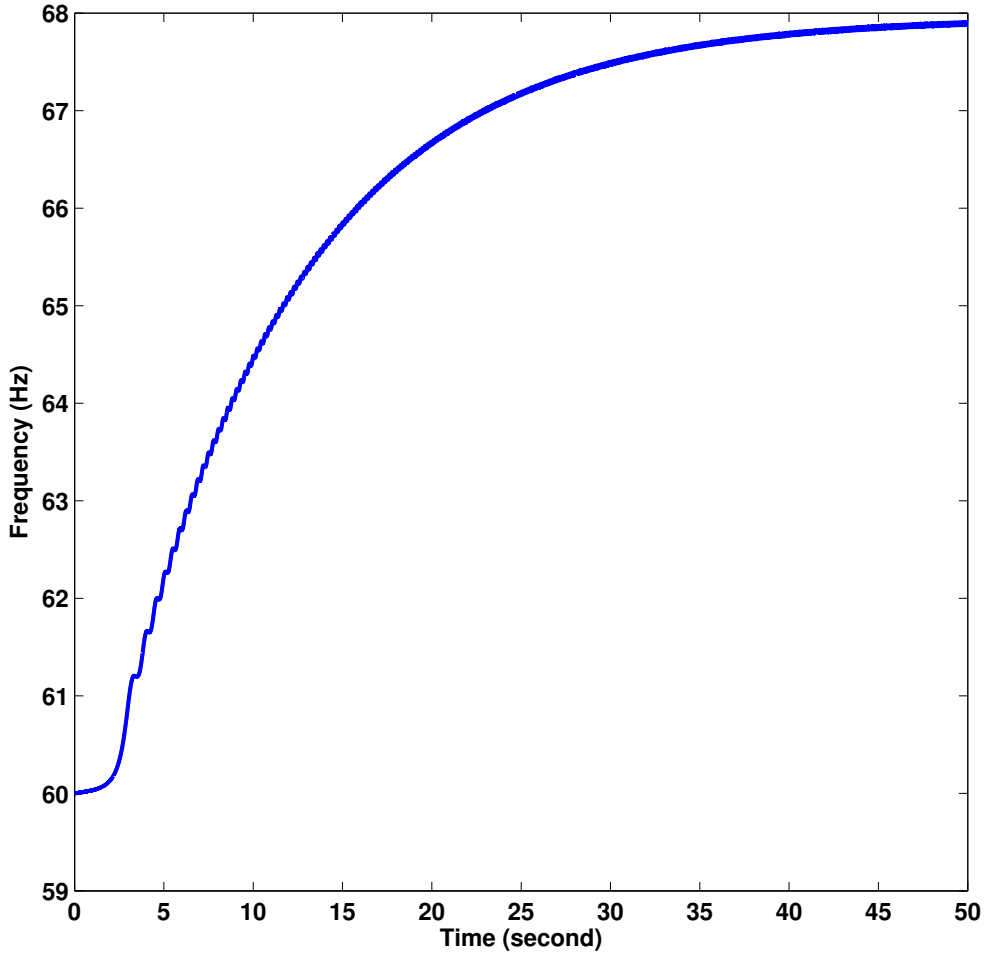

Figure 4.4: Evolution of the first principles model angular velocity (Example 1).

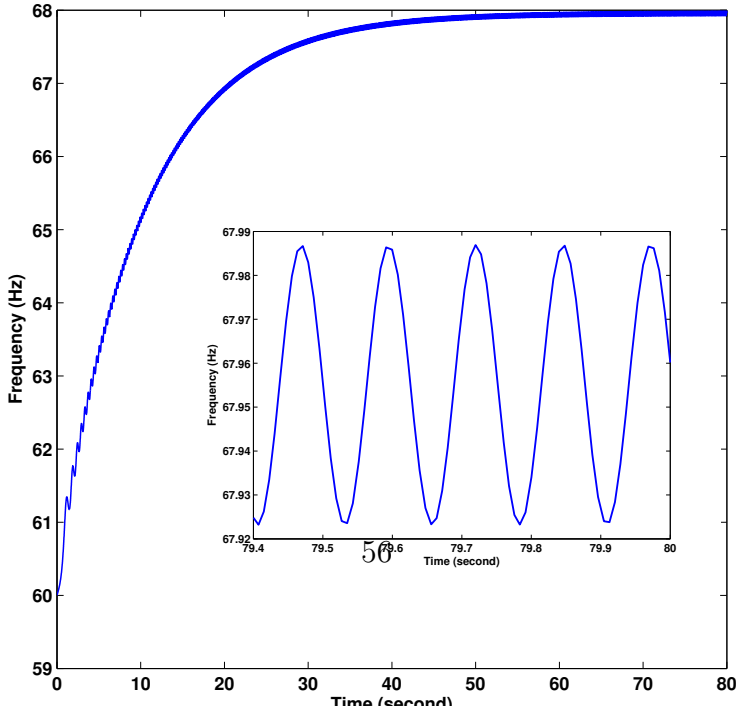

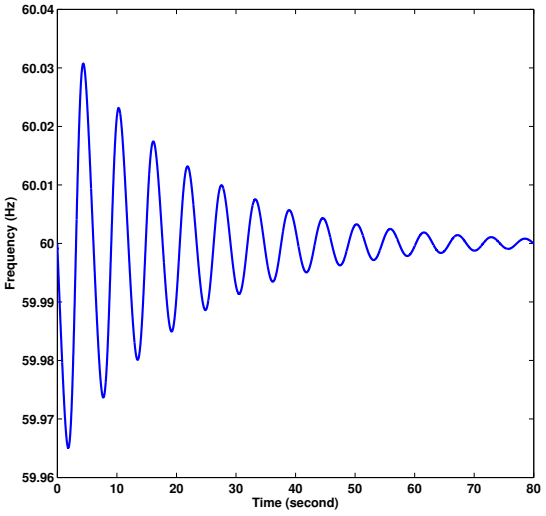

Figure 4.6: Evolution of the first principles model angular velocity (Example 2).

4.1.5.8 Example 3

Finally, we investigate the scenario in which the initial condition of the first principles model is $(\omega_0, I_{x,0}, I_{y,0}) = (0.133\omega_s, 1.74933, -1.08)$. This is one of the equilibrium points of the first principles model. Therefore $\omega(t) = 0.133\omega_s$ for all $t > 0$. The terminal voltages in this scenario are constant in xyz coordinates, i.e., $V_x^* = 0.545$, $V_y^* = 0$ and $V_z^* = 0$. Let $(0.133\omega_s, \delta^*)$ be the initial condition of the SMIB model. For any given δ^*, we expect the angular velocity of the SMIB model to stay constant at $0.133\omega_s$. We choose $\delta^* = \frac{\pi}{6}$. Although ω cannot remain constant in the SMIB model, as $(0.133\omega_s, \delta^*)$ is not an equilibrium point, we ask by how much will the SMIB model differ from the first principle model. The answer is given in Figure 4.7.

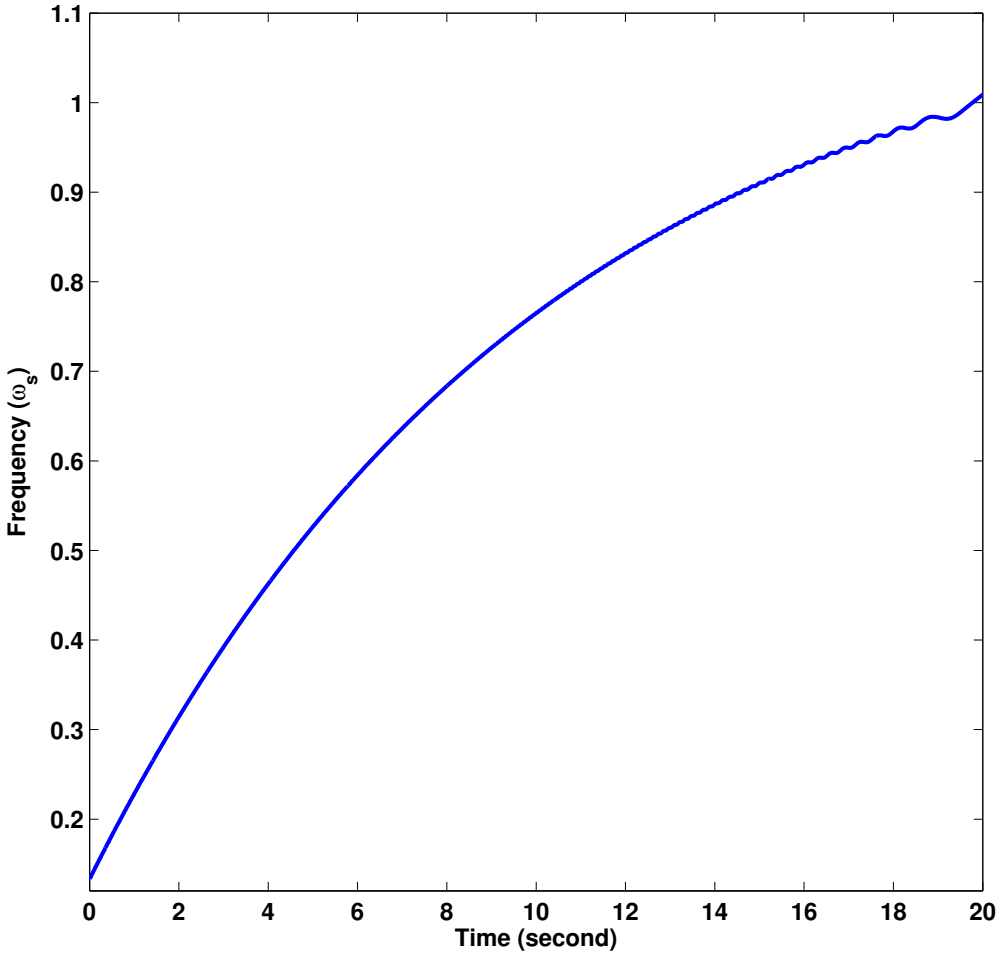

Figure 4.7: Evolution of the SMIB model angular velocity (Example 3).

4.2 Review of Classical Transient Stability Analysis

When power systems are working in normal operating conditions, i.e., in *steady-state*, the generators satisfy two main conditions: 1) their rotors rotate with the same velocity, which is also known as *synchronous velocity*, and 2) the generated voltages are sinusoidal waveforms with the same frequency. Keeping the velocity of the generators at the synchronous velocity and the terminal voltages at the desired levels are called *frequency stability* and *voltage stability*, respectively [40]. When all the generators are rotating with the same velocity, they are synchronized and

the relative differences between the rotor angles remain constant. The ability of a power system to recover and maintain this synchronism is called *rotor angle stability*. *Transient stability*, as defined in [40], is the maintenance of rotor angle stability when the power system is subject to large disturbances. These large disturbances are caused by faults on the power system such as the tripping of a transmission line.

In industry, the most common way of checking transient stability of a power system is to run extensive time-domain simulations for important fault scenarios [54]. This way of developing action plans for the maintenance of transient stability is easy and practical *if* we know all the "important" scenarios that we need to consider. Unfortunately, power systems are large-scale systems and the number of possible scenarios is quite large. Since an exhaustive search of all of these scenarios is impossible, power engineers need to guess the important cases that they need to analyze. These guesses, as made by humans, are prone to errors. Moreover, time-domain simulations do not provide insight for developing control laws that guarantee transient stability [55]. Because of these reasons, additional methods are required for transient stability analysis. Currently, the methods that do not rely on time-domain simulations can be collected in two different groups: direct methods and automatic learning approaches. The latter, automatic learning approaches [75], are based on machine learning techniques. In this work, we do not consider automatic learning approaches and we focus on direct methods.

Direct methods are based on obtaining Lyapunov functions for simple models of power systems [31, 54, 69]. Although in the power systems literature it is considered that Lyapunov-based methods for power systems were introduced in the early sixties, to the best of our knowledge, the origin of the idea can be found in the 1947 paper of Magnusson [46], which uses the concept of "transient energy" which is the sum of kinetic and potential energies, i.e. *Hamiltonian*, to study the stability of power systems. In 1958, Aylett, assuming that a two-machine system can be represented by the dynamical equation

$$\ddot{\theta} = B - \sin(\theta),$$

showed that there exists a separatrix on the two-dimensional plane of $\dot{\theta}$ and θ that

divides the two-dimensional plane into two regions [4]. One of the regions is an invariant set with respect to two-machine system dynamics, i.e., if the initial condition is in this set, trajectories stay inside this set for all future time. Aylett concluded that in order to check the stability of the system, we only need to check whether we are in the invariant set or not. Aylett also characterized the separatrix that defines the invariant set, extended the results from the two-machine case to the three-machine case in the same monograph. Although the term "Lyapunov function" was not stated explicitly in his work, Aylett's work used Lyapunov-based ideas. Some of the other pioneering works on direct methods include Szendy [61], Gless [33, 34], El-Abiad and Nagaphan [29], and Willems [77, 78, 79, 80]. There is a vast literature stemming from these early works, unfortunately without questioning the modeling assumptions. The later works in direct methods mainly focused on finding better Lyapunov functions that work for more detailed models and provide less conservative results. These Lyapunov functions are used for estimating the region of attraction of the stable equilibrium points that correspond to desired operating conditions. The obtained region of attraction estimates are used for reasoning about the stability of the power system after the clearence of a fault. For a detailed summary of these results, we refer the reader to [31, 54, 55, 56, 69]. There are several problematic issues with direct methods.

The first problem is the set of assumptions used to construct these models. The models used for the transient stability analysis implicitly assume that the angular velocity of the generators are very close to the synchronous velocity. In other words, it is assumed that the system is very close to desired equilibrium and the models developed based on this assumption are used to analyze the stability of the same equilibrium. The standard answer given to this objection is the following: the models that are used in transient stability studies are used only for the "first swing" transients and for these transients the angular velocities of the generators are very close to the synchronous velocity. Unfortunately, in real world scenarios this assumption is violated. One example of such violations is the August 14, 2003 blackout in Canada and the Northeast of the United States. As stated in the post-mortem report of

this blackout [66], frequency swings in the later stages of the blackout indicate that the assumption was violated. Using models based on these violated assumptions to analyze cases, like the August 14, 2003 blackout, seems unreasonable.

The second problem is the following: the models used for transient stability analysis, again implicitly, pose certain assumptions on the grid. The transmission lines are modeled as impedances and the loads are either modeled as impedances or as constant current sources. These modeling assumptions are used to eliminate the internal nodes of the network via a procedure called Kron reduction [5, 27]. The resulting network after Kron reduction is a strongly connected network. Every generator is connected every other generator via transmission lines modeled as a series connection of an inductor and a resistor. After this reduction process, the resistances in the reduced grid are neglected. The fundamental reason behind the neglect of the resistances lies in the strong belief, in the power community, about the non-existence of Lyapunov functions when these resistances are not neglected. The idea stems from the paper [17] which asserts the non-existence of global Lyapunov functions for power systems with losses in the reduced power grid. This belief is further supported by the fact that the Lyapunov functions that the power community have developed contain path-dependent terms unless these resistances are neglected. The reader should note that the resistors here represent both the losses on the transmission *and* the loads. Hence this assumption implies that there is no load in the grid (other than the loads modeled as current inductions), which is not a reasonable assumption. In addition to these problems that have their origin in neglecting the resistances of the grid, the process of constructing these reduced grids, i.e. Kron reduction, can only be performed for a very restrictive class of circuits *unless* we assume that all the waveforms in the grid are sinusiodal [10, 11]. In other words, in order to perform this reduction process for arbitrary networks, we need to use phasors, which in turn requires that all the waveforms in the grid are sinusoidals and every generator in the power grid is rotating with the same velocity. This assumption is not compatible with the study of transients.

There were several attempts to address the aforementioned issues. In order to

deal with the unreasonable "zero resistance" assumption, structure-preserving models were suggested by A. R. Bergen and D. Hill in [6]. In the structure-preserving model, instead of incorporating the loads into the reduced network by applying Kron reduction, the loads in the network, which are assumed to be frequency-dependent, are preserved. Since the loads are not absorbed to the reduced grid, the resistances on the grid represent the transmission line losses only. Neglecting the resistances in the reduced grid of the structure-preserving model is less problematic because transmission line losses are considered to be negligible in practice. Lyapunov functions that can be used for direct method studies of the structure-preserving models were also suggested in [65].

Direct method techniques analyze the transient stability of power systems. One can also design control laws that guarantee transient stability for power systems. Despite the long efforts to obtain control laws for power systems with nonnegligible transfer conductances, results only appeared in the beginning of the 21^{st} century. For the single machine and the two machine cases, a solution, under restrictive assumptions, is provided in [53]. In the same work, the existence of globally asymptotically stabilizing controllers for power systems with more than two machines is also proved but no explicit controller is suggested. An extension of the results in [53] to structure preserving models can be found in [23]. To the best of our knowledge, the problem of finding explicit globally asymptotically stabilizing controllers for power systems with nonnegligible transfer conductances and more than two generators has only been recently solved in [15, 16]. The proposed control law requires certain restrictive assumptions such as the uniqueness of equilibria. Although a solution has been offered for an important long-lasting problem, the models that are used in [16] are still the traditional models that we want to avoid in our work.

There are also some recent related results on synchronization of Kuramoto oscillators [25, 26, 28]. If the generators are taken to be *strongly overdamped*, these synchronization results can be used to analyze the synchronization of power networks. The synchronization conditions obtained in [25, 26, 28] can also be used in certain microgrid scenarios [60]. In our work, we provide results that do not require

any assumption on generator's damping. In this section, we explain the fundamental results based on direct methods. We refer the reader to the sources [31, 59, 54, 65, 69] for a more detailed treatment. We first state the assumptions on the equilibrium points of the power system. Then we present an estimate for the region of attraction of the stable equilibrium. This region of attraction estimate is the essence of the results based on direct methods. The method for computing the region of attraction is also introduced in this section.

4.2.1 Unstable Equilibrium Points (UEP)

In this section, we explain the concept of unstable equilibrium point (UEP) of multi-machine power systems. In the power systems literature, including the work related with the transient stability analysis, the system is assumed to have multiple equilibria. This idea has its roots in the ideas reviewed in this section. We consider a multi-machine power system with $N+1$ generators. We use the last generator, generator $N+1$, as a reference generator by assuming $\delta_{N+1} = 0$ and $E_{N+1} = 1$. The dynamical equations for the the reference generator are neglected. We begin by defining $P_i' = P_{m,i}' - E_{ii}^2 G_{ii}$ and assuming $G_{ij} = 0$ for all $j \in 1, \dots N+1$ and $j \neq i$. By setting $G_{ij} = 0$, we neglect the losses in transmission lines *and* loads. With these assumptions, (4.56) and (4.57) can be written as

$$\dot{\delta}_i = \hat{\omega}_i \tag{4.84}$$

$$M_i' \dot{\hat{\omega}}_i + D_i' \hat{\omega}_i = P_i' - \sum_{j=1, j\neq i}^{N+1} E_i E_j B_{ij} \sin(\delta_i - \delta_j) \tag{4.85}$$

At equilibrium, dropping the equations for the reference bus, we have $\hat{\omega}_i = 0$, i.e. $\omega = \omega_s$, for every $i \in \{1, \dots N\}$ and

$$P_i' - \sum_{j=1, j\neq i}^{N+1} E_i E_j B_{ij} \sin(\delta_i - \delta_j) = 0.$$

Since $\delta_{n+1} = 0$, we have N unknowns: δ_i for $i \in \{1, \dots, N\}$. It is *assumed* that the equilibria satisfy $-\pi < \delta_i \leq \pi$. Consider the special case $N+1 = 2$. This is the

case in which a single machine is connected to the infinite bus. In this case,

$$P_1' = E_1 E_2 B_{12} \sin(\delta_1). \tag{4.86}$$

If we have $-P_1' < E_1 E_2 B_{12} < P_1'$, we have two solutions for δ_1. One of the solutions is $\delta_1^1 = \arcsin\left(P_1'/(E_1 E_2 B_{12})\right)$ and the other solution is either $\delta_1^2 = \pi - \delta_1^1$ or $\delta_1^2 = -\pi - \delta_1^1$. Hence we have two equilibrium points: $(0, \delta_1^1)$ and $(0, \delta_1^2)$. One of these equilibrium points is stable and the other one is unstable [69]. Now, consider another special case in which $P_i = 0$ for all $i \in \{1, \ldots, N\}$. We have

$$\sum_{j=1, j\neq i}^{N} E_i E_j B_{ij} \sin(\delta_i - \delta_j) = 0. \tag{4.87}$$

We construct 2^N vectors in $(\delta_1, \ldots, \delta_N) \in (-\pi, \pi]^n$ by picking, for each $i \in 1, \ldots, N$, $\delta_i = 0$ or $\delta_i = \pi$. Each one of these 2^N vectors satisfies (4.87). Hence the (n+1)-tuple elements $(0, v)$, where $v \in (-\pi, \pi]^n$ is one of the constructed 2^N vectors, is an equilibrium point. One of these equilibrium points is a vector of zeros and it is stable. The other $2^N - 1$ equilibrium points are unstable [3, 69]. Based on these special cases, the following statement was conjectured in the power systems literature.

Conjecture 4.2.1 *The multi-machine power system represented by* (4.84), (4.85) *has* 2^N *equilibrium points. One of the equilibrium points* $(0, \delta_1^s, \ldots, \delta_N^s)$ *is stable. Other equilibrium points, different from the stable equilibrium point, are located in one of the small neighborhoods around the points of the form* $(0, \delta_1^u, \ldots, \delta_N^u)$*, where* $\delta_i^u = \delta_i^s$ *or* $\delta_i^u = \pi - \delta_i^s$ *or* $\delta_i^u = -\pi - \delta_i^s$.

We present Conjecture 4.2.1 because, to the best of our knowledge, all the results in the direct methods that we have encountered are based on Conjecture 4.2.1. In the power systems literature, there is no quantification of how "small" the neighborhoods introduced in Conjecture 4.2.1 are. This lack of formalism makes classical direct methods, which are based on Conjecture 4.2.1, imprecise. Estimating these $2^N - 1$ unstable (conjectured) equilibrium points is considered to be one of the most important problems in the transient stability analysis by the power systems community [31]. The compositional analysis in Section 4.3 does not require Conjecture 4.2.1 to hold.

4.2.2 Region of Attraction of the Stable Equilibrium Point

Let $x = (\hat{\omega}, \delta_1, \ldots, \delta_N) \in \mathbb{R}^n \times \mathbb{S}^n$. By Conjecture 4.2.1, there exists a stable equilibrium point $x^s = (0, \delta_1^s, \ldots, \delta_N^s)$ for the multi-machine power system described by the equations (4.84) and (4.85). Let $\xi(x_0, t)$ be the solution of (4.84) and (4.85) with initial condition $x_0 \in \mathbb{R}^n \times \mathbb{S}^n$.

Definition 4.2.2 *The region of attraction of the equilibrium point x^s of* (4.84), (4.85) *is the set*

$$A = \{x_0 \in \mathbb{R}^n \times \mathbb{S}^n \mid \lim_{t\to\infty} \xi(x_0, t) = x^s\}$$

We define the smooth function $V : \mathbb{R}^n \times \mathbb{S}^n \to \mathbb{R}$ as:

$$V(x) = \frac{1}{2}\sum_{i=1}^{N} M_i'\hat{\omega}_i^2 - \sum_{i=1}^{N}(\delta_i - \delta_i^s)P_i' - \sum_{i\neq j}^{N+1} E_i E_j B_{ij}\Big(\cos(\delta_i - \delta_j) - \cos(\delta_i^s - \delta_j^s)\Big). \quad (4.88)$$

It is easy to check that $V(x^s) = 0$ and $\frac{d}{dt}V(x) = -\sum_{i=1}^{N} D_i\hat{\omega}_i^2$. Following theorem is a restatement of [65, Theorem 5.2].

Theorem 4.2.3 *Let x^s be the stable equilibrium point. Define $A_v = \{x \in \mathcal{M} \mid V(x) < v\}$. Let $\bar{v}$ be the smallest positive real number such that there exists an unstable equilibrium point $x^u \in \partial A_{\bar{v}}$, where $\partial A_{\bar{v}}$ is the boundary of $A_{\bar{v}}$. Then $A_{\bar{v}} \subseteq A$.*

Assuming that Conjecture 4.2.1 is true, let U be the set of all $2^n - 1$ unstable equilibrium points. Define

$$x^{uc} = \text{argmin}_{x^u \in U} V(x^u). \quad (4.89)$$

This unstable equilibrium point x^{uc} is called *the controlling unstable equilibrium point* [31]. The following result follows from Theorem 2.3.

Corollary 4.2.4 *The set $\{x_0 \in \mathbb{R}^n \times \mathbb{S}^n \mid V(x_0) < V(x^{uc})\} \subseteq A$ is an estimate of the region of attraction of the stable equilibrium point x^s.*

In practice, these results are applied in the following manner. First, it is assumed that Conjecture 4.2.1 is true. Then, we use a numerical method, such as Newton's

method, to determine the unstable equilibrium points [69]. Conjecture 4.2.1 assumes that the actual unstable equilibrium points are located in small neighborhoods around $2^N - 1$ points and these $2^N - 1$ points are also specified. If Conjecture 4.2.1 is true, and we give one of these points as an initial condition to Newton's method, then the algorithm should converge to the corresponding unstable equilibrium point which is assumed to be located in a small neighborhood around the selected initial point. Note that Conjecture 4.2.1 assumes that the number of unstable equilibrium points is $2^N - 1$, hence the complexity of this step is exponentially increasing with the number of machines in the system. Once all the unstable equilibrium points are determined, the controlling unstable equilibrium is computed from (4.89). Using Corollary 4.2.4, the region of attraction of the stable equilibrium point can be estimated. Several ad-hoc methods have been suggested to approximate the region of attraction without checking all the unstable equilibrium points [59, Chapter 9]. The aim of these methods is to reduce the complexity of obtaining unstable equilibrium points. Unfortunately, none of the methods that we are aware of, including the "Potential Energy Boundary Surface" method that approximates the power system as a nearly Hamiltonian system [74], has a theoretical justification. We refer the readers interested in these methods to [31, 69].

The region of attraction estimation is followed by the simulation of the fault. After the fault is cleared, if the state is inside the estimated region of attraction, then the state will converge to the stable equilibrium point. One can also find an estimate for the critical clearing time by simulating the fault and computing the value of the function V, defined in (4.88), during the simulation. If at some time instance τ, the value of the function V is equal to $V(x^{uc})$, then τ is an estimate for the actual critical clearing time. If the fault is cleared by the estimate critical clearing time, the state of the system will converge to the stable equilibrium point after the fault is cleared [59]. We want to emphasize at this point that the region of attraction estimate in Corollary 4.2.4, is a conservative estimate [69] and based on Conjecture 4.2.1 being true.

4.2.3 Extensions

In Section 4.2.1, we assumed that $G_{ij} = 0$ in the swing equation (4.57). Since these G_{ij} terms represent resistive components of both the transmission lines and the loads, this implies that on average, there is no power dissipation at the loads. This is not a reasonable assumption. In order to address this limitation, a structure-preserving model is suggested in [6]. In this model, instead of treating loads and transmission lines as a single linear electrical circuit, the loads are preserved in the system and they are modeled separately as generators with $M_i = 0$. In the swing equation (4.57), if we replace $N + 1$ by $N + M + 1$ and set $M_i = 0$ for $i = N + 1, \ldots, M$, we obtain the structure preserving model presented in [6]. A Lyapunov function for direct-method studies is also provided in the same work. Different Lyapunov functions for the structure-preserving model are also suggested in [43]

Another limitation is the exclusion of the reactive power demand. When we derived the swing equation, we used the equation

$$P_{e,i} = \mathrm{Re}\{\mathbf{E}_i^* \mathbf{I}_i\} = E_{d,i} I_{d,i} + E_{q,i} I_{q,i},$$

to relate the electrical power in the mechanical equation for generator i with the electrical variables. The meaning of this equation is the following: electrical power is equal to the average power in one cycle of oscillation. However, this is not the whole picture. One can also define the reactive power for generator i as

$$Q_{e,i} = \mathrm{Im}\{\mathbf{E}_i^* \mathbf{I}_i\}.$$

The time-domain interpretation of this concept is not as obvious as the real power. One can think the reactive power as a concept that represents the gap between the average power and the instantaneous power or as a quantity that represents the power fluctuating between the generator and the grid. In [50], an additional set of equations that model the reactive power demand at the loads is introduced. In a relatively new paper, a different set of results is suggested by R. J. Davy and I. A. Hiskens in [8] that are using dynamic load models, introduced by D. J. Hill in [44].

The constant E_i assumption was relaxed by the more detailed models suggested in [7, 65]. A general procedure for constructing analytical Lyapunov functions is presented in [18]. There are other results for obtaining better estimates for the region of stability and constructing Lyapunov functions via iterative processes. These ad-hoc methods will not be covered in this section. We refer the reader to [31, 69] and the 2013 paper of M. Anghel, F. Milano and A. Papachristodoulou [2].

4.3 Compositional Transient Stability Analysis

In this section, we provide sufficient conditions for the equilibrium point computed in Section 4.1.2.2 to be globally asymptotically stable. All the previously described methods use classical models for power systems. They are only valid when the generator velocities are very close to the synchronous velocity. In this section, we abandon these models and use port-Hamiltonian systems [70] to model power systems from first principles. As already suggested in [62], a power system can be represented as the interconnection of individual port-Hamiltonian systems. There are several advantages of this approach. First of all, we have a clear understanding of how energy is moving between components. Secondly, we do not need to use phasors. Thirdly, we do not need to assume all the generator velocities to be close to the synchronous velocity. Finally, using the properties of port-Hamiltonian systems, we can easily obtain the Hamiltonian of the interconnected system, which is a natural candidate for a Lyapunov function. A similar framework, based on passivity, is being used in a research project on the synchronization of oscillators with applications to networks of high-power electronic inverters [64].

We first obtain transient stability conditions for generators in isolation from a power system. These conditions show that as long as we have enough dissipation, there will be no loss of synchronization. In [62] the port Hamiltonian framework is also used to derive sufficient conditions for the stability of a single generator. The techniques used in [62] rely on certain integrability assumptions that require the stator winding resistance to be zero. In contrast, our results hold for non-zero

stator resistances. Moreover, while in [62] it is assumed that synchronous generators have a single equilibrium, we show in this paper that generators have, in general, 3 equilibria and offer necessary and sufficient conditions on the generator parameters for the existence of a single equilibrium. With the help of useful properties of port-Hamiltonian systems, we obtain sufficient conditions for the transient stability of the interconnected power system from the individual transient stability conditions for the generators.

4.3.1 Stability of a Single Generator

A natural choice for Lyapunov function candidate is the Hamiltonian H of the single generator. However the minimum of H occurs at the origin instead of $\xi^* = (M\omega_s, \lambda^*_{xyz})$, where $\lambda^*_{xyz} = \mathbb{L}_{xyz} I^*_{xyz}$. We shift the minimum of the Hamiltonian to ξ^* by defining a function we call the *shifted Hamiltonian*. Explicitly, the shifted Hamiltonian is given as

$$\hat{H} = \frac{1}{2}\left(\lambda_{xyz} - \lambda^*_{xyz}\right)^T \mathbb{L}^{-1}_{xyz}\left(\lambda_{xyz} - \lambda^*_{xyz}\right) + \frac{1}{2}M\left(\omega - \omega_s\right)^2. \tag{4.90}$$

We also define the shifted state by $\hat{\xi} = \xi - \xi^*$. It is easy to check that we have

$$\frac{\partial \hat{H}}{\partial \hat{\xi}} = \frac{\partial H}{\partial \xi} - \frac{\partial H}{\partial \xi}\Big|_{\xi^*}. \tag{4.91}$$

where $\frac{\partial H}{\partial \xi}\Big|_{\xi^*}$ is the gradient of the Hamiltonian H with respect to ξ, evaluated at $\xi = \xi^*$. Note that $\hat{H}$ is positive definite and $\hat{H} = 0$ implies $\hat{\xi} = 0$, which in turn implies $\xi = \xi^*$. Therefore, in order to prove that ξ^* is globally asymptotically stable, it is enough to show that $\frac{d\hat{H}}{dt} < 0$. The time derivative of ξ^* is given by

$$\frac{d}{dt}\xi^* = 0 = \left(\mathcal{J}(\xi^*) - \mathcal{R}\right)\frac{\partial H}{\partial \xi}\Big|_{\xi^*} + g\begin{bmatrix} \tau^*_m \\ V^*_{xyz} \end{bmatrix}, \tag{4.92}$$

From equation (4.15) and $V_{xyz} = V^*_{xyz}$, we obtain

$$\begin{aligned}
\dot{\xi} = \dot{\hat{\xi}} &= (\mathcal{J}(\xi) - \mathcal{R})\frac{\partial H}{\partial \xi} + g \begin{bmatrix} \tau^*_m \\ V_{xyz} \end{bmatrix} \\
&= (\mathcal{J}(\xi^*) + \mathcal{J}(\hat{\xi}) - \mathcal{R}) \left(\frac{\partial \hat{H}}{\partial \hat{\xi}} + \frac{\partial H}{\partial \xi}\Big|_{\xi^*} \right) + g \begin{bmatrix} \tau^*_m \\ V_{xyz} \end{bmatrix} \\
&= \left((\mathcal{J}(\xi^*) - \mathcal{R})\frac{\partial H}{\partial \xi}\Big|_{\xi^*} + g \begin{bmatrix} \tau^*_m \\ V^*_{xyz} \end{bmatrix} \right) \\
&\quad + \mathcal{J}(\hat{\xi})\frac{\partial H}{\partial \xi}\Big|_{\xi^*} + (\mathcal{J}(\xi^*) + \mathcal{J}(\hat{\xi}) - \mathcal{R})\frac{\partial \hat{H}}{\partial \hat{\xi}} + g \begin{bmatrix} 0 \\ \hat{V}_{xyz} \end{bmatrix}. \qquad (4.93)
\end{aligned}$$

where $\hat{V}_{xyz} = V_{xyz} - V^*_{xyz}$ and we used the equality $\mathcal{J}(\xi) = \mathcal{J}(\xi^*) + \mathcal{J}(\hat{\xi})$. From (4.92), we know that the term inside parentheses in (4.93) is equal to zero. Hence (4.93) implies

$$\dot{\hat{\xi}} = \mathcal{J}(\hat{\xi})\frac{\partial H}{\partial \xi}\Big|_{\xi^*} + (\mathcal{J}(\xi^*) + \mathcal{J}(\hat{\xi}) - \mathcal{R})\frac{\partial \hat{H}}{\partial \hat{\xi}} + g \begin{bmatrix} 0 \\ \hat{V}_{xyz} \end{bmatrix}. \qquad (4.94)$$

Taking the time derivative of the shifted Hamiltonian $\hat{H}$, we get

$$\frac{d\hat{H}}{dt} = \frac{\partial \hat{H}}{\partial \hat{\xi}}^T \dot{\hat{\xi}} = \frac{\partial \hat{H}}{\partial \hat{\xi}}^T \mathcal{J}(\hat{\xi})\frac{\partial H}{\partial \xi}\Big|_{\xi^*} - \frac{\partial \hat{H}}{\partial \hat{\xi}}^T \mathcal{R}\frac{\partial \hat{H}}{\partial \hat{\xi}} + \hat{V}^T_{xyz}\hat{I}_{xyz} \qquad (4.95)$$

where $\hat{I}_{xyz} = I_{xyz} - I^*_{xyz}$. Note that the last element of $\hat{I}_{xyz}$ is zero since a constant field winding current implies $\hat{I}_f = I_f - I^*_f = 0$. We can write the first term in the right-hand side of (4.95) as a quadratic function of $\frac{\partial \hat{H}}{\partial \hat{\xi}}$. Explicitly,

$$\begin{aligned}
&\frac{\partial \hat{H}}{\partial \hat{\xi}}^T J(\hat{\xi})\frac{\partial H}{\partial \xi}\Big|_{\xi^*} = \hat{\omega}\hat{\lambda}_y I^*_x - \hat{\omega}\hat{\lambda}_x I^*_y + \omega_s \left(\hat{\lambda}_x \hat{I}_y - \hat{\lambda}_y \hat{I}_x \right). \\
&= \hat{\omega}\hat{I}_y L_{ss} I^*_x - \hat{\omega}\hat{I}_x L_{ss} I^*_y \\
&= \frac{\partial \hat{H}}{\partial \hat{\xi}}^T \begin{bmatrix} 0 & -\frac{1}{2}L_{ss}I^*_y & \frac{1}{2}L_{ss}I^*_x & 0 & 0 \\ -\frac{1}{2}L_{ss}I^*_y & 0 & 0 & 0 & 0 \\ \frac{1}{2}L_{ss}I^*_x & 0 & 0 & 0 & 0 \\ 0 & 0 & 0 & 0 & 0 \\ 0 & 0 & 0 & 0 & 0 \end{bmatrix} \frac{\partial \hat{H}}{\partial \hat{\xi}}. \qquad (4.96)
\end{aligned}$$

where we used $\hat{\lambda}_{xyz} = \mathbb{L}_{xyz}\hat{I}_{xyz}$ to eliminate the flux variables. Replacing (4.96) in (4.95), we obtain

$$\frac{d\hat{H}}{dt} = \frac{\partial \hat{H}}{\partial \hat{\xi}}^T \mathcal{P} \frac{\partial \hat{H}}{\partial \hat{\xi}} + \hat{V}_{xyz}^T \hat{I}_{xyz}, \tag{4.97}$$

where

$$\mathcal{P} = \begin{bmatrix} -D & -\frac{1}{2}L_{ss}I_y^* & \frac{1}{2}L_{ss}I_x^* & 0 & 0 \\ -\frac{1}{2}L_{ss}I_y^* & -r & 0 & 0 & 0 \\ \frac{1}{2}L_{ss}I_x^* & 0 & -r & 0 & 0 \\ 0 & 0 & 0 & -r & 0 \\ 0 & 0 & 0 & 0 & -r_f \end{bmatrix}. \tag{4.98}$$

The eigenvalues of the matrix $\mathcal{P}$ are $\lambda_1 = -r_f$, $\lambda_2 = \lambda_3 = -r$ and

$$\lambda_{4,5} = -\frac{D+r}{2} \pm \frac{\sqrt{D^2 - 2Dr + r^2 + (L_{ss}I_x^*)^2 + (L_{ss}I_y^*)^2}}{2}.$$

Since we have $V_{xyz} = V_{xyz}^*$, i.e. $\hat{V}_{xyz} = 0$, if $\mathcal{P}$ is negative definite, then $\frac{d\hat{H}}{dt} < 0$. It is easy to check that if

$$(L_{ss}I_x^*)^2 + (L_{ss}I_y^*)^2 < 4Dr. \tag{4.99}$$

holds, then $\lambda_{4,5} < 0$, which implies that the matrix $\mathcal{P}$ in (4.97) is negative definite. Hence, if (4.104) holds, we have $\frac{d\hat{H}}{dt} < 0$, which in turn implies that ξ^* is globally asymptotically stable. We can summarize the preceding discussion in the following result.

Theorem 4.3.1 *Let ξ^* be an equilibrium point of the single generator, described by equation* (4.15) *when we have $\tau_m = \tau_m^*$ and $V_{xyz} = V_{xyz}^*$. The equilibrium point ξ^* is globally asymptotically stable if*

$$(L_{ss}I_x^*)^2 + (L_{ss}I_y^*)^2 < 4Dr. \tag{4.100}$$

It is useful to express inequality (4.100) in terms of d-axis and q-axis currents. We know that the x-axis and y-axis currents are different from the traditional d-axis and q-axis currents during the transient stage. However, we have $(I_x^*)^2 + (I_y^*)^2 = (I_d^*)^2 + (I_q^*)^2$ at equilibrium. Thus, we can replace (4.100) with

$(L_{ss}I_d^*)^2 + (L_{ss}I_q^*)^2 < 4Dr$. Note that we are using motor reference directions. In order to find the generator currents, we need to replace I_x^* and I_y^* by $-I_x^*$ and $-I_y^*$, respectively. However, this change in reference directions does not effect (4.100). Condition (4.100) relates the total magnetic energy stored on the generator windings at steady state (left hand side of (4.100)) to the dissipation terms D and r. This relation gives us a set of admissible steady-state currents in xy-coordinates (or alternatively, dq-coordinates) that lead to global asymptotical stability.

Remark 4.3.2 *One can verify that if inequality* (4.100) *holds, then inequality* (4.28) *also holds while the converse is not true. This is to be excepted since global asymptotical stability requires a unique equilibrium.*

Remark 4.3.3 *In the single machine infinite bus scenario, a generator is connected to an infinite bus modeling the power grid as a constant voltage source. The analysis of the single machine in this section, which is based on the assumption that the terminal voltages are constant, can also be seen as the analysis of a single machine connected to an infinite bus. In the classical analysis of this scenario [1], there are multiple equilibrium points and energy based conditions for local stability are obtained. The analysis in this section shows that in fact a single equilibrium exists, under certain assumptions on the generator parameters, and that global asymptotical stability is also possible. Such conclusions are not possible to obtain using the classical models as they are not detailed enough.*

Inequality (4.100) is a sufficient condition for asymptotic stability. Typically, the stator winding resistance r is small and inequality (4.100) is only satisfied for small steady state currents. However, inequality (4.100) can be enforced by actively controlling the voltage at the generator terminals using a static synchronous series compensator (SSSC), a FACTS device that is typically used for series compensation

[37] of real and reactive power. Using a SSSC we can introduce voltage drops of

$$V_{FACTS,x} = R\left(I_x - I_x^*\right), \tag{4.101}$$

$$V_{FACTS,y} = R\left(I_y - I_y^*\right), \tag{4.102}$$

$$V_{FACTS,z} = R\left(I_z - I_z^*\right), \tag{4.103}$$

at the generator terminals without altering the current. The turn-on and turn-off times for the thyristors in a SSSC are at the level of microseconds [37], small enough to enforce a voltage drop that is a piece-wise constant approximation of $R\left(I_x - I_x^*\right)$, $R\left(I_y - I_y^*\right)$, and $R\left(I_z - I_z^*\right)$. The approximation error can always be reduced by increasing the number of converter valves in the SSSC. By repeating the stability analysis in this section, while taking into consideration the voltage drops (4.101)-(4.103), we arrive at the relaxed condition for global asymptotic stability:

$$\left(L_{ss}I_x^*\right)^2 + \left(L_{ss}I_y^*\right)^2 < 4D\left(r + R\right). \tag{4.104}$$

Since the power throughput of SSSC devices is in the order of megawatts [37] we can choose a value for R that is several order of magnitude larger than r_i. Therefore, the relaxed inequality (4.104) allows for large steady-state currents and is widely applicable to realistic examples. The following theorem summarizes this discussion.

Theorem 4.3.4 *Let ξ^* be an equilibrium point of the single generator, described by equation* (4.15) *when we have $\tau_m = \tau_m^*$ and $V_{xyz} = V_{xyz}^*$, and let* (4.101)-(4.103) *be the voltage drops introduced by the SSSC controller. The equilibrium point ξ^* is globally asymptotically stable if*

$$\left(L_{ss}I_x^*\right)^2 + \left(L_{ss}I_y^*\right)^2 < 4D(r + R). \tag{4.105}$$

It is assumed that $V_{xyz} = V_{xyz}^*$ in both Theorems 4.3.1 and 4.3.4. We can replace this assumption with $V_{abc} = V_{abc}^*$ by modifying the voltage drops (4.101)-(4.103) introduced by the SSSC device to

$$V_{drop,x} = R\left(I_x - I_x^*\right) + V_{cx}, \tag{4.106}$$

$$V_{drop,y} = R\left(I_y - I_y^*\right) + V_{cy}, \tag{4.107}$$

$$V_{drop,z} = R\left(I_z - I_z^*\right) + V_{cz}, \tag{4.108}$$

where

$$\begin{bmatrix} V_{cx} \\ V_{cy} \\ V_{cz} \end{bmatrix} = V^*_{xyz} - T^T_\theta V^*_{abc}, \tag{4.109}$$

and by introducing a current drop using a static synchronous compensator (STATCOM) device, where the current drops are given by

$$\begin{bmatrix} I_{drop,x} \\ I_{drop,y} \\ I_{drop,z} \end{bmatrix} = I^*_{xyz} - T^T_\theta I^*_{abc}. \tag{4.110}$$

By repeating the stability analysis in this section, while taking into consideration the voltage and current drops given by (4.109) and (4.110), respectively, we conclude that

$$\frac{d\hat{H}}{dt} = \frac{\partial \hat{H}}{\partial \hat{\xi}}^T \mathcal{P} \frac{\partial \hat{H}}{\partial \hat{\xi}} + \hat{V}^T_{abc}\hat{I}_{abc}, \tag{4.111}$$

where the matrix $\mathcal{P}$ is negative-definite if (4.104) holds. This discussion is summarized in the following theorem.

Theorem 4.3.5 *Let ξ^* be an equilibrium point of the single generator, described by equation* (4.15) *when we have $\tau_m = \tau^*_m$ and $V_{abc} = V^*_{abc}$. Let* (4.109) *and* (4.110) *be the voltage and current drops introduced by the FACTS controllers, respectively. The equilibrium point ξ^* is globally asymptotically stable if*

$$(L_{ss}I^*_x)^2 + (L_{ss}I^*_y)^2 < 4D(r + R). \tag{4.112}$$

4.3.2 Stability Analysis of Multi-Machine Power Systems

4.3.2.1 Multi-Machine Power System Model

We consider a multi-machine power system consisting of N generators, M loads and a transmission grid connecting the generators and the loads. We distinguish between different generators by labeling each variable in the generator model with the subscript $i \in \{1, 2, \ldots, N\}$. We make the following assumption about the multi-machine power system.

Assumption 4.3.6 *The transmission network can be modeled by an asymptotically stable linear port-Hamiltonian system with Hamiltonian H_{grid}.*

Concretely, this assumption states that whenever the inputs to the transmission network are zero, H_{grid} can be used as a quadratic Lyapunov function proving global asymptotic stability of the origin. Although it may appear strong, we note that it holds in many cases of interest. In particular, it is satisfied whenever we use short or medium length approximate models to describe transmission lines in arbitrary network topologies. Furthermore, we discuss in Remark 4.3.9 how it can be relaxed.

We denote the three-phase voltages across the load terminals and currents entering into the load terminals by $V_{\ell,abc,j}$ and $I_{\ell,abc,j}$, respectively. Here, we use the letter ℓ to distinguish the currents and voltages that correspond to a load from the ones that correspond to a generator. The current entering into the load terminals when we set $V_{\ell,abc,j} = V^*_{\ell,abc,j}$ is denoted by $I^*_{\ell,abc,j}$. It follows from the linearity assumption on the transmission network that we can perform an affine change of coordinates so that in the new coordinates we have

$$\hat{u}^T_{\text{grid}}\hat{y}_{\text{grid}} + \sum_{i=1}^{N} \hat{V}^T_{abc,i}\hat{I}_{abc,i} + \sum_{j=1}^{M} \hat{V}^T_{\ell,abc,j}\hat{I}_{\ell,abc,j} = 0 \tag{4.113}$$

where $\hat{u}_{\text{grid}}$ and $\hat{y}_{\text{grid}}$ are the input and the output of the port-Hamiltonian model of the grid in the new coordinates with shifted Hamiltonian $\hat{H}_{\text{grid}}$, $\hat{V}_{\ell,abc,j} = V_{\ell,abc,j} - V^*_{\ell,abc,j}$, and $\hat{I}_{\ell,abc,j} = I_{\ell,abc,j} - I^*_{\ell,abc,j}$. Equation (4.113) represents an "incremental power balance", i.e., a power balance in the shifted variables. Intuitively, it states that the net incremental power supplied by the generators and the loads is equal to the net incremental power received by the transmission grid.

4.3.2.2 Assumptions on Load Models

We make the following assumption regarding loads.

Assumption 4.3.7 *Each load is described by one of the following models:*

- *a symmetric three-phase circuit with each phase being an asymptotically stable linear electric circuit;*

- *a constant current source.*

The proposed load models are quite simple and a subset of the models used in the power systems literature. It has recently been argued [58] that the increase of DC loads, such as computers and appliances, interfacing the grid through power electronics intensifies the nonlinear character of the loads. However, there is no agreement on how such loads should be modeled. In fact, load modeling is still an area of research [47]. The first class of models in Assumption 4.3.7 contains the well-known constant impedance model in the power systems literature. Constant impedance load models are commonly used in transient stability analysis [31] and can be used to study the transient behavior of induction motors [32]. According to the IEEE Task Force on Load Representation for Dynamic Performance, more than half of the energy generated in the United States is consumed by induction motors [39]. This observation, together with the fact that these three-phase induction motors can be modeled as three-phase circuits with each phase being a series connection of a resistor, an inductor and a voltage drop justifies the constant impedance model usage in transient stability studies. The RL-circuit model suggested for induction motors in [39] is also captured by Assumption 4.3.7. In [39], it is also stated that lighting loads behave as resistors in certain operational regions. This observation also suggests the usage of constant impedances for modeling the aggregated behavior of loads. The second load model in Assumption 4.3.7 is also common in the power systems literature [47].

Any asymptotically stable linear electrical circuit has a unique equilibrium and admits a port-Hamiltonian representation with Hamiltonian $H_{\ell,abc,j}$. By performing a change of coordinates, we can obtain a port-Hamiltonian system for the shifted coordinates with the shifted Hamiltonian $\hat{H}_{\ell,abc,j}$ satisfying:

$$\frac{d\hat{H}_{\ell,j}}{dt} < \hat{V}_{\ell,abc,j}^T \hat{I}_{\ell,abc,j}. \tag{4.114}$$

Let us now consider constant current loads. If a load j draws constant current from the network we have $I_{\ell,abc,j} = I^*_{\ell,abc,j}$. This implies $\hat{I}_{\ell,abc,j} = 0$ and the contribution

of the constant current load j to the incremental power balance (4.113) is zero. This observation shows that we can neglect constant current loads since they do not contribute to the incremental power balance. Therefore, in the remainder of the paper we only consider the first type of loads in Assumption 4.3.7.

4.3.2.3 Stability of Multi-Machine Power Systems

Let $\hat{H}_i$ be the shifted Hamiltonian for generator i with respect to the equilibrium point $\xi_i^* = (M_i\omega_s, \lambda_{xyz,i}^*)$, as defined in Section 4.1.2.2. From Section 4.1.2.2, we know that, under the FACTS control law that introduces the voltage drops (4.106)-(4.108), for every generator i we have

$$\frac{d\hat{H}_i}{dt} = \frac{\partial \hat{H}_i}{\partial \hat{\xi}_i}^T \mathcal{P}_i \frac{\partial \hat{H}_i}{\partial \hat{\xi}_i} + \hat{V}_{abc,i}^T \hat{I}_{abc,i}, \tag{4.115}$$

where $\mathcal{P}_i$ is a matrix obtained by adding subscript i to the elements of the matrix $\mathcal{P}$ given by (4.98), where the stator resistance r is replaced by $r + R$. Using the definitions above, we select our candidate Lyapunov function as

$$\hat{H}_{\text{total}} = \hat{H}_{\text{grid}} + \sum_{i=1}^{N} \hat{H}_i + \sum_{j=1}^{M} \hat{H}_{\ell,j},$$

where $\hat{H}_{\text{grid}}$ is the shifted Hamiltonian of the transmission grid that was introduced in Assumption 4.3.6, Section 4.3.2.1. Our objective is to show that the equilibrium $\xi^* = (\xi_1^*, \ldots, \xi_N^*)$ for the generators is globally asymptotically stable. Note that every equilibrium ξ_i^* shares the same synchronous velocity ω_s. Hence, asymptotical stability of ξ^* implies that all the generators converge to the synchronous velocity ω_s. In addition to synchronize the generators' angular velocity we also need to ensure that the currents flowing through the transmission network converge to preset values respecting several operational constraints such as thermal limits of the transmission lines. This will also be a consequence of asymptotical stability of the equilibrium ξ^*. When this equilibrium is reached, the voltages and currents at the generator terminals are $V_{abc,i}^*$ and $I_{abc,i}^*$, respectively. If we now regard the transmission network and the loads as being described by an asymptotically stable linear system driven by the inputs $V_{abc,i}^*$ and $I_{abc,i}^*$, we realize that all the voltages and currents

in the transmission network and loads will converge to a unique steady state. We assume that such steady state, uniquely defined by $V^*_{abc,i}$ and $I^*_{abc,i}$, satisfies all the operational constraints.

Taking the time derivative of $\hat{H}_{\text{total}}$, we obtain

$$\frac{d\hat{H}_{\text{total}}}{dt} = \frac{d\hat{H}_{\text{grid}}}{dt} + \sum_{i=1}^{N} \frac{d\hat{H}_i}{dt} + \sum_{j=1}^{M} \frac{d\hat{H}_{\ell,j}}{dt} \tag{4.116}$$

$$\leq \hat{u}^T_{\text{grid}} \hat{y}_{\text{grid}} + \sum_{i=1}^{N} \frac{d\hat{H}_i}{dt} + \sum_{j=1}^{M} \frac{d\hat{H}_{\ell,j}}{dt} \tag{4.117}$$

$$= \sum_{i=1}^{N} \frac{\partial \hat{H}_i}{\partial \hat{\xi}_i}^T \mathcal{P}_i \frac{\partial \hat{H}_i}{\partial \hat{\xi}_i}, \tag{4.118}$$

where (4.117) follows from (2.20), and (4.118) follows from (4.113), (4.114), and (4.115). If

$$(L_{ss,i} I^*_{x,i})^2 + (L_{ss,i} I^*_{y,i})^2 < 4 D_i r_i. \tag{4.119}$$

holds for $i \in \{1, \ldots, N\}$, then $\mathcal{P}_i < 0$ for every $i \in \{1, \ldots, N\}$ by Theorem 4.3.1. Therefore, if (4.119) holds for every $i \in \{1, \ldots, N\}$, we conclude from (4.118) that

$$\frac{d\hat{H}_{\text{total}}}{dt} \leq \sum_{i=1}^{N} \frac{\partial \hat{H}_i}{\partial \hat{\xi}_i}^T \mathcal{P}_i \frac{\partial \hat{H}_i}{\partial \hat{\xi}_i} < 0. \tag{4.120}$$

This only shows that $\frac{d\hat{H}_{\text{total}}}{dt}$ is negative semi-definite. Since all of the Hamiltonians that constitute the total Hamiltonian $\hat{H}_{\text{total}}$ have compact level sets, the level sets of $\hat{H}_{\text{total}}$ are also compact. Hence, we can apply La Salle's Invariance Principle to conclude that all the trajectories converge to the largest invariant set contained in the set defined by

$$\sum_{i=1}^{N} \frac{\partial \hat{H}_i}{\partial \hat{\xi}_i}^T \mathcal{P}_i \frac{\partial \hat{H}_i}{\partial \hat{\xi}_i} = 0. \tag{4.121}$$

The left hand side of (4.121) is a sum of negative definite quadratic terms (recall that $\mathcal{P}_i < 0$) and thus only zero when $\frac{\partial \hat{H}_i}{\partial \hat{\xi}_i} = 0$ for all i. This implies $\xi = \xi^*$, hence the generator states globally asymptotically converge to ξ^* if (4.120) holds. The preceding discussion is summarized in the following result.

Theorem 4.3.8 *Consider a multi-machine power system with N generators described by equations* (4.15) *with $\tau_{m,i} = \tau^*_{m,i}$, and M loads satisfying Assumption*

4.3.7 interconnected by a transmission network satisfying Assumption 4.3.6. Let ξ^* be an equilibrium point for the generators that is consistent with all the equations describing the power system. Let (4.109) *and* (4.110) *be the voltage and current drops introduced by the FACTS controllers, respectively. The equilibrium ξ^* is globally asymptotically stable if*

$$(L_{ss,i}I^*_{x,i})^2 + (L_{ss,i}I^*_{y,i})^2 < 4D_i(r_i + R_i). \tag{4.122}$$

holds for all $i \in \{1, \ldots, N\}$.

Theorem 4.3.8 states that in order to check the stability of the multi-machine system, we only need to check a simple condition for each generator in the system. This makes our result compositional in the sense that the complexity of condition (4.122) is independent of the size of the network. All these conditions are bound together by I^*_x and I^*_y that obviously depend on the whole network. However, the computation of the desired steady state currents needs to be performed for reasons other than transient stability and thus are assumed to be readily available.

Remark 4.3.9 *We note that if Assumption 4.3.6 is weakened from asymptotic stability to stability of the transmission network, the equilibrium ξ^* is still globally asymptotically stable. However, the voltages and currents in the transmission network are no longer uniquely determined and may violate the operational constraints.*

Remark 4.3.10 *If there exists a reference trajectory for the grid that satisfies*

$$\hat{u}^T_{grid}\hat{y}_{grid} + \sum_{i=1}^{N} \hat{V}^T_{xyz,i}\hat{I}_{xyz,i} + \sum_{j=1}^{M} \hat{V}^T_{\ell,abc,j}\hat{I}_{\ell,abc,j} = 0, \tag{4.123}$$

then we can replace the FACTS controllers in Theorem 4.3.8 with the FACTS controller defined by (4.101)-(4.103)*. The multi-machine power system in Section 4.3.3 is an example of a power system where this replacement can be performed.*

4.3.3 Example

We apply our results to the two-generator single-load scenario depicted in Figure 4.8. The generators are connected to the load via transmission lines with impedances

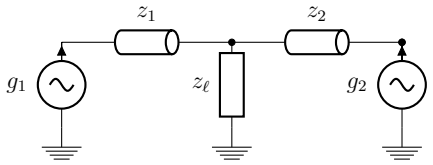

Figure 4.8: Two-generator single-load scenario

$z_1 = z_2 = (5 + j0.1\omega_s)\,\Omega$. The load impedance is $z_\ell = 1\text{k}\Omega$. We use the generator parameters provided in [59, Table 7.3]. Using the provided H_i values, the damping coefficients are selected as $D_1 = \frac{0.2H_1}{\omega_s} = 1.25$ MVAs and $D_2 = \frac{0.4H_2}{\omega_s} = 0.68$ MVAs as was done in [59, Example 7.1]. The stator winding resistances for the generators are taken to be $r_1 = r_2 = 0.05\Omega$. Using the values for $X_{d,i}$ and $X_{q,i}$ provided in [59, Table 7.3], we obtain $L_{s,1} = 0.2049$ H and $L_{s,2} = 1.2570$ H from the equations $X_{d,i} = \omega_s L_{s,i}$. Since the parameters $L_{s0,i}$ and $L_{m,i}$ cannot be obtained from [59, Table 7.3] we assume $L_{s0,i} = 0$ and $L_{m,i} = L_{s,i}$. The steady state phase-xyz voltages are $V^*_{x,1} = -17.56$ kV, $V^*_{y,1} = 280.16$ kV, $V^*_{x,2} = -24.14$ kV, and $V^*_{y,2} = 278.76$ kV. The steady state phase-xyz currents satisfying the circuit constraints are $I^*_{x,1} = 19.83$ A, $I^*_{y,1} = -227.33$ A, $I^*_{x,2} = 6.2$ A, and $I^*_{y,2} = -50.9402$ A. The mechanical torques and field winding currents are selected so as to be consistent with these steady-state values. For both generators, (4.28) is satisfied with this choice of parameters and the equilibrium is unique. We now investigate global asymptotic stability for this example. We connect a static synchronous series compensator (SSSC) in series with the generator terminals providing the voltage drops $R_i\left(I_{x,i} - I^*_{x,i}\right)$, $R_i\left(I_{y,i} - I^*_{y,i}\right)$, and $R_i\left(I_{z,i} - I^*_{z,i}\right)$ in phases x, y, and z, respectively. Condition (4.122) holds for generator i if:

$$R_i > \frac{(L_{ss,i}I^*_{x,i})^2 + (L_{ss,i}I^*_{y,i})^2}{4D_i}.$$

Replacing the generator parameters into this inequality, we obtain $R_1 > 0.437$ mΩ and $R_2 > 1.53$ mΩ. We choose $R_1 = R_2 = 10\Omega$ to satisfy these inequalities and provide enough damping.

We numerically simulated the dynamics of the circuit in Figure 4.8 to obtain the transient behavior following the occurrence of a fault. Without conjecturing anything about the nature of the fault or the pre-fault circuit, we simply assumed that

the initial condition for the frequencies of the generators lies in the set $[59.8, 60.2]$. For a generator current with steady state value I^*, we assumed that the initial condition for the current lies in the set $[I^* - 50, I^* + 50]$. With this assumption about the initial states, we performed numerical simulations for 25 randomly chosen initial state vectors. These simulations indicate that the generator states converge to the steady-state values as expected. We present in Figure 4.9 a typical trajectory corresponding to initial conditions $\omega_1(0) = 2\pi(60.08)$ rad/s, $\omega_2(0) = 2\pi(60.17)$ rad/sec, $I^*_{x,1}(0) = -62.46$ A, $I^*_{x,2}(0) = -46.95$ A, $I^*_{y,1}(0) = -249.61$ A, and $I^*_{y,2}(0) = -70.71$ A. The reader can appreciate how the states and the value of the total shifted Hamiltonian converge to the desired values.

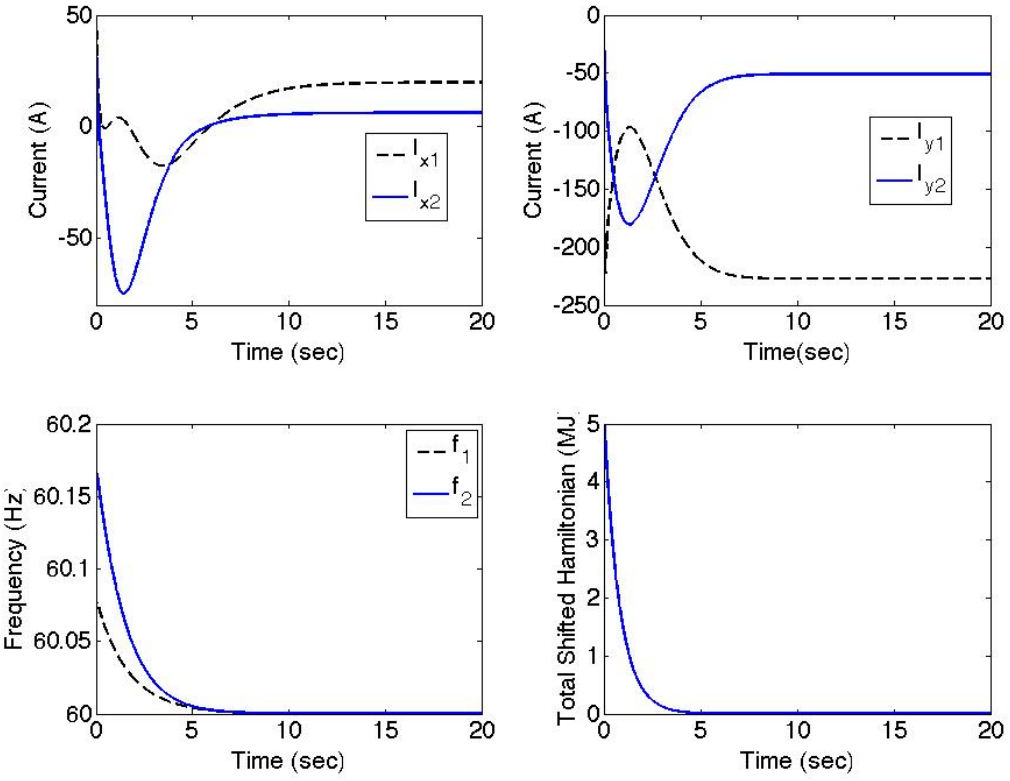

Figure 4.9: Evolution of the generators' states (x-axis currents on upper left, y-axis currents on upper right, frequencies on lower left) and the value of the total shifted Hamiltonian (on lower right).

CHAPTER 5

Conclusions and Future Work

In this thesis, we demonstrated through counter-examples that the usage of the swing equation to study transient stability leads to erroneous conclusions. We explained how to perform transient stability analysis using a first principles model instead of the traditional models based on the swing equation. The stability conditions we proposed in this thesis are compositional, that is, it is enough to verify that a simple stability condition holds for every generator to conclude that the power system is stable. We also showed that one can enforce these conditions by deploying local controllers on the generators. Finally, we presented a way of performing circuit reduction to reduce the complexity of the power system. In contrast to the circuit reduction methods, such as Kron reduction, that are widely used in the literature, the proposed method does not require the usage of phasors.

There are certain limitations in our framework. We want to address these limitations in future. First of all, we use FACTS devices to implement our control law. In practice, these devices are costly and thus not widely used. In the future, we want to design a controller that can act on the field windings of the generators to reduce the cost of implementation. Other limitations are the load models that we use. We can only deal with loads that can be modeled as linear circuits. We need to find alternative ways of dealing with loads that cannot be represented by this model. We also need to quantify the class of practical loads that can be modeled accurately with this model. Finally, higher order generator models can be used instead of the five state model that we use.

References

[1] P. M. Anderson, A. A. Fouad, *P*ower system control and stability, (2nd ed.), IEEE Press, New Jersey.

[2] M. Anghel, F. Milano, and A. Papachristodoulou, *A*lgorithmic construction of Lyapunov functions for power system stability analysis, IEEE Transactions on Circuits and Systems-I: Regular Papers, *Accepted for publication*, 2013.

[3] A. Arapostathis, S. Sastry, P. Varaiya, *A*nalysis of power-flow equation, Electrical Power & Energy Systems, Vol. 3, No. 3, pp. 115–126, July 1981

[4] P. D. Aylett, *T*he energy-integral criterion of transient stability limits of power systems, Proceedings of the IEE - Part C: Monographs, Vol. 105, Issue 8, pp. 527–536, September 1958.

[5] A. R. Bergen, V. Vittal, *P*ower system analysis (2nd ed.), Prentice Hall, New Jersey.

[6] A. R. Bergen, D. J. Hill, *A* structure-preserving model for power system stability analysis, IEEE Transactions on Power Apparatus and Systems, Vol. 100, No. 1, pp. 25–35, January 1981.

[7] A. R. Bergen, D. J. Hill, C. L. de Marcot, *L*yapunov function for multimachine power systems with generator flux decay and voltage dependent loads, Electrical Power and Energy Systems, Vol. 8, Issue 1, pp. 2–10, January 1986.

[8] R. J. Davy, I. A. Hiskens, *L*yapunov functions for multimachine power systems with dynamic loads, IEEE Transactions on Circuits and Systems-I: Fundamental Theory and Applications, Vol. 44, No. 9, pp. 796–812, September 1997

[9] C. A. Desoer, E. S. Kuh, *B*asic circuit theory , McGraw-Hill, New York, 1969.

[10] S. Y. Caliskan, P. Tabuada, *K*ron reduction of power networks with lossy and dynamic transmission lines, Proceedings of the 51st IEEE Conference of Decision and Control, pp. 5554–5559, December 10–13 2012, Maui, Hawaii, USA.

[11] S. Y. Caliskan, P. Tabuada, *T*owards Kron reduction of generalized electrical networks, Automatica, Vol. 50, Issue 10, pp. 2586–2590, October 2014.

[12] S. Y. Caliskan, P. Tabuada, *T*owards a compositional analysis of multi-machine power systems transient stability, Proceedings of the 52nd IEEE Conference of Decision and Control, pp. 3969-3974, December 10–13 2013, Firenze, Italy.

[13] S. Y. Caliskan, and P. Tabuada, *C*ompositional transient stability analysis of multi-machine power networks, IEEE Transactions on Control of Networked Systems, Volume 1, Issue 1, pp. 4–14, March 2014.

[14] S. Y. Caliskan, and P. Tabuada, *U*ses and Abuses of the Swing Equation Model, Submitted to 54th IEEE Conference of Decision and Control (2015)

[15] D. Casagrande, A. Astolfi, and R. Ortega, *G*lobal stabilization of non-globally linearizable triangular systems: application to transient stability of power systems, Proceeding of the 50th IEEE Conference on Decision and Control and European Control Conference, pp. 331–336, December 12-15 2011, Orlando, Florida, USA.

[16] D. Casagrande, A. Astolfi, R. Ortega, and D. Langarica, *A* solution to the problem of transient stability of multimachine power systems, Proceedings of the 51st IEEE Conference and Decision and Control, pp. 1703–1708, December 10-13 2012, Maui, Hawaii, USA.

[17] H.-D. Chiang, *S*tudy of the existence of energy functions for power systems with losses, IEEE Transactions on Circuits and Systems, Vol. 39, No. 11, pp. 1423–1429, November 1989.

[18] C.-C. Chu, H. D. Chiang, *C*onstructing analytical energy functions for network-preserving power system models, Circuits Systems Signal Processing, Vol. 24, No. 4, pp. 363-383, 2005.

[19] L. O. Chua, C. A. Desoer, and E. S. Kuh, *L*inear and nonlinear circuits, McGraw-Hill, New York, 1987.

[20] C. Concordia, *E*ffect of synchronous-machine transient rotor saliency, Electrical Engineering, Volume 74, page 123, February 1955.

[21] M. V. Deshpande, *Electrical power system design*, ISBN 978-0-074515-75-4 ,Tata McGraw-Hill, 2001.

[22] C. A. Desoer, and E. S. Kuh, *B*asic circuit theory, McGraw-Hill, New York, 2009

[23] W. Dib, R. Ortega, A. Barabanov, and F. Lamnabhi-Lagarrigue, *A* globally convergent controller for multi-machine power systems using structure-preserving models, IEEE Transactions on Automatic Control, Vol. 54, No. 9, pp. 2179–2185, September 2009.

[24] H. W. Dommel, *Techniques for analyzing electromagnetic transients*, IEEE Computer Applications in Power, Vol. 10, Issue 3, pp. 18–21, 1997.

[25] F. Dörfler and F. Bullo, *O*n the critical coupling for Kuramoto oscillators, SIAM Journal on Applied Dynamical Systems, Volume 10, Issue 3, pp. 1070–1099, September 2011.

[26] F. Dörfler, and F. Bullo, *S*ynchronization and transient stability in power networks and nonuniform Kuramoto oscillators, SIAM J. of Control and Optimization, Vol. 50, No. 3, pp 1116–1642, June 2012.

[27] F. Dörfler, and F. Bullo, *K*ron reduction of graphs with applications to electrical networks. IEEE Transactions on Circuits and Systems, Vol. 60, No. 1, pp. 150–163, January 2013.

[28] F. Dörfler, M. Chertkov, and F. Bullo, *S*ynchronization in complex oscillator networks and smart grids, Proceedings of the National Academy of Sciences, Volume 110, No. 6, pp. 2005–2010, February 2013.

[29] A. H. El-Abiad, and K. Nagappan, *T*ransient stability regions for multimachine power systems, IEEE Transactions on Power Apparatus and Systems, Vol. 85, No. 2, pp. 169–179, February 1966.

[30] H. Farhangi, *T*he path of the smart grid, IEEE Power and Energy Magazine, Vol. 8, Issue 1, pp 18–28, January/February 2010.

[31] A. A. Fouad, V. Vittal, *P*ower system transient stability analysis using the transient energy function method, Prentice Hall, New Jersey, 1992.

[32] A. E. Fitzgerald, C. Kingsley, S. D. Umans, *E*lectric machinery, 5$^{\text{th}}$ Ed., McGraw-Hill, New York, 1990.

[33] G. E. Gless, *A*pplication of the direct method of Liapunov to the power system stability problem, Ph.D. thesis, Iowa State University of Science and Technology, Ames, 1963.

[34] G. E. Gless, *D*irect method of Lyapunov applied to transient power system stability, IEEE Transactions on Power Apparatus and Systems, Vol. 85, No. 2, pp. 159–168, February 1966.

[35] C. Godsil, and G. Royle, *Algebraic graph theory*, Graduate Texts in Mathematics, Vol. 207, Springer-Verlag, New York, 2001.

[36] *H*andbook of Linear Algebra, 2$^{\text{th}}$ Edition, Edited by Leslie Hogben, Associate Editors: Richard Brualdi, Anne Greenbaum, Roy Mathias, Chapman and Hall/CRC, 2007.

[37] N. G. Hingorani, L. Gyughi, *U*nderstanding FACTS: Concepts and Technology of Flexible AC Transmission Systems, IEEE Press, New York, 2000.

[38] IEEE Task Force on Load Representation for Dynamic Performance, *L*oad representation for dynamic performance analysis, IEEE Transactions on Power Systems, Vol. 8, No. 2, pp. 472–482, May 1993

[39] IEEE Task Force on Load Representation for Dynamic Performance, *S*tandard load models for power flow and dynamic performance simulation, IEEE Transactions on Power Systems. Vol. 10. No. 3, pp. 1302–1313, August 1995

[40] IEEE/CIGRE Joint Task Force on Stability Terms and Definitions, *D*efinition and classification of power system stability, IEEE Transactions on Power Systems, Vol. 19, No. 2, pp. 1387–1401 May 2004.

[41] P. K. Kundu, and I. M. Cohen, *F*luid mechanics, Elsevier, 2008.

[42] A. Halim, and K. Takahashi, *A*n application of linear matrix inequality method for power system transient stability analysis, Proceeding of the IEEE Power Engineering Society Summer Meeting, Vol. 2, pp. 675–680, 2000.

[43] D. Hill, and C. N. Chong, *L*yapunov functions of Lur'e-Postnikov form for structure preserving models of power systems, Automatica, Vol. 25, No. 3, pp. 453–460, 1989.

[44] D. J. Hill, *N*onlinear dynamic load models with recovery for voltage stability studies, IEEE Transactions on Power Systems, Vol. 8, No. 1, pp. 166-176, February 1993.

[45] A. J. Laub, *M*atrix analysis for scientists and engineers, Society for Industrial and Applied Mathematics, Philadelphia, 2005.

[46] P. C. Magnusson, *T*he transient-energy method of calculating stability, Transactions of the American Institute of Electrical Engineers, Vol. 66, Issue 1, pp. 747–755, January 1947

[47] J. V. Milanović, K. Yamashita, S. M. Villanueva, S. Ž. Djokic, and L. M. Korunović, *I*nternational industry practice on power system load modeling, IEEE Transactions on Power Systems, Vol. 28, No. 3, pp. 3038–3046, August 2013.

[48] G. Miranda, *B*e prepared!, IEEE Industry Applications Magazine, Vol. 9, Issue 2, pp. 12–20, March/April 2003.

[49] K. Moslehi, and R. Kumar, *A* reliability perspective of the smart grid, IEEE Transactions on Smart Grid, Vol. 1, No. 1, pp. 57–64, June 2010.

[50] N. Narasimhamurthi, and M. R. Musavi, *A* general function for transient stability analysis of power systems, IEEE Transactions on Circuits & Systems, Vol. 31, No. 7, pp. 637–645, July 1984.

[51] National Institute of Standards, *N*IST Framework and Roadmap for Smart Grid Interoperability Standards, Release 1.0, NIST Special Publication 1108.

[52] North American Electric Reliability Corporation, *B*alancing and Frequency Control, January 2011.

[53] R. Ortega, M. Galaz, A. Astolfi, Y. Sun and T. Shen, *T*ransient stabilization of multimachine power systems with nontrivial transfer conductances, IEEE Transactions in Automatic Control, Vol. 50, No. 1, pp. 60–75, January 2005.

[54] M. Pavella, and P. G. Murthy, *T*ransient stability of power systems: theory and practice, West Sussex: John Wiley & Sons, 1994.

[55] M. Pavella, D. Ernst, D. Ruiz-Vega, *T*ransient stability of power systems: a unified approach to assesment and control, Kluwer's Power Electronics and Power Systems Series (Editor: M. A. Pai), Kluwer Academic Publishers, Dordrecht, 2000.

[56] M. A. Pai, *E*nergy function analysis for power system stability, Kluwer Academic Publishers, Boston, 1986.

[57] J. W. Polderman, and J. C. Willems, *Introduction to the mathematical theory of system and control: A behavioral approach*, New York, Springer-Verlag, 1998.

[58] M. J. H. Raja, D. W. P. Thomas, and M. Sumner, *H*armonics attenuation of nonlinear loads due to linear loads, 2012 Asia-Pacific Symposium on Electromagnetic Compatibility (APEMC), pp. 829–832, 21-24 May 2012, Singapore.

[59] P. Sauer, M. A. Pai, *P*ower system dynamics and stability, Stipes Publishing L. L. C., Champaign, IL, 1997.

[60] J.W. Simpson-Porco, F. Dörfler, and F. Bullo, *S*ynchronization and Power-Sharing for Droop-Controlled Inverters in Islanded Microgrids, Automatica. To appear. Available electronically at http://arxiv.org/.

[61] K. Szendy, *K*riterium der dynamischen Stabilität in Dreigeneratorensystemen und dessen Verallgemeinerung auf Mehrgeneratorensysteme, Archiv f. Elektrotechnik, XLVII. Band, 3. Heft, pp. 149–160, 1962.

[62] F. Shaiz, D. Zonetti, R. Ortega, J. M. A. Scherpen, and A. J. Van Der Schaft, *O*n port-Hamiltonian modeling of the synchronous generator and ultimate boundedness of its solutions, 4th IFAC Workshop on Lagrangian and Hamiltonian Methods for Non Linear Control, August 29-31 2012, Bertinoro, Italy.

[63] F. Shaiz, D. Zonetti, R. Ortega, J. M. A. Scherpen, and A. J. Van Der Schaft, *P*ort Hamiltonian modeling of power networks, 20th International Symposium on Mathematical Theory of Networks and Systems, July 9-13 2012, Melbourne, Australia.

[64] L. A. B. Torres, J. Hespanha, and J. Moehlis, *S*ynchronization of oscillators coupled through a network with dynamics: a constructive approach with applications to the parallel operation of voltage power supplies, September 2013, Submitted to journal publication, available at http://www.ece.ucsb.edu/ hespanha.

[65] N. A. Tsolas, A. Araphostatis, P. Varaiya, *A* structure preserving energy function for power system transient analysis, IEEE Transactions on Circuits and Systems, Vol. 32, No. 10, pp. 1041–1049, October 1985.

[66] The United States Department of Energy, *I*nterim Report: Causes of the August 14th Blackout in the United States and Canada, U.S.-Canada Power System Outage Task Force, November 2003

[67] The United States Department of Energy, *2*010 Smart Grid System Report to Congress, February 2012.

[68] The United States Department of Energy, *T*he Future of the Grid: Evolving to Meet America's Needs, December 2014.

[69] P. Varaiya, F. F. Wu, R.-L. Chen, *D*irect methods for transient stability analysis for power systems: recent results, Proceedings of the IEEE, Vol. 73, No. 12, pp. 1703–1715, December 1985.

[70] A. J. van der Schaft, L_2-gain and passivity techniques in nonlinear control, Lecture Notes in Control and Information Sciences, Vol. 218, Berlin - Heidelber, Springer-Verlag, 1996.

[71] H. Nijmeijer, and A. J. van der Schaft, *N*onlinear dynamical control systems, Springer, New York, 2010.

[72] A. J. van der Schaft, B. M. Maschke, *Conservation laws and lumped system dynamics*, Model-Based Control; Bridging Rigorous Theory and Advanced Technology, P.M.J. Van den Hof, C. Scherer, P. S. C. Heuberger, eds., Springer, ISBN 978-1-4419-0894-0, pp. 31–48, 2009.

[73] A.J. van der Schaft, *C*haracterization and partial synthesis of the behavior of resistive circuits at their terminals, System & Control Letters, Vol. 59, pp. 423–428, June 2010.

[74] V. Vittal, A. N. Michel, and A. A. Fouad, *P*ower system transient stability analysis: formulation as nearly Hamiltonian systems, Circuits Systems Signal Processing, Vol. 3, No. 1, pp. 105–122, 1984

[75] L. Wehenkel, *A*utomatic learning techniques in power systems, Kluwer Academic Publishers, 1998.

[76] J. C. Willems, and E. I. Verriest, *The behavior of resistive circuits*, Joint 48th IEEE Conference on Decision and Control and 28th Chinese Control Conference, December 16-18, 2009, Shanghai, P.R. China.

[77] J. L. Willems, *I*mproved Lyapunov function for transient power-system stability, Proceedings of IEE, Vol. 115, No. 9, pp. 1315–1317, September 1968.

[78] J. L. Willems, *O*ptimum Lyapunov functions and stability regions for multimachine power systems, Proceedings of IEE, Vol. 117, No. 3, pp. 573–577, March 1970.

[79] J. L. Willems, J. C. Willems, *T*he application of Lyapunov methods to the computation of transient stability regions for multimachine power systems, IEEE Transactions on Power Power Apparatus and Systems, Vol. 89, No. 5/6, pp. 795–801, May/June 1970.

[80] J. L. Willems, *D*irect methods for transient stability studies in power system analysis, IEEE Transactions on Automatic Control, Vol. 16, No. 4, pp. 332–341, August 1971.

[81] E. I. Verriest, and J. C. Willems, *The behavior of linear time invariant RLC circuits*, 49th IEEE Conference on Decision and Control, December 15-17, 2010, Atlanta, GA, USA.